Original

Bouali, A.; Serdechnova, M.; Blawert, C.; Tedim, J.; Ferreira, M.; Zheludkevich, M.:

Layered double hydroxides (LDHs) as functional materials for the corrosion protection of aluminum alloys: A review.

In: Applied Materials Today. Vol. 21 (2020) 100857.

First published online by Elsevier: 28.10.2020

https://dx.doi.org/10.1016/j.apmt.2020.100857

Applied Materials Today 21 (2020) 100857

Contents lists available at ScienceDirect

Applied Materials Today

journal homepage: www.elsevier.com/locate/apmt

Layered double hydroxides (LDHs) as functional materials for the corrosion protection of aluminum alloys: A review

A.C. Bouali[a,*], M. Serdechnova[a], C. Blawert[a], J. Tedim[b], M.G.S. Ferreira[b], M.L. Zheludkevich[a,c]

[a] Institute of Materials Research, Helmholtz-Zentrum Geesthacht, Max-Planck-Straße 1, Geesthacht 21502, Germany
[b] Department of Materials and Ceramic Engineering, CICECO - Aveiro Institute of Materials, University of Aveiro, Aveiro 3810-193, Portugal
[c] Faculty of Engineering, Kiel University, Kaiserstraße 2, Kiel 24143, Germany

ARTICLE INFO

Article history:
Received 27 July 2020
Revised 20 September 2020
Accepted 11 October 2020

Keywords:
Layered double hydroxide
Self-healing
Corrosion protection
Aluminum alloys

ABSTRACT

The search for new alternatives to replace chromate-based coatings is a matter of great importance. Since their official ban due to the raised concerns of hexavalent chromium to the human health and the environment, significant efforts have been devoted to finding a more suitable alternative for the corrosion protection of aluminum alloys. However, the task has been quite challenging since the potential replacement needs to fulfill several requirements both in terms of cost and exceptional corrosion performance. Layered double hydroxides (LDHs) have generated a lot of interest in the past few years. They have been proposed as prospective candidates to replace chromate based protective systems. The particular structure of LDH nanocontainers allows them to intercalate a number of corrosion inhibitors and release them on demand under the action of corrosion relevant triggers. Moreover, their flexible use as pigments in paints or as a pre-treatment directly as conversion layers makes their implementation even more convenient. This review presents a critical view to the studies performed till today on LDHs for corrosion protection of aluminum alloys.

1. Introduction

Layered clay materials are currently the focus of many studies and innovations. The interest for these materials arises from the nature and composition of their stacked layers and interlayer galleries offering many options for modification and tuning [1–7]. However, layered double hydroxides (LDHs) (or hydrotalcite-like structures) have recently gained a key position not only due to their unique two-dimensional structure but more importantly because of their anion-exchange properties. As a result, their application has been continuously expanding, especially owing to new emerging demands such as in corrosion protection [8–20].

The first studies on hydrotalcite-like structures can be traced back to Hochstetler (1842) using materials originating from a natural deposit in Snarum/Norway [21,22]. However, it was not until the works of Manasse (1915) and Frondel (1941), that the mineral was given the final formula of $[Mg_{4+x}\ Al_2(OH)_{\ 12+2x}](CO_3)\bullet 4H_2O$ $(0 \leq x \leq 2)$ [23,24]. Allmann [25] and Taylor [26–28] reported a few years later a more detailed study including an understanding of the LDH structure. Using single crystal X-ray diffraction, the authors were able to reveal a rhombohedral lattice symmetry (R-3m) with a stacking of positively charged brucite-like layers alternating with disordered negatively charged interlayers [25,26,29]. LDHs are typically described as a stacking of positively charged mixed metal M^{I}/M^{II}-M^{III} hydroxide layers, balanced by the presence of anions (A^{y-}) together with water molecules between the inter-galleries. The most common LDH can be represented by the

Abbreviations: 3- or 4-ABSA, 3 or 4- aminobenzensulfonic acid; BTA, benzotriazole; CA, contact angle; CCC, chromate conversion coatings; CFRP, carbon fiber reinforced plastics/polymer; DC, direct current; EDTA, ethylenediaminetetraacetic acid; FAS-13, F-triethoxy-1H,1H,2H,2H-tridecafluoro-n-octylsilane; FFC, filiform corrosion; GDOES, glow discharge optical emission spectroscopy; 2-HEP, 2-hydroxyethyl phosphate; 3,4-HHBA, 3,4-dihydroxybenzoic acid; 8-HQ, 8-hydroxyquinoline; IMC, intermetallic; L-Cys, L-cysteine; LbL, layer-by-layer; LDH, layered double hydroxide; LDH-CC, layered double hydroxide conversion coating; MBT, 2-mercaptobenzothiazol; MW, microwave; ORR, oxygen reduction reaction; PANI, polyaniline; PEO, plasma electrolytic oxidation; PFDTMS, 1H,1H,2H,2H-Perfluorodecyltrimethoxysilane; PFDTS, 1H, 1H, 2H, 2H perfluorododecyl trichlorosilane; PVA, polyvinyl alcohol; PVB, polyvinyl butyral; QA, quinaldic acid; RT, room temperature; SEM, scanning electron microscopy; SKP, Scanning kelvin probe; SST, salt spray test; SVET, scanning vibrating electrode technique; TCC, trivalent chromium conversion coating; TSA, tartaric sulfuric anodizing; XRD, X-ray diffraction.

* Corresponding author.
E-mail address: anissa.bouali@hzg.de (A.C. Bouali).

https://doi.org/10.1016/j.apmt.2020.100857

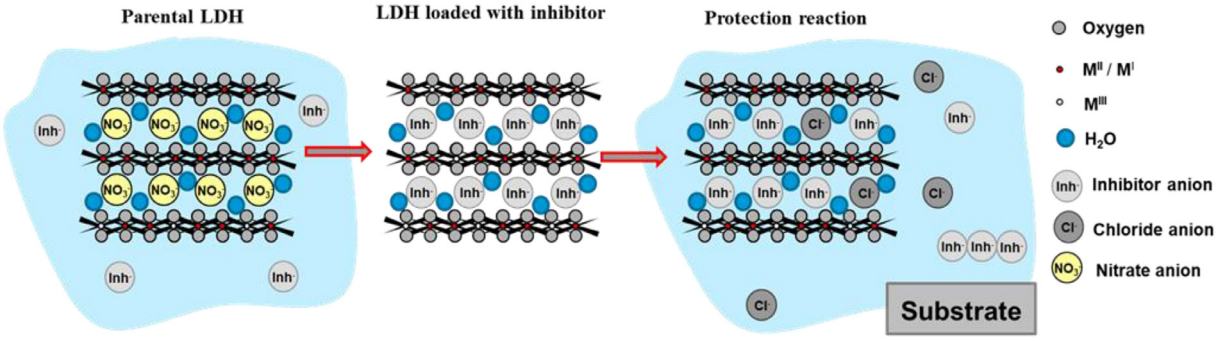

Fig. 1. The schematic presentation of LDH structure, the anionic exchange with inhibitor ion (Inh-) and their triggered release for corrosion protection.

formula $[M^{II}_{1-x}M^{III}_{x}(OH)_2]^{x+}(A^{y-})_{x/y}\bullet zH_2O$ (with M^{II}, M^{III}: divalent and trivalent metallic cations, and (A^{y-}) anions) [3,4]. Accordingly, the structural characteristics of LDHs allows the possibility to use a wide variety of intercalation compounds either by modification of the chemical composition of the hydroxide layer [8,18,30–47] or by chemical /structural modification of the interlayers [14,17,32,48–56].

The ability of LDHs to be used in their derived form or/and as incipient (host for different species) along with their other interesting properties make them valuable for an extended range of functionalities [57,58]. Some of the interesting LDH properties can be listed as follows:

(1) LDHs biocompatibility, prolonged buffering effect, antacids and ability to host pharmaceutically active molecules (e.g. diclofenac sodium, gemfibrozil, ibuprofen, naproxen, tolfenamic) were extensively investigated and reported in the area of drug delivery [58–62].
(2) The high surface area, homogeneous and thermally stable composition of the metal cations of the LDHs, makes them good candidates as catalysts [63–65].
(3) LDHs highly tunable architecture, non-toxicity and anion exchange properties are exploited as adsorbent for inorganic contaminants (eg. AsO_4^{3-}, CrO_4^{2-}, F^-, Br^-, I^-) in water purification [58,66,67].
(4) The crystallinity, morphology and conductivity (depending on the LDH composition) of LDH contribute to enhance the electrochemical performance of materials for energy conversion and storage in the form of electrodes for batteries, fuel cells, super capacitors and so on [68–72].

This review focuses on the use of LDH for corrosion protection of aluminum alloys. Because of the ban of toxic chromate-based corrosion protective systems [73], there is a growing need to redirect the research in the field of corrosion protection into more environmentally friendly concepts. Moreover, these systems should be cost-effective while maintaining a good performance in terms of corrosion protection, hence the recent developments in the area of self-healing "smart" approaches. The latter include the use of nanocontainers [51,74–78] that have the aptitude to host and release healing agents in a controlled manner. Due to the above listed properties and the remarkable anion-exchange capacity, LDHs have been dominating the area of active corrosion protection for a few years now [8,9,13,34,48,79–81]. The protective action of LDH loaded with inhibitive anions is based on the anion-exchange reaction induced by particular triggers, such as pH [30,82] and/or presence of aggressive species [35,83]. The operative mode of LDH nanocontainers involve (a) the release of inhibiting anions [53,84] while (b) capturing corrosive species such as Cl^- [15,83,85] and/or (c) cathodic formation of a hydroxide film [86] (Fig. 1).

This review begins with an overview of the former Cr(VI)-based protective systems and their mechanism of action in Al alloy. A short and comprehensive outline in respect to the corrosion protective strategies proposed as potential replacement to Cr(VI), will be given next. Finally, a critical review of the studies accomplished on LDH as a "smart" active corrosion protective system for Al alloys is provided. The literature review of LDH will be divided in two main parts: first, discussing the studies on the application of LDH in form of pigment and second, on LDH applied as a conversion layer. At the end, a concise outlook on the overall application of LDH for corrosion protection of Al alloy and their current or/and possible implementation in industry, is addressed.

2. Overview of Cr(VI) - based coatings and potential green alternatives

2.1. Cr (VI) based coatings

Chromate-containing coatings were extensively used in the past in many different applications. In the specific case of aerospace industry, they have perhaps been the main tool against corrosion for nearly 100 years [73,87]. These coatings are very effective, providing corrosion protection to critical aerospace parts (fuselage, wings, engines, etc.), that are required to operate in highly demanding environments for extended periods. The remarkable corrosion resistance of Cr-based systems is based on their so-called "self-healing" properties [88]. As the term "self-healing" can be defined in various ways, it is worth specifying that in the current context of corrosion, the term refers to the capacity of a coating system to heal (complete to partial recovery of the coating's main function, which is corrosion protection [89,90]) by releasing corrosion inhibiting species into the area of the defect or damage [90].

Recent interpretations of the formation of chromate conversion coatings (CCC) on the surface of Al alloy suggest to be based on a sol-gel mechanism that involves three steps: hydrolysis, polymerization and condensation of Cr(III) [88,91,92]. Frankel et al. [88] explained that the formation of CCCs begins with the reduction of Cr(VI) to Cr(III) followed by a series of condensation reactions leading to the formation of a Cr(III) oxy-hydroxides polymer chain. The accumulation of high amounts of Cr(VI) on the $Cr(OH)_3$ polymer chain during the polymerization as a result of nucleophile attacks of OH^- ligands, leads to the establishment of covalent Cr(VI)-O-Cr(III) bonds. In this way the Cr(VI) is stored and released when necessary (Fig. 2) [88,91]. In most cases, additional anions (fluorides, phosphates, ferricyanides etc.) are added into the working baths to accelerate the formation of CCCs by preventing the Al surface passivation and promoting a faster reduction of the Cr(VI) to Cr(III) [87].

The formation mechanism of CCC is strongly related with its functionality to provide active corrosion protection. Indeed, the

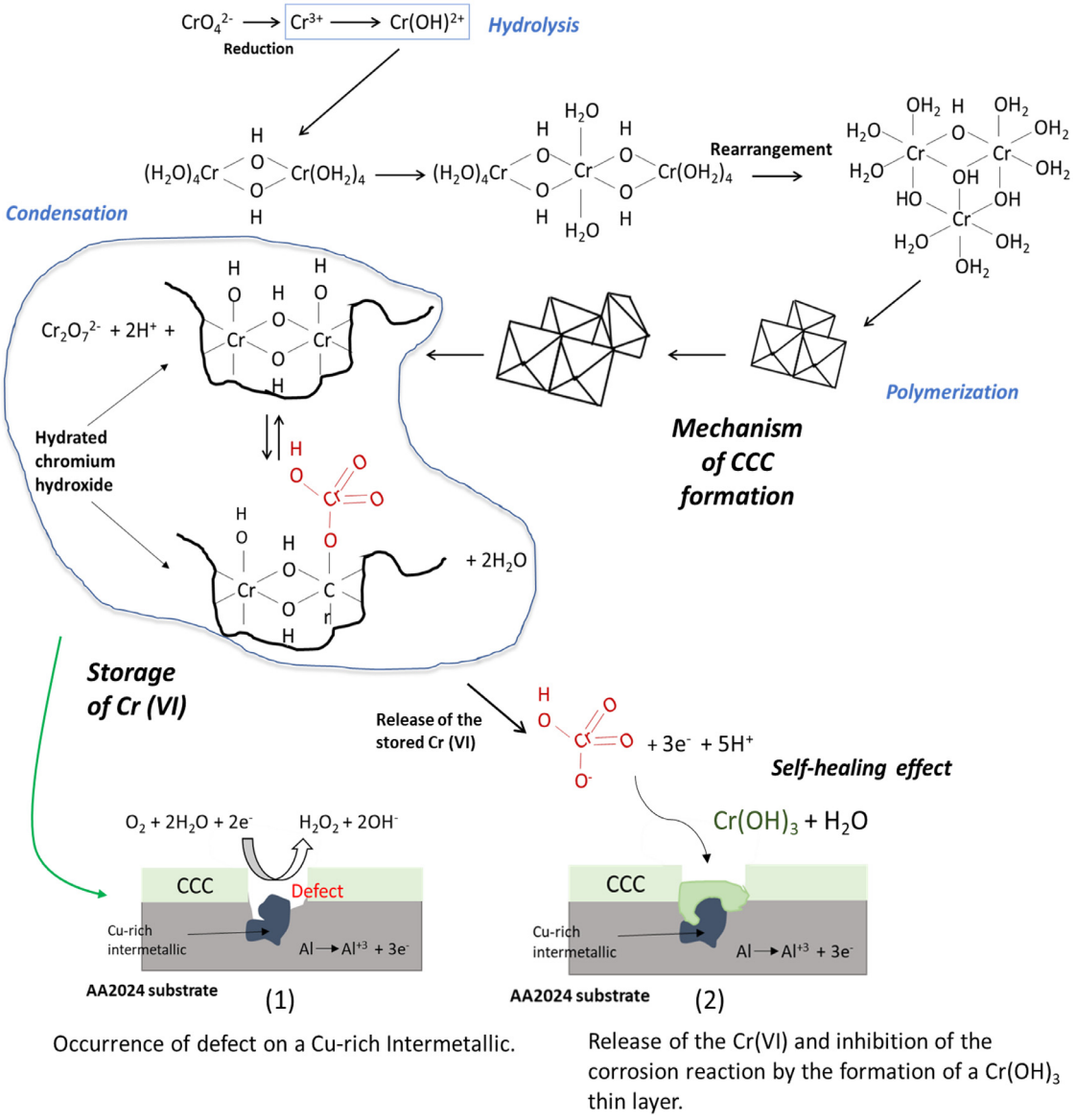

Fig. 2. Scheme representing the mechanism of CCC formation and the storage of Cr(VI) within the Cr(VI)-O-Cr(III) backbones (with permission from [88]), followed by their mechanism of inhibition/self-healing on AA2024 upon mechanical damage [88,93,94].

previously mentioned reaction leading to the formation of the mixed oxides Cr(III) / Cr(VI) is reversible. Hence, upon contact with an aggressive media, the Cr(VI) is released and transported to the affected zones to inhibit any corrosion activity.

A similar operating mode is found for chromates stored in primers or/and topcoats (generally in form of $SrCrO_4$). Cr(VI) are leached in form of CrO_4^{2-} anions into the electrolyte to undergo a corrosion inhibition process. An illustration of the different discussed mode of intervention of Cr-based systems with their different speciation is provided in Fig. 3 [95]. The first mode of action (Fig. 3 a) is associated to the chromate capacity to function in wide range of pH, which in turn makes it a good candidate to be incorporated into different polymer matrices. When incorporated into a primer in form of $SrCrO_4$ (Fig. 3 b) or used directly as a conversion coating CCC (Fig. 3 c), chromates offer a self-healing functionality by the release of CrO_4^{2-} into the surface upon mechanical damage or defect on the coating [95].

The operating principle of Cr(VI) inhibition relies on a complex dual function mechanism. It has the aptitude to impede the rate of cathodic reduction reactions whilst mitigating the anodic metal dissolution (Fig. 2) [92,96]. For instance, in high strength Al alloys, studies reported that the cathodic inhibition involves the reduction of Cr(VI) to Cr(III) which adsorbs on the Cu-rich particles and suppress the oxygen reduction reaction (ORR) [92,97]. The formed layer is irreversible, therefore even after removing chromates from the solution, the ORR stays inhibited [88]. When it comes to anodic inhibition, it is considered more to be a consequence of the cathodic inhibition process rather than actually an independent process. Hurley et al. [92] stated that the inhibition of the oxidation reactions related to the anodic dissolution of Al is a result of a general hindrance of the electron transfer imposed by the formation of a protective Cr (III) monolayer during the above mentioned cathodic inhibition process.

Despite the exceptional corrosion protective properties of chromate-based coatings, their use is highly restricted due to the striking toxicity for humans and the environment [98]. Cr(VI) was first listed as a human carcinogen in 1980 on the annual report published by the National Toxicology Program and the Depart-

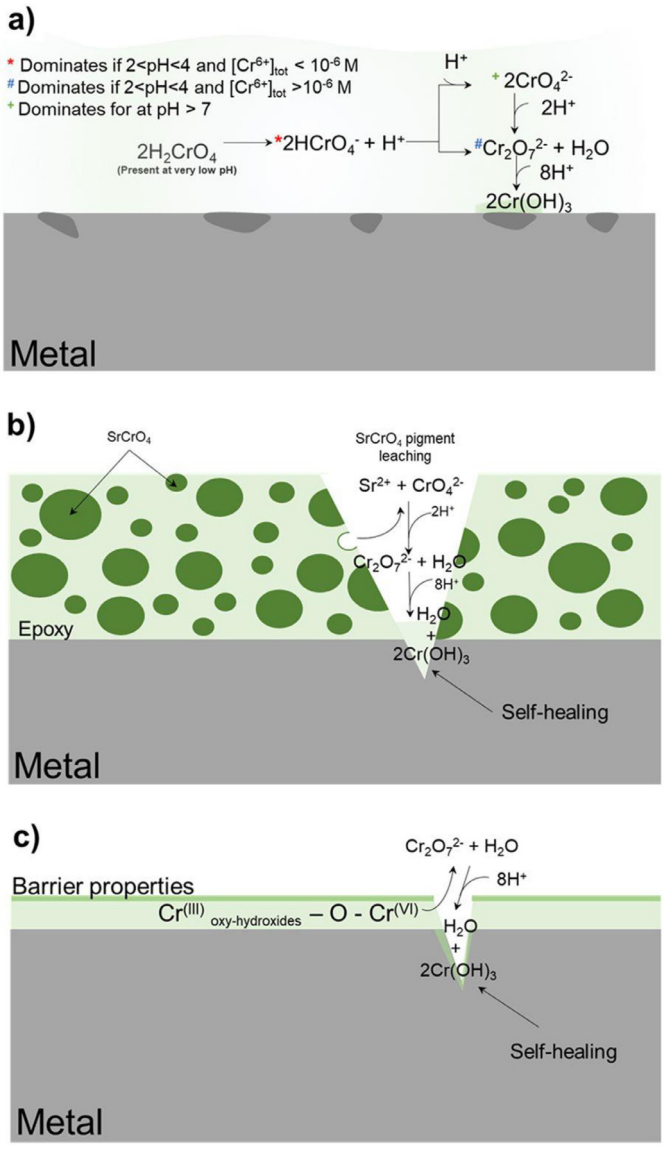

Fig. 3. Schematic illustrations of the different inhibition scenarios associated with Cr(VI) compounds in: (a) aqueous solution, or when a morphological defect occurs (b) in the presence of a Sr–Cr-based primer, or (c) a Cr(VI) conversion coating, with a particular emphasis on the self-healing and barrier properties. (Reprinted with permission from [95])

ment of Health and Human Services (US) [99]. The restrictions for the use of chromate in automotive and aerospace industries were being gradually issued through the following years. On the 21st of September 2017, under the Europe's Registration, Evaluation, Authorization & Restriction of Chemicals (REACH) regulation, chrome-plating chemicals such as sodium dichromate were completely banned. The ban of some other chromate containing compounds such as strontium chromate used in primers followed on January 2019 [73].

However, the replacement of a well-known technologically relevant additive such as chromate, with new alternatives is challenging especially for critical applications.

Therefore, the European Chemicals Agency (ECHA) has extended the sunset date for the use of Cr(VI) plating treatment for aerospace to the year 2024 and a few Cr(VI) additives for paints to the year 2026 [73].

The performance of an alternative is expected to be comparable or even exceed the corrosion resistance of chromate-based systems and should comply with several requirements, some of which are:

- Applicable in a wide range of pH (which makes it possible to be stored in primers and paints).
- Fitting the minimal requirements for concentrations (in aqueous solution the concentration of Cr(VI) is generally between 0.05 to 0.075 M and are found in form of CrO_3 with a concentration of approx. 50 mM in coating formulations [91]).
- Similar or less time for processing steps in comparison to Cr-based processes [100,101].
- Low bath temperatures 60°C > T, ideally room temperature (RT) [100,101].
- Cost-effective and more importantly ecologically acceptable [95].
- Suitable for all relevant Al alloys [100].

Over the course of many years, a large number of studies devoted to potential alternatives for chromates have been developed and a number of reviews [95,102,103] summarizing these alternatives were written. A list of a few examples of the most discussed alternatives that were applied to Al alloys is provided in the next section.

2.2. Alternatives to Cr (VI)-based coatings

Since the ban of Cr(VI)-based coatings, an important number of possible alternatives were proposed and some are already available commercially. In the following sections some examples are described and a summary is presented in Table 1.

2.2.1. Trivalent chromium

Following the ban of Cr(VI), many studies focused on the use of Cr(III), considering it as the "second-best" option [104]. Trivalent chromium pre-treatments are commonly available as zirconium/trivalent chromium-based conversion coatings (TCC). The formation of the latter conversion coating takes place in an acidic bath (pH 3.8-4) generally containing trivalent chromium, zirconate, fluoride and sulfate salts. The mechanism of formation relies on a co-precipitation of hydrated zirconia and $Cr(OH)_3$ initiated by an increase of pH at the active cathodic sites (e.g. Cu-rich intermetallic in the case of AA2024) [105].

Qi et al. [105] performed a deeper investigation on the composition of the Cr(III)-CC and its influence on the mechanism of corrosion protection of Al alloys. The authors found that the coating is composed of two layers: the thick outer layer consists of compounds such as AlF_3 $Cr(OH)_3$, ZrO_2 and ZrF_4 (depending on the starting species on the bath) and the inner layer is mostly aluminium-rich and is responsible for providing the main corrosion protection which is mostly barrier-based.

Although, no Cr(VI) is used for the TCC growth process, some concerns were raised due to the high possibility of Cr(III) oxidizing to Cr(VI) [105–107]. For instance, using Raman microprobe spectroscopy method, Li et al. [107] revealed the presence of Cr(VI) oxide species formed via oxidation of Cr (III) in the presence of hydrogen peroxide. The authors linked the production of hydrogen peroxide to the local reduction of dissolved oxygen at the Cu-rich intermetallic. Qi et al. [108] also detected Cr(VI) species in an air-aged coating after exposure to a corrosive electrolyte (NaCl) and it was associated to corrosion processes. However, Cr(III)-based treatments are still being extensively employed in industry [95,109,110], as the estimated amount of Cr(VI) found is minimal (< 0.1 wt. % which complies with to REACH regulations [111]),therefore presenting no risk. Moreover, the toxicological data published in the last few years do not allege any high risk to human health or the environment related to Cr(III). Nevertheless, some uncertainties are

Table 1
Summary of possible alternatives to Cr(VI)- based coatings discussed in this section.

Coat. system	Al substrate	Most Common process and parameters of formation					Characteristics	Ref.
		Method	Temp.*	pH	Time	Acc.*		
Cr (III)-based	AA7075-T6, AA6063, AA5052, AA2024	Coprecipitation of $Cr(OH)_3$ and hydrated zirconia.	RT, 40°C	2-3.9	5 - 9 min	NaF, Na_2SiF_6, or Na_2ZrF	- Barrier protection, no self-healing effect due to the absence of active species such as Cr(VI) - Possible oxidation of Cr(III) to Cr(VI)	[102,104–108, 175-180]
Phosphate-based	AA6061, AA6063, AA5754, AA2024	Precipitation/deposition of insoluble tertiary phosphates.	40°C, 60°C	3-4	3 min	$NaNO_3$, $NaNO_2$, $Zn(ClO_3)_2$ or H_2O_2	- Barrier protection, no self-healing effect. - Risk of disbonding - limited pH stability. - Environmental impact of the waste related to the process bath	[112–115,118,119,181–184]
REMS-based (when used as CC)	AA7075-T6, AA6061, AA5083, AA2618, AA2024	Precipitation of $Ce(OH)_3$	25°C, 90°C,	1.9 -2.2	5-20 min	H_2O_2	- Slow mechanism of inhibition especially to ORR - Highly costly and not easily accessible in the market.	[101,121,136,139,154,185–192]
Zr/Ti-based	AA7075, AA6060, AA6061, AA2024, AA1050	Deposition of Zr/Ti oxides	20 -25°C	2.5 -4.5	3-6 min	NaF, KF, HF	- Barrier protection, no self-healing effect	[157,193,194]

*Temp. and *acc. are short for temperature and accelerators, respectively

still persistent and the non-self-healing aspect of the Cr(III)- systems could be a disadvantage when competing with other proposed alternatives to chromate.

2.2.2. Phosphates

Phosphate treatments were originally based on a mixture of chromate/phosphate conversion coatings that were known for their outstanding corrosion resistance and adhesion properties. Due to its banning, chromate was replaced by zinc, and the resulting zinc/phosphate coatings continued to be applied widely on steel [103,112] and were further extended to Al alloys [113–117].

For the phosphating process, an acidic bath typically composed of phosphoric acid, zinc dihydrogen phosphate, fluoride and an oxidation accelerator (e.g. NO_2) is used [103,112].

Akhtar et al. [113,114] showed that the phosphating process on Al alloys is a two-step process which starts at the active sites by the dissolution of Al (1) and an increase of the local pH (2). This increase of pH will lead to a shift in the hydrolytic equilibrium between the soluble primary phosphates and the insoluble tertiary phosphates of the heavy metals, driving into the systematic conversion and deposition of the latter species and the generation of the phosphate coating (3) and (4) [113,114]:

$$Al \rightarrow Al^{3+} + 3e^- \quad (1)$$

$$2H^+ + 2e^- \rightarrow H_2 \quad (2)$$

$$H_3PO_4 \leftrightarrow H^+ + H_2PO_4^- \leftrightarrow 2H^+ + HPO_4^{2-} \leftrightarrow 3H^+ + PO_4^{3-} \quad (3)$$

$$3Zn^{2+} + 2PO_4^{3-} \rightarrow Zn_3(PO_4)_2 \downarrow \quad (4)$$

The final obtained $Zn_3(PO_4)_2$ coating is reported to be reasonably hard, electrically non-conductive, adherent and with a good wear and corrosion resistance [112]. However, some studies have revealed a number of cons to the use of phosphate-based conversion coatings. Phosphate coatings generally present limited stability at higher pH and their destruction may lead to disbonding issues, if used under a polymer layer [118,119]. More critical, the waste resulting from the phosphating process is considered hazardous by the European Union as well as the US environmental protection agency. The phosphate coating sludges contain an important amount of heavy metals which makes the disposal of the phosphating baths detrimental [120]. With the presented evidence and the fact that phosphate coatings can offer only a barrier protection, phosphating may no longer be viable as an alternative to Cr(VI) based coatings.

2.2.3. Rare earth-based coatings

The first use of rare earth metal salts (REMS) for the corrosion protection of aluminum alloys dates back to the works of Hinton et al. [121–125], where an inhibition effect on aluminum alloys was observed with cerium. After that, other REMS compounds such as lanthanum [126–130] and praseodymium [129,131–134] salts were investigated for the same purpose. However, cerium salts were the ones that attracted most attention [101,102,121,135–137]. Cerium salts were implemented in various ways, for example as conversion coatings [121,135,138,139], incorporated into polymer coatings either directly as corrosion inhibitors (e.g. cerium nitrate) [140–145] or, in form of encapsulated pigments (e.g. silica and chitosan loaded with cerium) [141,146]. In addition, cerium can also serve as a sealing post-treatment for anodized Al alloys [147–149].

It was suggested that the inhibition mechanism of cerium salts is a localized process that interferes with the corrosion reactions occurring around the intermetallic (IMC). In an investigation performed by Yasakau et al. [130], it was shown that an increase of the local pH due to the cathodic process at the interface of

AA2024, leads to the formation of cerium hydroxo-complexes. This continuous increase of pH until approx. 10 resulted in the formation of cerium hydroxide deposits on top of the S-phase IMCs, thus obstructing both the cathodic and anodic processes on the IMCs [130]. It was also pointed out that the advantage of cerium relies on its aptitude to be oxidized from Ce(III) to Ce(IV) and form insoluble hydroxides. This oxidation reaction is generally driven by the hydrogen peroxide generated from the cathodic ORR Eq. (5)) [130,150,151] and can be illustrated by the Eqs. (6)–((8) [130,151]:

$$O_2 + 2H_2O + 2e^- \rightarrow H_2O_2 + 2OH^- \quad (5)$$

$$Ce^{3+} + \frac{1}{2}H_2O_2 + 3OH^- \rightarrow Ce(OH)_4\ (CeO_2 \cdot 2H_2O) \downarrow \quad (6)$$

$$Ce(OH)^{2+} + \frac{1}{2}H_2O_2 + 2OH^- \rightarrow Ce(OH)_4\ (CeO_2 \cdot 2H_2O) \downarrow \quad (7)$$

$$Ce(OH)_2^{+} + \frac{1}{2}H_2O_2 + OH^- \rightarrow Ce(OH)_4\ (CeO_2 \cdot 2H_2O) \downarrow \quad (8)$$

This mode of operating of cerium salts resembles that of chromates, which could make them possible alternatives for chromate-based conversion coatings. However, the efficiency of cerium inhibition at lower pH has been questioned more than once [152,153]. Moreover, the fact remains that the price of REMS is high. The reason behind the high cost of REMS is not much related to their abundance on earth but more to the production process and their availability in the market [154,155]. Despite being relatively abundant on earth's crust (e.g. Ce is present at similar amounts as Cu but twice less than Cr), the REMS market is mainly controlled by the Chinese state-owned industries with production levels close to 85% (in 2015) of the world's supply and the imposition of strong restrictions (e.g. export quotas, taxes, prices, etc.), especially between the years 2008 and 2014 [154,156].

One other factor that may make the access to REMS difficult for corrosion protection purposed, is the high demands of other competing technologies that would also require considerable amounts of these elements [154]. All these listed factors make the industrial application of cerium or REMS for the sake of corrosion protection highly uncertain.

2.2.4. Zr/Ti based coatings

Zirconium and/or titanium-based conversion (Zr/TiCC) coatings have been receiving an increasing interest since their introduction as potential replacement for chromates and phosphates in the late 20th century [157]. Ever since, the technology has significantly progressed and is proposed in various commercially available product trademarks [157,158]. Although the main application of these Zr/TiCCs are used for the automotive bodies composed of the 5xxx [159,160] and 6xxx [161–164] series of Al alloys [165], they are also highly suited for other Al alloys such as AA2024 used in the aerospace industry [88,102,166,167].

Many studies were devoted to the understanding of the formation mechanism of Zr/TiCCs and the influence of the Al alloy composition on it [161,163,164,166,168]. In a recent review by Milošev et al. [157], the authors divided the formation of Zr/TiCC on Al alloys into different stages. The first stage is the dissolution of the Al native oxide layer activated by the presence of aggressive hexafluorometallate complexes (e.g. H_2ZrF_6, Na_2ZrF_6, H_2TiF_6, etc.), in the bath at low pH (2.8 to 4). This is then followed by the formation of hexafluoroaluminate compounds according to Eqs. (9) and (10). The second stage involves the precipitation of the of Zr/Ti metal oxide layers driven by the increase of the local pH (to approx. 8.5) initiated at the cathodic sites (see Eqs. (11) to (14)) [157].

Stage I:

$$Al^{3+} + ZrF_6^{2-} \rightarrow AlF_6^{3-} + Zr^{4+} \quad (9)$$

$$Al^{3+} + TiF_6^{2-} \rightarrow AlF_6^{3-} + Ti^{4+} \quad (10)$$

Stage II:

$$ZrF_6^{2-} + 4OH^- \rightarrow 6F^- + ZrO_2 \cdot 2H_2O \downarrow \quad (11)$$

$$TiF_6^{2-} + 4OH^- \rightarrow 6F^- + TiO_2 \cdot 2H_2O \downarrow \quad (12)$$

$$Zr^{4+} + 3H_2O \rightarrow ZrO_2 \cdot 2H_2O + 4H^+ \quad (13)$$

$$Ti^{4+} + 3H_2O \rightarrow TiO_2 \cdot 2H_2O + 4H^+ \quad (14)$$

Besides their good corrosion resistance and remarkable adhesion performance to the metallic substrate, the use of Zr/TiCCs is energy and cost-effective as the formation process requires less time and lower temperatures in comparison to other conversion coatings [157]. Moreover, less sludge is induced from the preparation bath (low concentration of ionic species) and the involved compounds during the whole operation are classified as non-carcinogenic and non-eutrophic [169].

Although the list of advantages in regard to Zr/TiCCs is quite relevant, there is still a large room for improvement, starting from the fact that these coatings are not self-healing but only barrier protective [157] and second, the Zr/Ti layer tends to be inhomogeneous [157]. One way to enhance the performance of the Zr/TiCCs is by the addition of inhibitors in form of inorganic and/or organic pigments. For the case of self-healing implementation, several studies have been published on the possibility of adding corrosion inhibitive agents such as vanadate [170], cerium [171] and trivalent chromate [172] into the Zr/Ti formation bath for the corrosion protection of Al alloys. Similarly, a combination of additives such as poly-(4-vinylphenol and $Mn_3(PO_4)_2$ have shown to favorize a homogeneous formation of the Zr/Ti-CC, when added into the reaction bath [173,174]. Both methods presented significant potential in improving the Zr/Ti- CC.

2.3. Alternative pigments in coatings

The list of potential substitutes to chromates does not end with the few examples mentioned in the previous sections, since when referring to an efficient corrosion protective system for Al alloys or any other metal alloy for that matter, there is no constraint on the chemistries or the nature of the system to be exploited. The only requirement is for the technology to be so-called green and REACH conform.

One can think of a multi-level protective system that can comprise both barrier and active corrosion protection functionalities.

Organic coating systems confer corrosion protection by acting as a barrier and preventing the mass transport of aggressive elements such as water and chloride into the metal surface [195]. However, this protection can easily be compromised upon mechanical damage or defects. Moreover, some organic coatings are very often prone to degradation due to their permeability to air and moisture. These issues were previously countered by the presence of active chromate pigments (e.g. $SrCrO_4$) in the coating formulation. Since their ban, few other technologies have been highlighted to optimize the anti-corrosion properties of the organic coating, when applied to Al alloy. The most common pathway is the direct addition of corrosion inhibitors into the coating formulation. A few examples of direct addition of corrosion inhibitors in coating formulation used in Al alloy are given in Table 2.

In addition to corrosion inhibitors, sacrificial metal pigments such as Mg, can also be added into primers to impart cathodic protection to the underlying Al alloy [207–210]. Mg having a more negative potential than the Al substrate will lead to the cathodic

Table 2
Example of corrosion inhibitors incorporated directly into organic coatings for the corrosion protection of Al alloys.

Corrosion inhibitor	Al substrate	Coating	Ref.
Cerium	AA2024-T3	sol-gel and Epoxy	[196–200]
Lanthanum	AA2024	Sol-gel	[201]
Molybdate	AA2017	Sol-gel	[199]
Permanganate	AA2017	Sol-gel	[199]
Sr-Al-polyphosphate	AA2024	sol-gel	[202]
Benzotriazole	AA2024, AA2024-T3 and AA7075	sol-gel	[198,202–205]
8-hydroxyquinoline	AA2024	sol-gel	[198]
Tolyltriazole	AA2024-T3	sol-gel	[197]
Chloranil (tetrachloro- p -benzoquinone)	AA2017	sol-gel	[206]

Table 3
Summary of the most common delivery systems applied to corrosion protection

Delivery system	Chemical nature	Type of exchanger	Ref.
Silica	Modified	Neutral	[216–222]
Polymer capsules	Various	Neutral	[223–226]
Halloysite	Aluminosilicate minerals	Cationic	[74,222,227–229]
Titania	Titanium oxide	Neutral	[76,230,231]
Zeolite	Aluminosilicate minerals	Cationic	[19,232–234]
Bentonite	Montmorillonite	Cationic	[78,235–238]
Layered double hydroxides (LDH)	Mixed oxides/hydroxides	Anionic	[34,35,145,236,239]

polarization of the latter and the dissolution of the Mg particulates. A study also showed the formation of a porous barrier Mg oxide layer on the Al substrate [207].

It is important to stress out that the addition of corrosion inhibitors and sacrificial metal pigments are just two methods among various others. The content of this section was restricted to these particular two types of pigments since they are more relevant to the current review.

Despite the promising results achieved with the addition of corrosion inhibitors or/and sacrificial particles into the organic coatings, these methodologies present a few disadvantages and need to be re-evaluated. For instance, in the corrosive media, a corrosion inhibitor to be incorporated needs to be have the right degree of solubility. A low solubility leads to insufficient self-healing properties whereas a high solubility results in a fast leaching of the inhibitor compromising the long-term active corrosion protection, along with a degradation of the coating due to possible delamination and blistering (caused by an increase of the osmotic pressure within the coating) [89]. The last effect was for example observed on Mg-rich primers applied on AA2024-T3 [211,212]. Moreover, the chemical nature of the corrosion inhibitor may also lead to its interaction with the polymer coating which will induce a loss of the inhibition property and degradation of the coating. The inhibition property of the corrosion inhibitor can also be lost due to its sensitivity to environmental factors. As a matter of fact, organic corrosion inhibitors such as 2-mercaptobenzothiazole and 1,2,3-benzotriazole that were reported to inhibit corrosion activities on Al alloys, are subject to photodegradation [213].This means that the direct incorporation of these inhibitors in a polymer coating may not provide the active corrosion performance that is needed.

Nevertheless, significant progress has been made to avoid some of the above-mentioned drawbacks. One key solution is to encapsulate the active agent using LDH nanocontainers, as it will be explained in the next section.

2.4. A nanocontainer based strategy

To avoid the direct incorporation of corrosion inhibitors into coatings and the limitations that can come by doing so, specific micro/nano delivery systems were designed and synthesized to host active agents such as corrosion inhibitors [77,89,90,214,215]. A wide variety of encapsulation approaches has been proposed in the past few years and were used for isolating/protecting the incorporating agents from the polymer resin, store the corrosion inhibitors and release them on demand when triggered by changes on the metal interface or upon mechanical damage. Some of these nanocontainer-based strategies were originally derived from other fields such as the food and pharmaceutical industry. A brief list of the most reported nanocontainer based strategies for corrosion protection, are given in Table 3.

Three types of nanocontainers can be distinguished, according to the charge of the guest ions; the cationic exchangers, the anionic exchangers and neutral nanocontainers. Several triggering mechanisms can lead to the activation of these nanocontainers and the release of the intercalated inhibitor, namely: pH perturbations, presence of specific ions, change of the redox potential, mechanical rupture etc.

For instance, the cation-exchangers (e.g. zeolites and bentonites) may release the inhibitors in the presence of other cations in the interface (metal cations in the case of corrosion processes) [215]. For anion-exchangers (e.g. LDH), the aim is more directed to the capture of corrosive agents such as chlorides or sulfates followed by the release of the inhibitors. Finally, neutral nanocontainers rely on a desorption process and can have the advantage of hosting both anionic and cationic inhibitors.

The reason behind the choice of selecting LDH for this review, to the detriment of other nanocontainers can be explained by the following points; i) LDH have the remarkable option to be used both in form of anticorrosion pigments incorporated into a coating system [77], as well as a conversion coating on the metal [48,84]. This means that it can be easily adapted according to different requirements. On one hand, LDH can be used as a powder/slurry if the wish is to confer additional active protection properties to a barrier coating by the addition of a self-healing functionality [15,18,55,89]. On the other hand, LDH can be applied directly to the metal surface as a conversion coating if there is a need for the first defensive layer (close to the metal) to be an active corrosion protective system [48,79,240]. ii) LDHs are among

the most investigated and with more application potential anion-exchange nanocontainers for “smart” active corrosion protection [9,13,18,48,81,84,241–249].

In the course of this review, we will be going through these two manners of using LDH and examine the latest progress in this area for the protection of aluminum alloys.

3. LDH in form of pigments

3.1. Synthesis of LDH pigments

The availability of LDH in their natural form is limited, but their preparation can be easily achieved in both laboratory and industrial scales at a moderate cost. Depending on the application, several methods were reported for the formation of LDH powders relying mostly on soft chemistry (*chimie douce*) reactions [2,45,250]. Some of these methods are; synthesis by co-precipitation, sol-gel method using alkoxides and/or acetylacetonate as starting precursors [39,251,252], urea hydrolysis method [253–256], hydrothermal method [257,258], reformation [259] and mechanical milling [260–262]. Since the co-precipitation method is the most straightforward and commonly applied “one-pot” method, it will be given more attention in this review.

Typically, the synthesis by co-precipitation can be achieved at either variable pH (titration co-precipitation) or constant pH conditions. The latter option is preferable to obtain pure, crystalline LDHs. During the reaction, the pH of the solution is kept constant by the simultaneous addition of an alkaline solution (e.g. NaOH or $NH_3 \bullet H_2O$) together with the precursor solution of mixed metal salts (metals that will be part of the LDH). Usually, an alkaline solution is chosen according to the corresponding metal salts and the desired anion to be intercalated between the LDH galleries. Additionally, since it is difficult to avoid the presence of CO_2 in air, it is further advised to work under nitrogen or argon flow to avoid the formation of LDH intercalated with carbonates, if these are not desirable. The following equations were proposed as an example for the formation of ZnAl LDH pigment by co-precipitation method [263]:

$$Zn(OH)_2 + 2NaOH \rightarrow Na_2\ ZnO_2 + H_2O \quad (15)$$

$$Al(OH)_3 + NaOH \rightarrow NaAlO_2 + 2H_2 \quad (16)$$

$$AlO_2^- + ZnO_2^- + NO_3^- + H_2O \rightarrow \left[Zn_{1-x}^{2+}Al_x^{3+}(OH)_2\right]^{x+}(NO_3^-)_X \cdot yH_2O \quad (17)$$

The LDH product of the synthesis by co-precipitation Eqs. (15) to ((17)) relies upon a crucial control of the pH of the reaction medium, the concentration and nature of both alkaline and metal precursor solutions (besides the molar ratio of the metal cation itself), the temperature and aging time.

However, despite the above precautions, it remains very challenging to avoid the segregation of unwanted products (eg. oxide/hydroxide mixtures) [264] during the precipitation reaction, and this is mostly due to supersaturation and local increase of the pH. Therefore, it is advised to find a compromise between the different preparation conditions (see Fig. 4 a).

For instance, as a solution to the local pH increase, urea can be used to favor a homogeneous precipitation at a controlled pH [255,256,265]. This method leads to the formation of LDH with a high degree of crystallinity and larger flakes but with a narrower particle size distribution [255]. However, depending on the temperature, the urea procedure relies on a continuous release of ammonia and carbonate, generally yielding to the formation of carbonate-intercalated LDH [256].

The above-mentioned modification of the synthesis bath, can intervene both in the nucleation and growth steps of the LDH. The conventional synthesis methods may help further optimize the LDH growth, but in most cases, they require a long synthesis time, high temperatures or pressure to obtain a pure-phased, well crystallized LDH that has a homogeneous oriented layer and a high specific area. Therefore, several assisted or/and post-synthesis treatment routes have been introduced for tuning the structural and textural properties of LDH powders, during the phase of growth (e.g. good dispersion and uniform distribution of the LDH particles), with the additional benefit of a reduced time and preconditioning (Fig. 4 b). LDH synthesis using MWs (microwaves) allows to obtain an enhanced crystallinity together with considerable reduction of synthesis time [41,266–268]. This is achieved due to a well volumetrically distributed heating, which helps reduce thermal gradients. Indeed, in a study by Benito et al. [266], SEM (scanning electron microscopy) micrographs of Mg-Al LDH have shown well-defined and very uniformly sized hexagonal platelets (Fig. 5 b) in comparison with the Mg-Al LDH synthesized under constant pH conditions without microwaves treatment (Fig. 5 a).

In addition to MWs treatment, *ultrasound irradiation treatment* was also applied to achieve a rapid synthesis and improve the crystallinity of the LDH phases. Compared to the traditional stirring, ultrasonic treatment allows a better dispersion of particles in solution. In this way, the reaction time is shortened and a more uniform LDH size distribution is obtained (Fig. 5 c and d) [31,269–272].

3.2. LDH pigment anionic exchange for corrosion protection

Various pathways have been disclosed in order to obtain LDH pigments intercalated with the desired guest anion between the interlayers. Among the methods for intercalation/immobilization of the species in LDH, the most common ones are: (1) the direct intercalation during the synthesis by co-precipitation, as long as the precursors and the reaction medium contain the guest (and not contaminated by the presence of other anions susceptible to be intercalated) [83], (2) the post ion-exchange reaction where the already formed LDH powder is immersed into a solution medium containing the salts of the desired guest anion and an anion-exchange reaction takes place [12,273], and (3) the calcination-reconstruction procedure based on a so-called “memory effect”. During heat treatment of the parent LDH (450°C $\geq$ T), the interlayer water molecules are evaporated followed by a dihydroxylation coupled to transition metal oxide crystallization and the decomposition of the intercalated anions [274,275]. The mixed oxides can be brought into contact with an aqueous solution containing the anion to be intercalated; afterwards the LDH containing the desired anion can be reconstructed [276]. However, a prerequisite of this method is that the anion initially intercalated between the layers must be volatile and should decompose completely without forming any mixed compounds with the matrix cations [276].

In the area of corrosion protection, most authors use the second method of post-synthesis treatment by anion-exchange reaction to obtain LDH with the aimed intercalated species.

The anionic exchange in LDH depends on several factors such as the electrostatic and H-bonding interactions between the mixed-metal hydroxide layers and the exchanging anions [277]. Nevertheless, similarly to the synthesis process of LDH, there are different factors that must be taken into account to promote a successful anion-exchange reaction. Amongst these factors is the affinity of the anion. Miyata et al. [278] claimed that the equilibrium constant for the exchange reactions increases when the radius of the bare anion decreases. The smaller the radius and the higher the charge densities of the anions, the more favorable is the exchange. Based on the calculation of various exchange reaction’s equilibrium

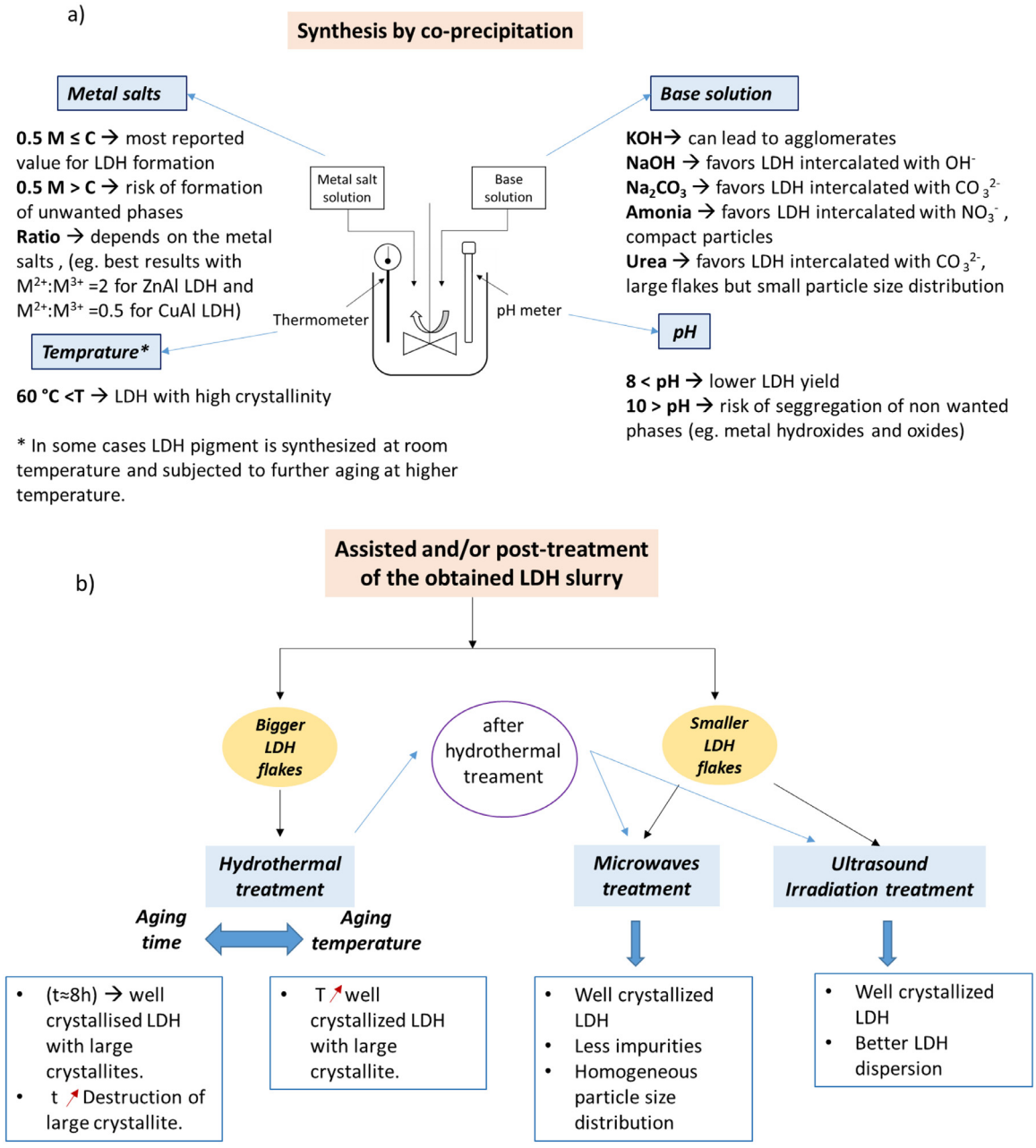

Fig. 4. Scheme summarizing the influence (a) of the different parameters during the synthesis of LDH pigments and (b) methods that can be additionally used during the synthesis and/or after as a post-treatment.

constant, an order of affinity of LDH to monovalent anions was established as following [279,280]:

$OH^- > F^- > Cl^- > Br^- > NO_3^- > I^-$

And for divalent anions as:

$CO_3^{2-} > C_{10}H_4N_2O_8S^{2-} > SO_4^{2-}$

Accordingly, since NO_3^- anion has a relatively low affinity, it can be easily replaced by other anions. Therefore, nitrate-containing LDHs are commonly used as parent compounds for subsequent intercalations (e.g. with corrosion inhibitors).

Despite the above assertions, it remains possible for low-charge and large anions (including organic species) to be intercalated. Indeed, other parameters involved in the anion-exchange reactions can be manipulated to facilitate the insertion of different anions. As a matter of fact, it was shown that some solvents such as methanol [281] and glycerol [282] can enlarge the space between the LDH interlayers allowing bigger species to be hosted [281,282].

Hibino [283] also highlighted the importance of the parent LDH crystallinity and the ratio of the metal cations of the LDH hydroxide layers, on the anion exchange selectivity. Choosing MgAl LDH as a model system, the following trends were established for a well-crystallized MgAl LDH: the higher is the Mg/Al molar ratio, the higher is the selectivity towards NO_3^- whereas the selectivity towards SO_4^{2-} and F^- is lower. The selectivity toward the different anions is less apparent for low-crystallinity LDHs [283].

It should be pointed out that from a kinetic point of view, the anion exchange reaction is still subject to controversy. Next to the early studies by Miyata et al. [278,279] and Costa et al. [280], several investigations were carried out to understand the mechanism and kinetics involved during the LDH anion exchange reaction es-

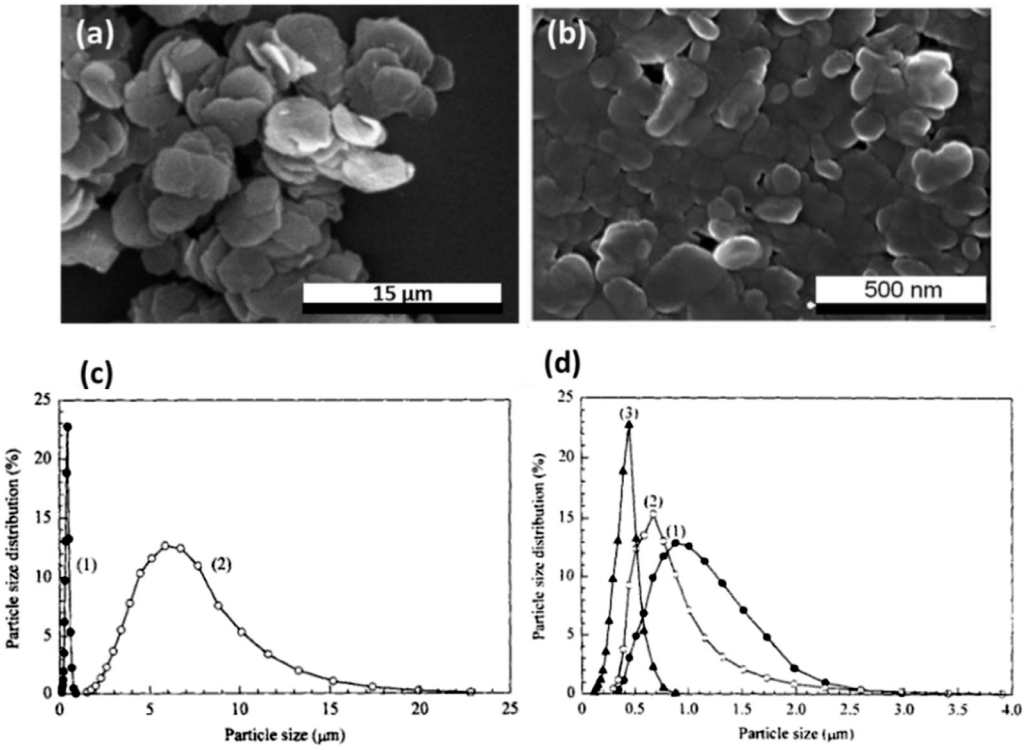

Fig. 5. SEM images of the Mg-Al LDH synthesized with (a) and without (b) microwave treatment (Reprinted with permission from [266] and [50]); particle size distribution of Zn-Al LDH modified with stirring methods (1) and ultrasonic crystallization (2), and (c) as function of different ultrasonic powers (1) 88 W, (2) 175 W, (3) 250 W (d). (Reprinted with permission from [31]).

pecially for bigger species. Meyn et al. [284] investigated the kinetics of the anion exchange reaction of five LDHs; ZnCr, ZnAl, MgAl, CaAl and LiAl LDHs, with several long chain organic species (carboxylic acid anions, arenesulfonates, secondary alkanesulfonates, alkynebenzensulfonates and ether sulfates). The parent LDHs were synthesized by co-precipitation and intercalated with nitrate. The anion-exchange was carried out by the immersion of the parent LDH into a solution containing the organic species to be intercalated. On one hand, it was found that the LDH is highly reactive to most organic anions characterized by a fast kinetic and a high exchange rate (80-100 %). Moreover, the rate and degree of reaction is generally independent of the chain length of the anion to be exchanged. On the other hand, the investigation showed that due to the small equivalent area of the LDH, the alkyl chain compounds (fatty acid anions, dicarboxylates, alkyl sulfates) are pushed to point away from the interlamellar surfaces and to form monomolecular films of high regularity [284]. Secondary alkanesulfonates and other specific anionic surfactants (mixtures of isomers and of compounds with different chain lengths) form well-ordered bimolecular films of constant thickness, between the LDH interlayers [284].

The mechanism of anion exchange of LDH with inorganic and/or organic species is of particular interest in the field of corrosion protection since it is a determinant factor to whether this novel technology can compete with formal Cr(VI)-based coatings. Indeed, the aptitude of LDH to host actives species such as corrosion inhibitors and promote self-healing/active corrosion protection, is the main reason for it to be considered as a suitable alternative. Therefore, several studies have been devoted to understanding mechanisms of ion-exchange of corrosion inhibitors [49,50,283,285]. For instance, Serdechnova et al. [50], has investigated the anion exchange reaction of ZnAl-NO_3 and MgAl-NO_3 LDHs with two known corrosion inhibitors 2-mercaptobenzothiazole (MBT) and 1,2,3-benzotriazole (BTA). Using X-ray diffraction (XRD) as the main investigation tool, it was demonstrated that MBT can be easily exchanged and intercalated between the ZnAl LDH and MgAl LDH layers whereas BTA can only be intercalated within the MgAl LDH galleries. The anion-exchange reaction of NO_3^- with MBT/BTA was determined to be fast, without formation of intermediate phases and more interestingly with a rearrangement step where both organic species adopt a herringbone-like arrangement [50].

Altogether, the intercalation of smaller and bigger corrosion inhibitors into LDH has proven to be very attainable. Recent works involving the corrosion protection of aluminum alloys reported the LDH intercalation with different inorganic inhibitors such as nitrate [48,264], vanadate [286,287] and phosphate [16] as well as organic inhibitors such as MBT [50,288], quinaldic acid (QA) and BTA [34,236], which were effective for AA2024 and other Al alloys (An overview list of the intercalated inhibitors into LDH will be provided in the next section). For the cited organic inhibitors, a prior deprotonation in NaOH was performed to convert the molecules into salts, so that they can be intercalated in the anionic form within the LDH galleries [50].

3.3. Application of LDH pigments for corrosion protection

The use of LDH as functional additives in an effort to implement self-healing/active attributes in a multi-level corrosion protection system was addressed in several works [10,12,13,15,34,83,85,289,290]. In this particular case, a multi-level protective system refers to the combination of one or several corrosion preventive and/or protective mechanisms into one system [290] (Fig. 6). It is possible to integrate these different functions into one coating systems (e.g. polymer) or distribute them within a frame composed of several layers of coatings. The last approach is generally what is used in industries such as the automotive [165,291].

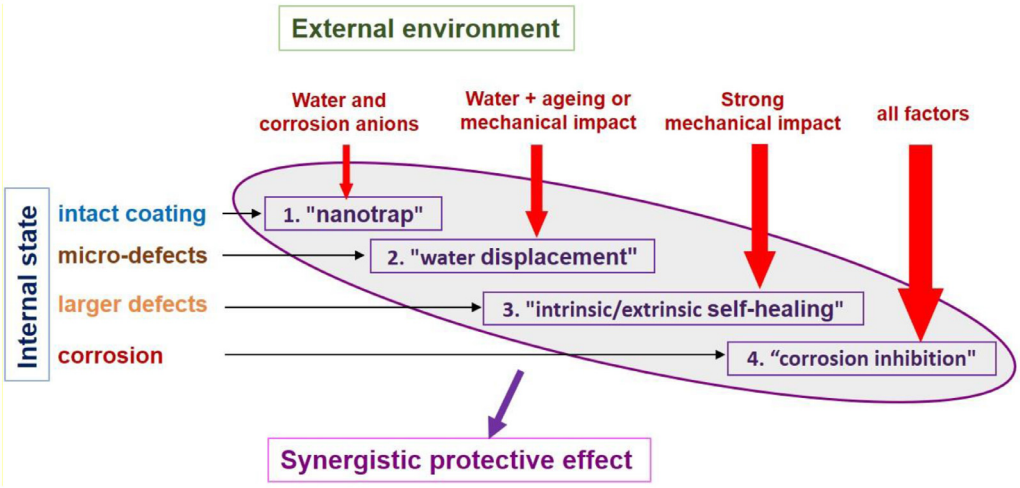

Fig. 6. Illustration of the multi-level protection approach (modified with permission from [90])

Relevant features to the mechanism of active corrosion protection as well as the durability of the hosting coating matrix were highlighted, some of which are:

- Efficient encapsulation of corrosion inhibitors, avoiding their direct contact with the coating's matrix, hence preventing both an unwanted deactivation and/or depletion of the inhibitor and the degradation of the coating [15,292].
- Triggered response to an external (e.g. scratch, mechanical damage) or internal stimuli (e.g. local change of pH) and release of the corrosion inhibitors. This also implies a controlled release over an extended period of time and/or a progressive release of the active agent into the affected area.

Buchheit et al. were the first to put forward a concept based on LDH as anticorrosion pigments in protective coatings. In a pioneering work published in 2003, Buchheit et al. [83] prepared ZnAl LDHs (referred to hydrotalcites) by co-precipitation of $ZnCl_2$ and $AlCl_3.6H_2O$ precursors in a solution containing vanadate as the corrosion inhibitor in its decavanadate form ($V_{10}O_{28}^{6-}$). The XRD patterns obtained for LDHs intercalated with decavanadates and chlorides are shown in Fig. 7 a. Accordingly, the layered structure of LDH is characterized by the reflections appearing at lower 2θ values (between 10° to 35°) whereas the larger 2θ values are associated to the structure within the mixed metal hydroxide layer in the compound (Fig. 7 b). Therefore, during anion exchange reaction, a displacement of typical (*003l*) reflections (l =1, 2, 3) can be observed. The anion exchange reaction of vanadate with chlorides within the LDH intergalleries will lead to the contraction of the latter and the formation of smaller crystallites of LDH-Cl. This phenomenon can be identified by the shift of the LDH containing vanadate reflections (003, 006 and 009) into lower angles (Fig. 7).

The corrosion protection provided by vanadate-containing LDHs to aluminum alloy 2024-T3 was evaluated by incorporating the LDH particles (3 wt. %) into a polyvinyl alcohol-based coating (PVA) [83]. Both salt spray tests (SST) as well as electrochemical impedance spectroscopy (EIS) revealed significant improvement of corrosion behavior for AA2024-T3 plates coated with LDH-loaded coatings. Mahajanam et al. [32] demonstrated a few years later that in addition to decavanadate, Zn^{2+} leached from the LDH structure upon mechanical damage can also contribute to the protection of AA2024-T3. This conclusion was made after the analysis of cathodic polarization curves in the presence of Zn^{2+}. It was shown that a significant decrease of the diffusion limiting current density is observed when the concentration of Zn^{2+} increases. This could be explained by the formation of a protective $Zn(OH)_2$ film [32,34].

Williams and McMurray promoted further the use of LDH pigments as a mean to impart AA2024-T3 with a resistance against filiform corrosion (FFC). Commercial LDH with a chemical formula of $Mg_6[Al_2(OH)_{16}]CO_3 \bullet 4H_2O$ were subjected to calcination-rehydration procedure in order to insert the corrosion inhibitors [12,13,85]. As a first proof of concept, LDH intercalated with nitrate, carbonate and chromate were incorporated into a polyvinyl butyral (PVB) coating and applied to AA2024-T3 panels. After visual examination and kinetics investigation by scanning kelvin probe (SKP), an effective hindrance to the propagation of FFC was observed for the AA2024-T3 LDH-containing coated panels. The FFC inhibition by LDH pigments occurred due to an uptake of aggressive Cl^- anions, hence favoring an increase of the electrolyte pH (since the formation of HCl is unlikely after the capturing of Cl^-), which allows the repassivation of the AA2024-T3 surface [13,85]. At the same time, the inhibition effect depends highly on the intercalated inhibitor and increases in the following order: CO_3^{2-} < NO_3^- < CrO_4^{2-}. In another study, the authors renewed the above experiment with a selection of organic inhibitors namely benzotriazolate, ethyl xanthate and oxalate. The resulting LDH pigments were also found to inhibit FFC in AA20204-T3, with the inhibiting efficiency increasing in the order of ethyl xanthate << oxalate < benzotriazolate [13].

Kendig et al. [14] optimized the approach suggested by Williams and McMurray by using 2,5-dimercapto-1,3,4-thiadiazolate as an organic corrosion inhibitor. The polarization tests were performed directly on a rotating Cu disk and have shown that this particular 2,5-dimercapto-1,3,4-thiadiazolate loaded LDH acted on inhibiting the oxygen reduction reaction (ORR). Moreover, similarly to strontium chromate, the inhibition effect of this organic inhibitor is irreversible which could imply that its mechanism of action relies on the formation of a possible protective layer. These results suggest that 2,5-dimercapto-1,3,4-thiadiazolate loaded LDH could effectively inhibit filiform corrosion on AA2024-T3.

In 2010, Zheludkevich et al. [15] reconsidered the use of LDH intercalated with speciated vanadates (VO_x^-). Two methods for LDH synthesis were tested: direct co-precipitation in a bath already containing the vanadate species and anion-exchange after synthesis by co-precipitation with nitrate-based precursors. Although a successful intercalation of vanadate was indicated by the XRD for both synthesis methods, vanadate-intercalated LDHs obtained by

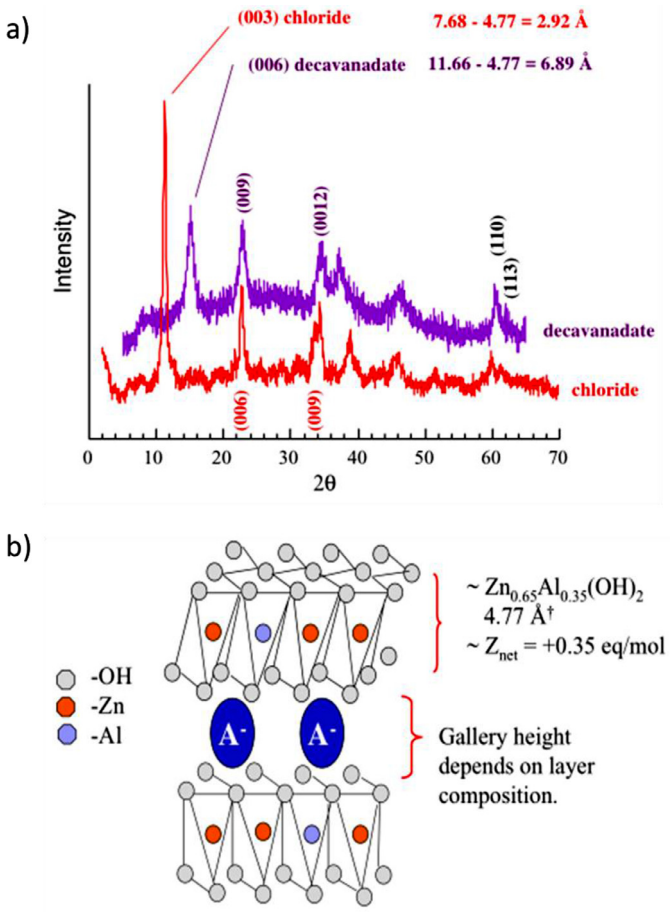

Fig. 7. X-ray diffraction patterns for Al–Zn-decavanadate and Al–Zn-chloride hydrotalcite compounds. The approximate ratio of Zn–Al in these compounds is 2–1 (a) and schematic illustration of the layered structure in hydrotalcite compounds. The structure consists of alternating layers of positively charged mixed metal hydroxide sheets and anions. The Gallery heights are calculated from the difference between the basal plane spacing and the thickness of the Al–Zn-hydroxide layer (4.77Å) (b). (Reprinted with permission from [83]).

anion-exchange were found to be more crystalline than the ones obtained by direct co-precipitation. The LDH vanadate powders obtained by direct synthesis generated a relevant amount of amorphous aluminum vanadate phase, which had an immediate impact on the release behavior. Indeed, the release profiles of vanadate from ZnAl LDHs obtained by direct synthesis showed a lower concentration of vanadate released into the solution in comparison to the ones obtained by anion exchange. Moreover, the release profile of the LDH vanadate obtained by anion-exchange revealed a fast-occurring release during the first hours followed by a chemical equilibrium. It was also noted that the saturation limit for the vanadate release diminishes when more LDH-vanadate is added into the solution. The authors argued in this respect, that the exchange reaction between vanadate and chloride is chemical in nature and is dominated by an anion-exchange equilibrium rather that a solubility equilibrium.

A multilayer painting scheme was prepared by incorporating the above LDH-VO_x pigments (prepared by direct synthesis and by anion-exchange) into an aeronautical based painting scheme and applied to AA2024 specimens [15]. The EIS curves together with their fitting models displayed a higher oxide barrier resistance than that of a conventional chromate-loaded paints. The coating resistance was also higher under prolonged immersion conditions in the presence of LDHs. In addition, standard tests were performed, including FFC and Q-panel condensation testing (QCT). While FFC testing revealed that LDHs led to better protection against FFC than chromate-loaded paint, QCT testing showed a higher number of blisters in the presence of LDHs when compared to reference (without any inhibitor additive) and chromate-doping systems [15]. A similar study on the corrosion protection efficiency of ZnAl LDH intercalated with vanadate was reported by Vega et al. [286]. Alkyd based primers with different LDH pigment concentration (5 %, 10 % and 15 % ZnAl LDH intercalated with vanadate) were prepared and their anticorrosion performance were compared to that of a chromate-based coating containing 10 % zinc chromate. The best results were obtained with the alkyd primer containing 10 % ZnAl LDH with vanadate, and confirmed the high potential of ZnAl LDH intercalated with vanadate to replace chromate- based systems. However, much care must be given to the content and dispersion of the pigment in a polymer matrix so that they do not interfere with other coating properties such as adhesion.

Although efficient for the corrosion inhibition of AA2024, vanadate was not the only candidate proposed to be intercalated into LDH pigments and used to enhance the anticorrosive properties of polymer coatings. Other groups proposed the use of organic corrosion inhibitors. For instance, Poznyak et al. [34] investigated the use of MBT and QA as possible organic inhibitors to be loaded into ZnAl LDH and MgAl LDH nanocontainers for AA2024 corrosion protection. The different LDHs loaded with organic inhibitors were added to a solution of 0.05 M NaCl (50mg of LDH in 10ml solution) and their anticorrosion performance were tested on AA2024-T3 by EIS. The best corrosion performance was demonstrated with the LDH loaded with MBT. Optical micrographs of the AA2024-T3 samples exposed to the above solution for 2 weeks showed the formation of a protective layer with samples exposed to solutions with LDH loaded with QA and MBT. However, the layer formed from the LDH loaded with MBT presented a much denser and compact structure. This formed compact layer allows to provide a long-term corrosion protection to the AA2024-T3 panels.

Over the years, many studies examined the possibility of intercalating bigger organic corrosion inhibitors for the protection of aluminum alloys were published. For instance, Stimpfling et al. have explored through various studies a number of organic inhibitors to be intercalated within the LDH intergalleries. Among them 2-hydroxyethyl phosphate (2-HEP) [54], ethylenediaminetetraacetic acid (EDTA) [55], organo-modified compounds by aniline and benzene derivatives [17] as well as various α-amino acid molecules [56]. In all mentioned studies, the different produced LDHs loaded with the organic inhibitors were incorporated into a primer polymer coating and were tested by DC polarization and EIS techniques. They have all shown viability as potential self-healing corrosion protective systems for AA2024.

An attractive feature of encapsulation of corrosion inhibitors in nanocontainers is the possibility to combine different inhibiting species in the same coating system. Tedim et al. [16] examined the possibility of combining LDHs loaded with different inhibitors in the intention of achieving synergistic effect for active corrosion protection of AA2024. The inorganic inhibitors vanadate (VO_x^{n-}) and phosphate ($H_xPO_4^{n-}$) together with the organic inhibitor MBT, were chosen to be loaded separately into LDH and the mix was incorporated in a polymer matrix (ratio 1:1 and total amount of dry LDH was 10 %) or directly dispersed in the electrolyte (ration 1:1 and total concentration of LDH was 5 $g.L^{-1}$). In the latter case, EIS results showed that the combination of vanadate-containing LDH with MBT- or phosphate-containing LDHs revealed a clear synergistic effect. Once the LDH pigments were added into the coating, the synergistic effect was limited due to the interaction between the LDHs and the polymer matrix. The best corrosion performance was observed for the system constituted by LDH-MBT added in sol-gel pre-treatment + LDH-VO_x in the primer. Both coating and oxide resistances obtained from EIS fitting showed the highest values

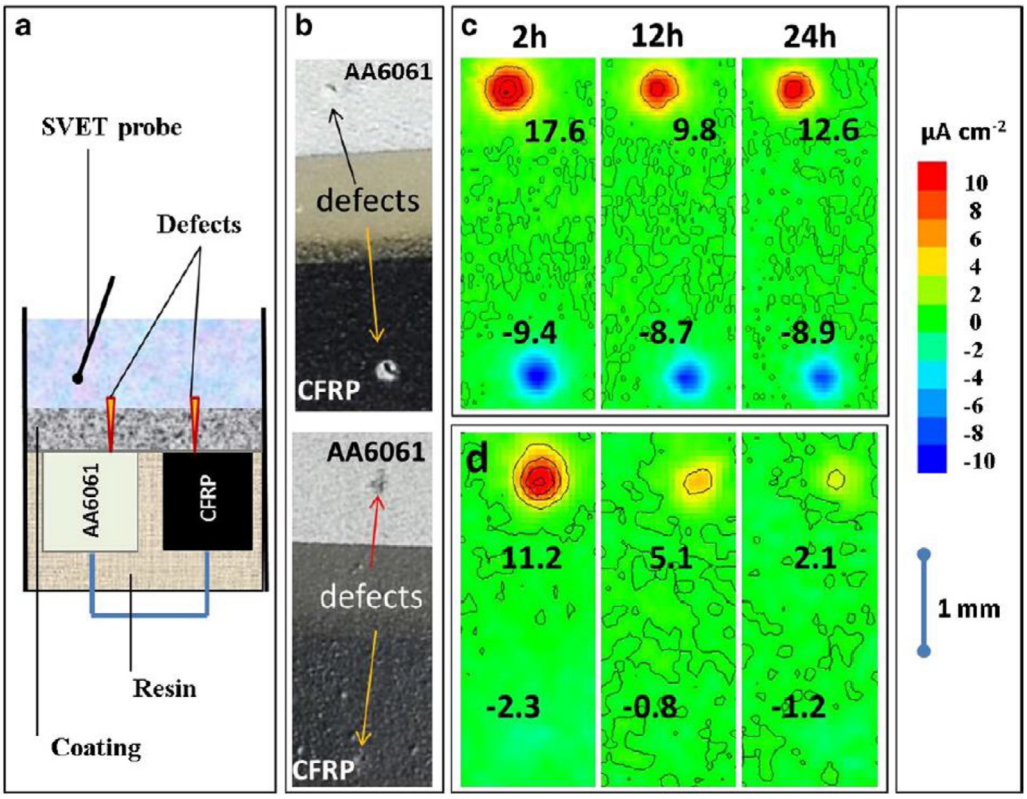

Fig. 8. Scheme of AA6061 + CFRP setup (a), microphotographs of coated galvanic model-cell (b). The SVET maps for the sample with blank epoxy coating (c) and for the coating loaded with combination of nanocontainers (LDH-BTA + bentonite-Ce^{3+}) (d) obtained after 2 h, 12 h and 24 h of immersion in 0.05 M NaCl (reprinted with permission from [236])

among the investigated systems. The proximity of the LDH-MBT to the substrate provides a short protection while LDH-VO_x present in the primer can provide a long-term protection.

In a similar experiment, Subasri et al. [18] prepared Zn-Al LDH pigments loaded separately with vanadate, MBT, molybdate, phytic acid and 8-hydroxyquinoline (8-HQ). The loaded LDH were then taken and dispersed individually in a hybrid sol-gel silica matrix. The obtained LDH- containing sol-gel silica coatings were applied to AA2024-T3 substrates according to a bilayer configuration, with the first sol-gel layer containing LDH loaded with either MBT, molybdate, phytic acid or 8-HQ and the second layer being in every case silica with LDH-vanadate. EIS, DC polarization and SST assessment of the different configurations showed enhanced corrosion resistance even when compared to chromate conversion coated samples owing to a barrier protection combined with the triggered response from the release of the corrosion inhibitors. The best corrosion performance was achieved with the bilayer configuration containing LDH-vanadate/LDH-molybdate. Besides, no interference with the adhesion strength was found for all five systems.

The idea of mixing inhibitors has been also applied to prevent the galvanic corrosion of aluminum alloy (AA6061) coupled with carbon fiber reinforced plastic (CFRP). Serdechnova et al. [236] exploited a combination of two nanocontainers, one being MgAl LDH loaded with BTA and the other was bentonite impregnated with cerium. Fig. 8 a and b represent the specimen design, which illustrates the AA6061 alloy galvanically-coupled with CFRP and embedded in an inert epoxy resin. The sample was coated with a commercially available bi-component epoxy resin containing the two nanocontainers. The self-healing ability of this model specimen was tested by applying two artificially made needle-like defects, located in both materials of the AA6061 + CFRP galvanic couple. The activities on the surface with immersion time was monitored by scanning vibrating electrode technique (SVET) (Fig. 8 c and d). Anodic and cathodic current densities are well defined and located strictly at the artificial defect zones over AA6061 and CFRP in both cases at the beginning of immersion [293]. The blank system demonstrated relatively stable values of corrosion currents in the defects during the measurement time of 24 hours, while a well-defined self-healing effect is observed in the case of the coating impregnated with nanocontainers.

The above cited works prompt one to think on possibilities of using rare earth compounds such as cerium for the corrosion protection of Al alloys. In this regards many attempts were done to introduce rare earth compounds into the LDH structure, most of which involve the rare earth cations (e.g. Ce^{3+}, La^{3+} etc.) to be adsorbed or directly integrated into the brucite-like sheet of the LDH layers and this mostly for other application than corrosion [40,273,294–297].

Nevertheless, the procedure used to benefit from rare earth and LDH together in one framework is not straightforward owing to the fact that they are positively charged (not possible to intercalate) and have a large ionic radius (difficulties to insert in the mixed-metal composition of the double hydroxide layers). However, some strategies mostly focusing on cerium, were developed for the corrosion protection of AA2024.

Liu et al. [298] prepared ZnAlCe-LDH powders with different Ce^{3+}/ (Al^{3+}+ Ce^{3+}) ratios by the co-precipitation method. The XRD results showed an increase of the d-spacing to higher values proportionally to the content of cerium. The authors argued that this increase is proof of successful insertion of Ce^{3+} within the hydroxide sheets. It was demonstrated that the best corrosion performance on AA2024 was attained using the ZnAlCe-LDH with the above ratio of 0.1 because of a synergistic mixture of ZnAlCe-LDHs and CeO_2 nanoparticles.

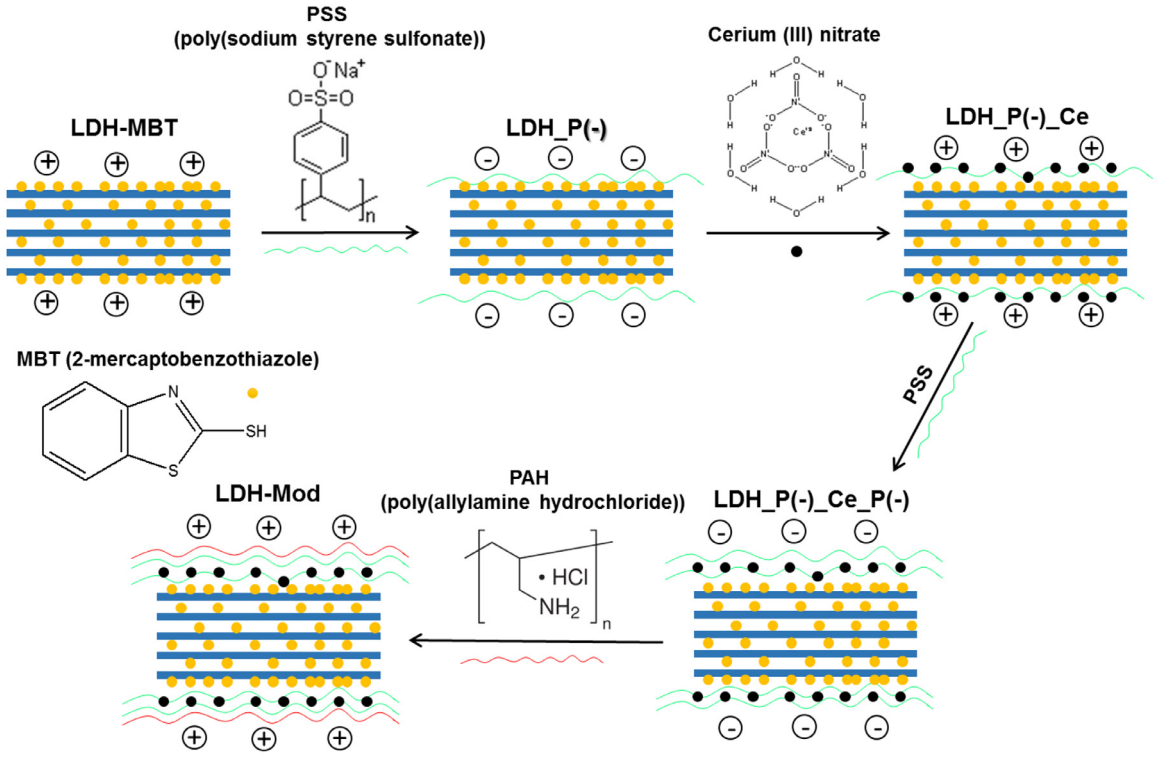

Fig. 9. Approach used in the surface modification of LDHs with PSS, PAH and cerium (III) nitrate (reprinted with permission from [51])

Relying on a different method, Carneiro et al. [51] managed to build an optimized LDH framework through a layer by layer (LbL) approach in order to allow the hosting of two type of corrosion inhibitors (MBT + Ce^{3+}). The MBT organic anion was loaded into the LDH galleries whereas the Ce^{3+} was hosted between the PSS/PAH layers (see Fig. 9). This concept allows to obtain a synergistic inhibition effect by the combination of MBT and Ce^{3+} within one nanocontainer.

Electrochemical studies based on EIS and direct current (DC) polarization on AA2024 coated with a sol-gel coating containing these LbL modified LDHs (0.5 wt. %), revealed an improvement of the corrosion resistance properties in comparison to the reference coating and the one loaded with just LDH-MBT. This behavior was associated to the poor interaction of MBT (which may be released at an early stage of coating preparation) with the sol-gel matrix, when LDHs are not covered with polyelectrolytes. Therefore, the additional polyelectrolyte treatment allowed not only to integrate cerium inhibitors into the LDH framework but also to promote compatibility between the pigments and the polymer matrix.

Aside from offering the possibility of a "smart" active corrosion protection, LDH pigments can also play a role in the prevention of corrosion. In some of the above reviewed studies, the nano-trapping and sensing aspects of LDH nanocontainers has often been mentioned [34,83,238]. These two features are often related since the first action, nano-trapping, is an indication of changes happening at the interface of the Al alloy which is translated as a sensing property. This was emphasized in a work by Buchheit et al. [83]. According to this investigation, a change in the basal spacing of LDH would mean a nucleation of a new LDH phase containing the corrosive species chlorides or sulfate. This change in basal spacing can be uncovered by XRD analysis and would be a primary indication of electrolyte permeation in the coating.

The entrapment of aggressive ions such as chlorides was also addressed in more details in the study by Tedim et al. [35]. ZnAl LDH loaded with nitrate and chlorides were prepared and incorporated into an aliphatic- and acrylic-based polyurethane (automotive coating) and were subjected to permeability tests in a solution of 0.5 M NaCl. It was found that the permeability of the coatings is 20 times lower in the presence of ZnAl LDH loaded with nitrates than it was in the presence of ZnAl loaded with chloride or without LDH. This positive effect was associated to the entrapment of the chloride by the ZnAl LDH nitrate through an anion exchange process. This was demonstrated by the shift of the XRD reflection of the ZnAl LDH nitrate to higher angles, due to the substitution of nitrate with chlorides between the LDH layers. After a month of measurement, 70 % of the nitrate were exchanged with chloride ions.

In a different manner, the sensing functionality of LDH was addressed by Wong et al. [289]. The structural memory effect of $Li_2[Al_2(OH)_6]_2CO_3 \bullet nH_2O$ LDH powder was utilized to detect the water uptake in optically opaque organic coatings in a remote and non-destructive manner. The LDH was synthesized by co-precipitation and calcined in air (220°C < T) and the resulting LiAl mixed hydrated oxide powder were incorporated into a commercial epoxy resin. The coating was applied on AA2024-T3 plates and exposed to 0.5 M NaCl solution for different periods. Using XRD as the main investigating tool, the rehydration transformation of the calcined LDH could be monitored and quantified by evaluating the peak height ratio (PHR) of the LDH characteristic reflection (003). Water-uptake is generally considered as the first step of more serious consequences for metal corrosion such as blisters, delamination and adhesion loss. This approach is suggested to prevent this from happening by an efficient and early detection of water-uptake in organic coatings.

As highlighted in the earlier sections, LDH nanocontainers have been exploited in different ways to offer extrinsic self-healing

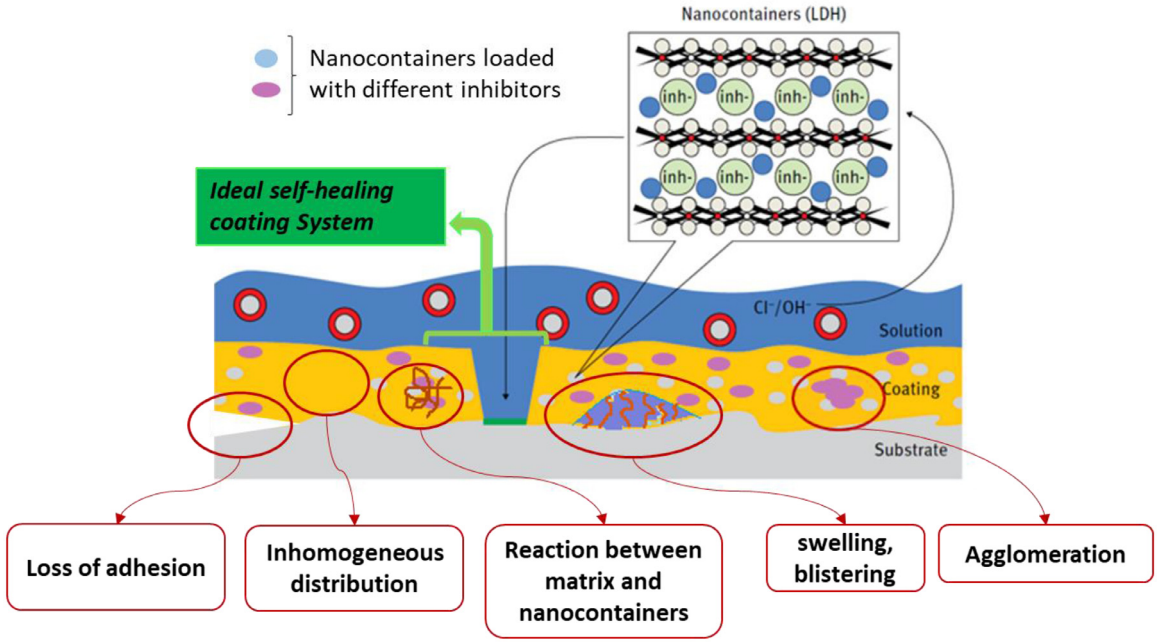

Fig. 10. Scheme summarizing a few challenges that may be encountered when using LDH nanocontainers as additives in a polymer matrix (modified from [293]).

functionalities (see Table 3). They can be integrated in frame of a much complex multi-level corrosion protective system. However, one would think that using LDH as pigments would still lead to the encountering of some of the issues discussed in Section 2.3 and described in Fig. 10. However, through the previous sections, we learned that LDH can be tuned to fit the various requirements in order to obtain a reliable active corrosion protective system.

For instance, osmotic blistering that is caused because of a concentration difference across the coating membrane, can be prevented by controlling the amount of inhibitor loaded into the nanocontainer as well as the amount of LDH nanocontainers hosting the so-called inhibitor. This could also contribute for the reduction of coating disbonding and delamination. There are established testing and monitoring methodologies that can be followed to obtain an optimized coating system. For instance, Mahajanam and Buchheit managed to define a critical percentage/concentration of LDH pigments below which blistering starts to take place for a primer [299]. This was achieved by visual examination of epoxy primers containing different LDH concentration, applied into glass substrates and immersed them into an aggressive media. Zheludkevich et al. relied on Q-Panel condensation test (QCT) (ASTM D 4585–99) to evaluate the degree of blistering caused by the incorporation of LDH pigments into a water-based epoxy primer [15]. Chico et al. compared the degree of blistering of LDH, chromate and Ca/Si pigments added into an alkyd coating based on ASTM D714-56. Vega et al. [286] tested and evaluated different LDH/coating ratios using the same standard.

The issue of compatibility between the LDH pigment and the polymer can be overcome by modification of their outer surface using surfactants or other organic compounds. Studies have reported the modification of the LDH surface to achieve different properties. Just to cite a few examples; LDH was modified with cetyl trimethyl ammonium bromide (CTAB) and octadecyl trimethyl ammonium bromide (ODTMA) surfactants to obtain better photocatalytic properties [300]. In another work, the hydroxyl groups on a MgAl LDH surface were altered by the introduction of amine groups to help improve the LDH drug delivery property by enhancing their compatibility with blood [301,302] but also their physical adsorption of CO_2, when it comes to environmental application [303]. MgAl LDH surface could also be changed from hydrophilic to hydrophobic to enhance flammability properties using different surfactants [304]. For anti-corrosion applications, Hu et al. [305] reported the possibility of chemically grafting ZnAl LDH nanocontainers loaded with vanadate in order to make it compatible for incorporation in a commercial epoxy coating. Briefly, the ZnAl LDH-nitrate was prepared by co-precipitation followed by an anion-exchange reaction to intercalate vanadate. The obtained ZnAl LDH loaded with decavanadate was then subjected to a hydroxylated treatment before its immersion in a solution of γ-aminopropyltriethoxysilane (APTS) to form a bonding layer at the surface of the LDH. The final step consisted of an in-situ polymerization of polyaniline (PANI) in the presence of the APTS modified ZnAl LDH to produce a polymer–clay composite PANI/ZnAl LDH loaded with decavanadate (see Fig. 11). The resulting surface engineered LDH could easily be incorporated in an epoxy based coating and offer efficient corrosion protection to mild steel substrate [305]. A similar surface modification was also attained with the work of Du et al. [306], where camphorsulfonic acid doped polyaniline(CPANI)-modified MgAl LDH composites were fabricated through an oxidative polymerization process. The altered LDH pigments allowed not only to ensure compatibility between the LDH pigment and the waterborne epoxy resin, but also to allow a better dispersion of the LDH and avoid the probability of agglomeration. Although this coating presented no active corrosion protective functionalities (no inhibitor loaded into LDH), it did exhibit superior barrier protection to the mild steel.

Industrial coating systems such as primers are generally composed of several different components and fillers that enhance the properties of the coating and guarantees a long-lasting use. For instance, different types of surfactant can be found on a paint system such as: i) dispersing agents that promote the dispersion of solid particles and prevent their flocculation/segregation through charge stabilization and, ii) wetting agents that help reduce the interfacial tension at the solid-liquid interface (e.g. between a solid pigment and the liquid polymer coating) enables the water to wet the pigment particles, hence allowing the good insertion of the lat-

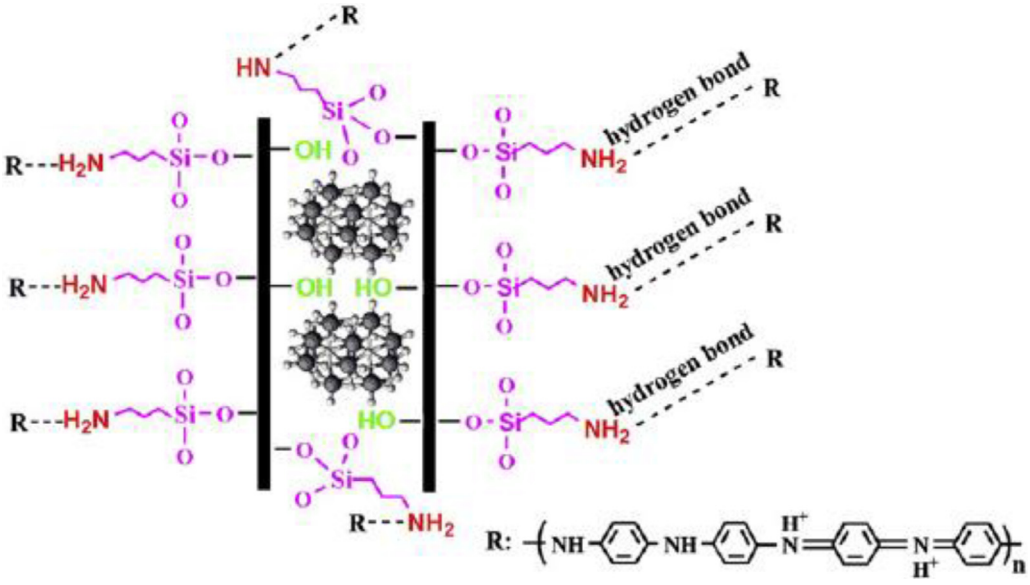

Fig. 11. Schematic illustration of the obtained PANI grafted APTS modified ZnAl LDH loaded with decavanadate. (Reprinted with permission from [305]).

ter. Some wetting surfactants can also facilitate the application of the coating on a substrate, thus improving adhesion [307]. Aside from the additives in the coating itself, the mixing process of the pigments and polymer matrix is generally achieved with sophisticated industrial mixing tools or agitators that contribute greatly in the optimization of the final coating formulation. Consequently, all these parameters should be taken into consideration as they can significantly facilitate the incorporation of LDH pigments into an organic coating.

It should be emphasized that, to this day, the reported studies on LDH nanocontainers and their incorporation in an organic coating, do not show an important diversity in terms of the selected coatings. It is important to perform more systematic and comparative investigations to find a range of formulations that are most suitable for the different available LDH pigments. Moreover, some of these investigations should include mechanistic and kinetic understanding of the inhibitor release from the LDH nanocontainers. The selected coating formulations should not interfere with the inhibitor release characteristics of the LDH nanocontainers but instead, it should allow an efficient diffusion of the released inhibitors into the unprotected area. It has been recently shown that the leaching kinetics of corrosion inhibitors and their diffusion and transport through the coating matrix are two independent phenomena. Accordingly, the leaching of the corrosion inhibitors starts from a cluster of connected inhibitors pigments and proceeds until no more species are left in the clusters. The removal of the connected inhibitor leads to the formation of a percolating network of connected voids that will enable the easy transport of further corrosion inhibitor species [308]. Therefore, when it comes to LDH pigments, one can suppose that the first stage related to the release of inhibitor from the LDH pigments, depends on the trigger and the solubility of the inhibitor whereas, the second stage that is the leaching process over time, is controlled by the creation of a percolating network of voids that will allow further transport of the inhibitors [308–311]. The described model was summarized into a parameter called the “percolation threshold”, which is the critical value of inhibitor pigment volume concentration (PVC) that needs to be considered during a coating formulation [310]. However, this model above was established on the basis of a direct addition of inhibitors into the coating formulation and it is expected that the mechanism may differ for an encapsulated inhibitor. Therefore, for the coating formulation containing LDH loaded with corrosion inhibitors, the percolation threshold should be defined by considering the following factors: the percentage of inhibitor loaded into the LDH, the volume of the final LDH loaded with inhibitors, the efficiency and dissolution of the corrosion inhibitor, the release kinetics of the inhibitors from the LDH.

Adjusting the model to a system based on LDH encapsulated inhibitor is key for the smooth integration of these nanocontainers into industry.

Through the previous sections, it could be undoubtedly confirmed that the use of LDH nanocontainers as “smart” carriers for active agents in a coating framework, can be considered as a potent strategy to replace Cr(VI) pigment-based systems. The LDH pigments can be prepared through various methods with a chemical composition that can be easily varied according to the needs. They can host several corrosion inhibitors, organic and inorganic inhibitors either in frame of the same LDH nanocontainer or as a combination of several LDHs containing different inhibitors. It can be surface engineered to allow the intercalation of a diversity of corrosion inhibitors (e.g anions and cations inhibitors in an LbL framework), or surface modified to promote compatibility within a coating formulation. It offers protection to the hosted corrosion inhibitor and allows its controlled release when triggered by specific factors (e.g. pH, chlorides…). These are just a few advantages among others. A summery of the reviewed studies in this section are represented in Table 4.

LDH pigments may be regarded as possible alternatives to Cr(VI) pigments but not to chromate-based conversion coatings (CCC). This fact is simply due to the distinct role played by an organic coating containing active pigments and a conversion layer directly generated on the surface of an Al substrate. A conversion coating does not only improve the corrosion resistance, but also strengthens the adhesion to subsequent organic coatings. As a direct alternative to CCC, LDH conversion coating (LDH-CC) is suggested . And it offers as much advantages as presented for the LDH as pigments. This will be reviewed in the following sections.

Table 4
Summary of the studies reporting the use of LDH pigments for the corrosion protection of Al alloys.

Parent LDH	Synthesis	Intercalation		Polymer matrix	Properties	Alloy	Ref.
		Method	Anion				
ZnAl/VO_x	Co-precip.	Direct- synthesis	VO_3^- $V_{10}O_{28}^{6-}$	PVA/thick.: 3 μm (dry)	Anticorrosion/ sensing	AA2024-T3	[32,83]
LiAl/CO_3	Co-precip.	Direct- synthesis	CO_3^{2-}	Epoxy resin /thick.: 126 μm (dry)	Sensing by calcination/reconstration	AA2024-T3	[289]
MgAl/CO_3	Commercial	Calcination-reconstraction	NO_3^- CrO_4^{2-}	PVB/ thick.: 30 μm (dry)	Inhibition of FFC	AA2024-T3	[12,13,85]
		Anion-exchange	ethyl xanthate, oxalate and BTA	PVB/ thick.: 30 μm (dry)	Inhibition of FFC	AA2024-T3	[13]
		Anion-exchange	2,5-dimercapto-1,3,4-thiadiazolate	Tested in solution (5 % NaCl)	Inhibition of FFC and ORR	AA2024-T3	[14]
ZnAl/NO_3 **MgAl/NO_3**	Co-precip	Direct synthesis and anion-exchange	VO_3^-	Water based epoxy primer / thick.: 30 μm (dry)	Active corrosion protection	AA2024-T3	[15]
ZnAL/VO_x	Co-precip	Direct synthesis	VO_x^{n-}	Alkyd based primer /thick.: 60±10 μm (dry)	Active corrosion protection	AA2024-T3	[286]
ZnAl/NO_3 **MgAl/NO_3**	Co-precip	Anion-exchange	QA and MBT	Tested in solution (0.05 M NaCl)	Inhibition of corrosion processes	AA2024-T3	[34]
ZnAl/NO_3 **MgAl/NO_3**	Co-precip.	Anion-exchange	2-HEP	Epoxy-primer/thick.: 50 μm (wet)	Active corrosion protection	AA2024-T3	[54]
ZnAl/NO_3			EDTA				[55]
ZnAl/NO_3			3-ABSA, 4-ABSA, 3,4-HHBA				[17]
MgAl/NO_3 **LiAl/NO_3**			L-Cys				[56]
ZnAl/NO_3	Co-precip	Anion-exchange	VO_x^{n-}, $H_xPO_4^{n-}$ and MBT	Water based epoxy primer / thick.: 25 μm (dry)	Active corrosion protection	AA2024	[16]
ZnAl/NO_3	Co-precip.	Anion-exchange	VO_x^{n-}, MBT, MoO_4^{2-}, phytic acid and 8-HQ.	Sol-gel/thick.: 20 μm (dry)	Active corrosion protection	AA2024-T3	[18]
ZnAl/NO_3	Co-precip.	Anion-exchange	BTA	Water based epoxy primer / thick.: 40 μm (wet)	Active corrosion protection	AA6061 (coupled with CFRP)	[236]
ZnAlCe/ NO_3	Co-precip.		Ce^{3+} insertion on the LDH hydroxode layers (not intercalated)	Sol-gel/ thick: undefined	Synergistic inhibition/ Active corrosion protection	AA2024	[298]
ZnAl/NO_3	Co-precip.	Anions-exchange	MBT + Ce^{3+} (inserted by LBL surface modification of LDH)	Sol-gel/ thick.: undefined	Synergistic inhibition/ Active corrosion protection	AA2024-T3	[51]

4. LDH as a functional conversion layer

In previous sections, studies on the use of LDH as pigments to improve corrosion protection of different hybrid and organic coatings were reviewed and, in some cases, their performance would match or exceed chromate-based pigments. However, similarly to Cr(VI) technology, LDH can also be directly applied to the metal surface in form of a conversion layer [10,33,38,48]. Keeping in mind that most well-known and studied LDHs are based on compositions such as ZnAl or MgAl, attempts to develop LDH-based conversion films have occurred during the last 25 years [8,10,11,48,86,240,244,312–317]. On one hand, this work can be considered as a new field with methodologies competing with chrome-free conversion treatments. On the other hand, it is an extension and improvement of already existing processes such as the sealing steps in anodizing processes.

Just like the conversion coatings described in Section 2.2, LDH conversion layers can be prepared directly on the surface of the Al substrate through a chemical/electrochemical conversion process. The active corrosion protective property is implemented by the intercalation of corrosion inhibitors between the LDH-CC galleries. In the event of mechanical damage or changes the interface (e.g. pH, presence of chlorides or/and sulfate, etc.), the LDH-CC is triggered and a subsequent release of the corrosion inhibitors takes place, followed by the entrapment of aggressive species. Hence, impeding the corrosion activity at the affected zone (Fig. 12).

A comprehensive understanding of the LDH-CC synthesis and mechanism of corrosion protection of Al alloys, is provided in the next sections.

4.1. LDH-CC Synthesis

From the time of the first reported achievement of LDH as conversion coatings for Al alloys [8–11], studies on the optimization and modification of the morphology and properties of these LDH films have been constantly increasing. According to the recent review by Guo et al [63], two main pathways can be adopted to obtain LDH-films, by physical deposition or in-situ formation.

Physical deposition methods include Layer-by-layer (LbL) [241,318–321], solvent/colloid evaporation [322–325], and sol-gel spin-coating techniques [63,326]. Although these physical deposition methods allowed the preparation of diverse LDH films with interesting properties, they have not been relevant for anti-corrosion applications. This may be associated with the fact that physical deposition does not allow an intimate connection between the substrate and the LDH film. Indeed, the substrate

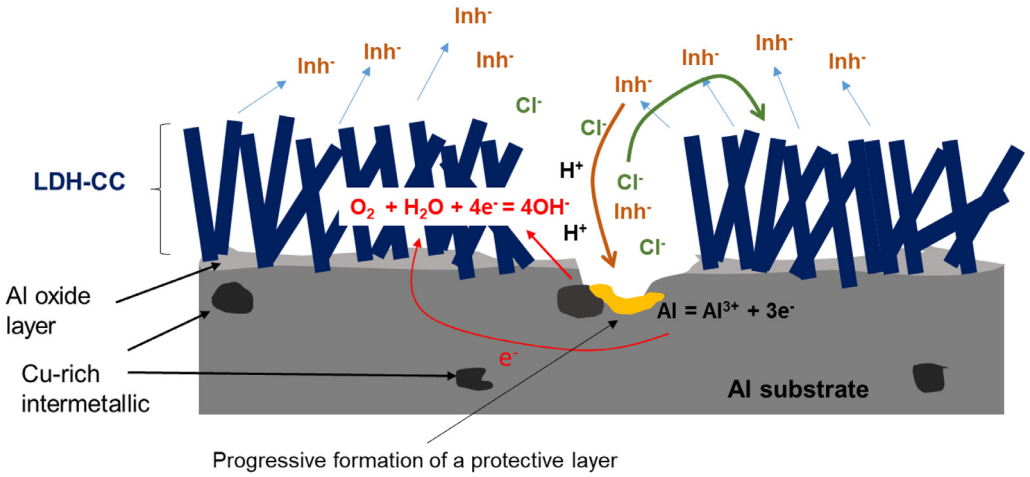

Fig. 12. Scheme describing the corrosion protection mechanism of LDH-CC prepared on an Al substrate.

does not serve as precursor. This means that the adhesion is weak which clearly is an obstacle for corrosion protection purposes. Moreover, the shape of the substrate could be an issue since with deposition methods, it may be challenging to cover surfaces with complicated shapes [63,327].

Contrary to physical deposition methods, in-situ LDH preparation allows an immediate contact of the LDH film layer and the Al substrate. In-situ LDH growth can be achieved either by electrodeposition or by co-precipitation treatment.

In-situ growth by electrodeposition is fairly known [33,38,63,312,326]. Most reported studies state that the electrodeposition of LDH film is based on the reduction of nitrate ions and the generation of OH^- ions (see Eq. (14)), which will lead to an increase of the local pH of the working electrode namely the substrate to be treated [33].

$$NO_3^- + H_2O + 2e^- \leftrightarrow NO_2^- + 2OH^- \quad E_0 = 0.01\ V \tag{14}$$

This increase of pH drives the precipitation and formation of the LDH film on the substrate. However, the substrate to be treated is not the source of the cations involved on the LDH film growth. This is why various conducting materials such as Pt [33,43,328], Au [33], glassy carbon [329] and Ni [330] could be treated with LDH films. This approach is more adequate for the area of energy conversion and storage [70,71] and has not been adopted for corrosion protection purposes, up to now. The reason might be that the resulting LDH has a disordered orientation with low crystallinity and purity due to the formation of unwanted intermediate phases (eg. metal hydroxides/oxides). This could interrupt further growth and thickening of the LDH film during the preparation process. The other important drawback of this method is the poor adhesion of the formed LDH film to the metallic substrate [331].

The second and most known pathway for *in-situ* LDH growth is by co-precipitation, which allows the formation of 2D perpendicular oriented LDH flakes [326]. From a chemical point of view, *in-situ* LDH growth is considered more advantageous since it involves the formation of chemical bonds, which strengthen the adhesion of the film. Moreover, *in-situ* LDH film formation is a one-step process and occurs independently of the shape of the substrate. This means that this method can be applied to a large area of application [63]. The simplest *in-situ* LDH growth can be achieved by a co-precipitation process, which is an extension of the LDH powder synthesis by co-precipitation. In this case, the substrate to be treated is generally also one of the precursors. In the case of Al substrate, M/Al LDH films can be fabricated by the immersion of the substrate in a bath containing a metal cation M^{2+}/M^{+} (Zn^{2+}, Mg^{2+}, Li^{+}...etc.) precursor in certain conditions (pH, temperature, concentration etc.) while the Al^{3+} ions are generated by the dissolution of the Al substrate. Since this process is derived from the co-precipitation method for LDH powder synthesis, most facts associated with the former method apply for the LDH film formation. In other words, the synthesis can be achieved by using urea [312], ammonia [314] or simply sodium hydroxide [44] as precipitating agents. However, as mentioned in the first section of this review, the final morphology of the 2D LDH flakes will vary according to the used precipitating agent. About corrosion application, the co-precipitation synthesis using ammonia or sodium hydroxide is generally the method of choice. The reason being the same as for LDH synthesis as pigments, the urea hydrolysis tends to release carbonates that will in turn be intercalated into the LDH galleries which is unwanted (since carbonate cannot be easily exchanged).

In the following sections, most of the LDH functional layers were prepared by *in-situ* hydrothermal/co-precipitation method.

4.2. LDH- CC anionic exchange for corrosion protection

Contrary to LDH nanocontainers in form of pigments, there has not been many studies in terms of intercalation possibilities for LDH in form of conversion coatings especially in the area of corrosion protection. In the context of corrosion protection, vanadate was the most utilized model corrosion inhibitor. First, because vanadate is a known efficient inhibitor for the corrosion protection of Al alloys [92,332,333] and second, the successful intercalation of vanadate anions between the LDH layers has been evidenced throughout several investigations [44,48,286,287,314]. Other corrosion inhibitors namely molybdate (MoO_4^{2-}) [52], MBT [52,334] and 8HQ [335] have also been claimed as potential candidates to be intercalated between the LDH layers.

So far, the intercalation process of the cited species was carried out through anion-exchange reaction by simple immersion of the LDH treated Al alloy into a solution containing the respective species at a specific pH, concentration and temperature. Most of these conditions were derived from the knowledge acquired from the anion-exchange reactions carried out with LDH in form of pigments [18,19,50,288]. This also includes the preference of selecting LDH intercalated with nitrate as a parent LDH, since similarly to the LDH pigments, LDH films intercalated with OH^- and CO_3^{2-} are challenging to exchange [79,334].

One can suppose that the lack of possibilities in terms of species that could be intercalated in the LDH-CC can be associated to the inelastic nature of the LDH film lamella. Indeed, as shown in earlier sections, a wide range of inorganic and organic species could be intercalated into LDH powders and most argued that it was due to the nature of the LDH pigments to expand and host even bigger molecules. In the case of LDH-CC a strain

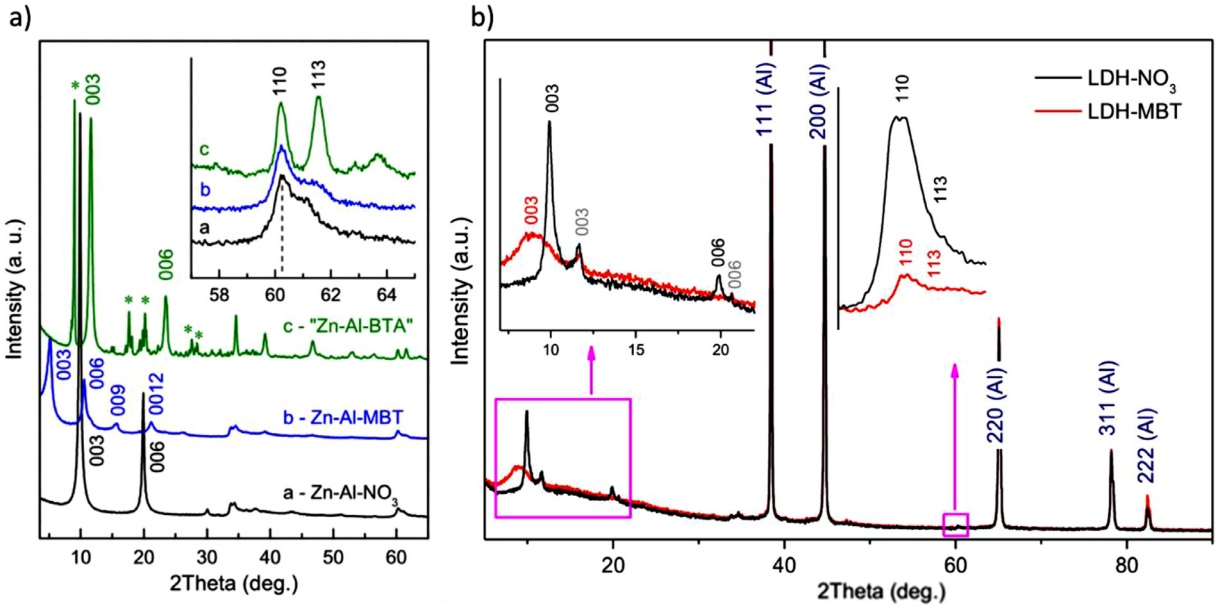

Fig. 13. XRD pattern of ZnAl LDH in form of powder a) and film b) before and after anion- exchange reaction NO_3^- → MBT^-. (reprinted with permission from [50] and [334]).

may exist, since the LDH films are chemically bonded into the treated metal substrate. Hence, two possible scenarios can be predicted; (i) the bigger molecules may cause a forced expansion of the LDH flakes that will be accompanied by a fragmentation of the LDH crystallites [334,336] or, (ii) the LDH will not expand and the species do not intercalate between the layers. For instance, Neves et al. [334] noticed that after anion exchange reaction from NO_3^- to MBT^- in ZnAl LDH-CC the XRD reflections (003) and (006) corresponding to the LDH-NO_3 phase have disappeared and a new peak has appeared at lower angles (to the left) (Fig. 13 b). This is in agreement with the peak shift observed with ZnAl LDH in form of powders (Fig. 13 a). Moreover the (001) and (113) reflections associated to the LDH hydroxide structure have not changed after anion-exchange reaction. This was enough to prove the successful intercalation of the organic corrosion inhibitor (Fig. 13 b).

However, when comparing XRD patterns obtained with ZnAl LDH intercalated with MBT^- in form of pigment (Fig. 13 a) and in form of conversion coatings (Fig. 13 b), it can be disputed that the amount of LDH phase, in the case of LDH-CC, after the anion exchange process with $MBT^-$is much lower and less crystalline in comparison to the parent LDH-CC with NO_3^-. The latter finding was explained by the fact that since LDH-CC are attached to the metal surface, there is a high probability for the LDH film to be fragmentated [334].

The hypothesis of possible fragmentation was also suggested in a recent work by Bouali et al. [248]. The authors monitored the anion exchange reaction (NO_3^- → Cl^-) of ZnAl LDH film grown on AA2024 and zinc substrate to track the kinetics differences. The measurements were carried out in *in-situ* mode, using synchrotron high performance X-ray diffraction. In both cases, when ZnAl LDH is grown on AA2024 and pure zinc, an important amorphous phase was noticed on the XRD patterns which was associated to a decomposition of the LDH crystallite as a result of the exchange reaction. This is an interesting fact, considering that Cl^- anions are much smaller than both NO_3^- and MBT^-. In other words, an expansion or contraction of the LDH galleries may always induce stress leading to a partial or a total fragmentation of the LDH crystallites. The study also revealed some other characteristics of the anion placement between the LDH galleries. For instance, it is claimed that the nitrate anions are positioned in a 70° angle, perpendicular to the cationic layers to achieve the highest compensation of the charge. After intercalation with chlorides, the basal spacing is reduced, followed by a decrease of the LDH crystallite size [248]. The latter effect is more pronounced for the LDH grown on pure zinc. Although this review focused on LDH films produced on Al alloys, it is important to point out that this comparative investigation showed that the kinetics of exchange reaction (NO_3^- → Cl^-) is faster for the LDH films grown on pure zinc than the ones on AA2024. Moreover, the resulting interlayer arrangement of the LDH-Cl is dissimilar in both cases. This entails that the starting substrate for LDH growth may greatly influence the kinetics of anion-exchange reactions.

Based on the same investigation tools of the above cited work [248], Iuzviuk et al. [317] managed to establish a kinetic trend of anion-exchange for a few corrosion relevant species namely Cl^-, SO_4^{2-} and VO_x^{n-}. The parent ZnAl LDH film intercalated with nitrates were produced on a pure zinc substrate. Three exchange reactions were monitored: ZnAl LDH-NO_3 → ZnAl LDH-SO_4, ZnAl LDH-NO_3 → ZnAl LDH-Cl and ZnAl LDH-NO_3 → ZnA LDH-VO_x. It was found that the first two reactions occur faster than the latter reaction. Based on an Avrami-Erofeev (AE) analysis, it was found that the above anion-exchange processes happen in two stages, the first is a two-dimensional diffusion-controlled reaction, and the second is characterized by a one-dimensional diffusion-controlled reaction. Both stages include a decelerator nucleation effect. The last anion-exchange reaction Zn-LDH-NO_3 → Zn-LDH-VO_x is governed by a slow reaction, which the authors attributed to an influence of the vanadate speciation characteristics. Indeed, two LDH structures were identified that were attributed to the ZnAl LDHs intercalated with $V_4O_{12}^{4-}$ and $V_2O_7^{4-}$. These polyvanadates were claimed to be promoting efficient corrosion inhibition of Al alloys [44]. The results of their kinetic study helped define a sequence of priority for anion-exchange reactions, with the parent ZnAl LDH -NO_3:

$$Cl^- > SO_4^{2-} > V_4O_{12}^{4-} \text{ or } V_2O_7^{4-}$$

As mentioned before, the starting substrate may affect the kinetics of anion exchange reaction [248] therefore it might be in-

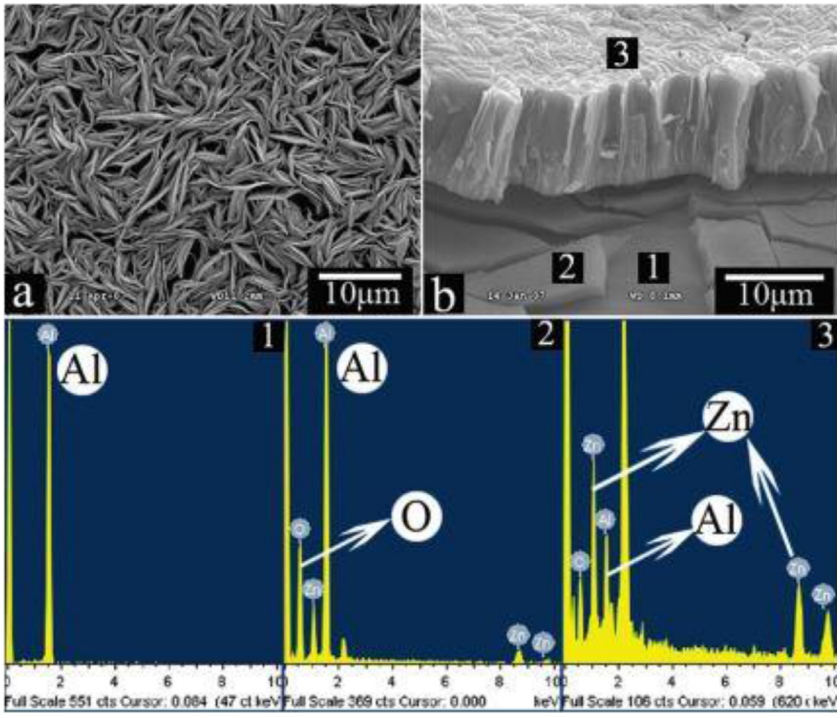

Fig. 14. SEM micrographs of the top (a) and cross-section (b) views of the ZnAl-LDH/alumina bilayer film crystallized for 48 h. The EDX spectra of the three different positions (1-3) in the cross section of the film are also shown. (reprinted with permission from [337])

correct to extend the finding from [317] into LDH film formed on Al alloys.

Most known kinetics and modelling studies have been carried out on LDH in form of powder. For example, the work by Miyata et al. [278,279] and Costa et al. [280] are considered as basics in terms of LDH anion affinity and exchange reaction. However, till recently there has not been a clear study that asserts that the knowledge can be extended to LDH conversion coatings.

When dealing with LDH films, there are more challenging aspects that need to be taken into account such as the nature of the substrate and the induced stress from the expansion/contraction of the LDH lamellae during the exchange reaction. The latter aspect concern mostly in-situ LDH grown film. For films produced by deposition pathways (LbL, solvent evaporation or spin coating), the restrictions may be different since the resulting LDH is not attached to the metal substrates.

4.3. LDH-based surface treatments for corrosion protection

4.3.1. LDH conversion coatings on aluminum alloys

The first reported studies on surface modification of aluminum alloys by LDH films for the sake of corrosion protection, appeared earlier than that of LDH pigments. Indeed, before the group of Buchheit and co-workers reported their studies on LDH as pigments for corrosion protection, they first promoted the use of LDH as functional surface treatment for the corrosion protection of Al alloy in 1994 [8].

Buchheit et al. demonstrated a formation of what they called a talc film formation on four different Al alloys (AA1100, AA2024-T3, AA6061-T6, and AA7075-T6), when immersed in an alkaline Li-containing salt bath. Their investigation revealed that this talc film had the typical structure and stoichiometry of the hydrotalcite-like compound $Li_2[Al_2(OH)_6]_2{\bullet}CO_3{\bullet}nH_2O$ and provided an efficient corrosion resistance towards standard salt spray testing [8]. In 2002, three more studies by the same group were published with each revealing more about the likelihood of these nanocontainers to replace the toxic CCC [9–11]. For instance, the authors claimed that the development of these systems was done with a reduced number of processing steps using non-toxic chemicals. Moreover, the requirements essential to produce these LiAl LDHs on Al substrates are the following: (i) dissolution of the native Al-oxide, (ii) sufficient concentrations of the reactants in order to cause precipitation, (iii) in a reasonable short time of coating formation. To accelerate the LDH film formation [11], it was shown that the addition of oxidizing agents such as hydrogen peroxide into the hydrotalcite baths accelerated the dissolution of the Al-oxide and the formation of the LDH-CC. Even better, the resulting LDH coatings presented superior corrosion resistance.

Several years after the first studies of Buchheit et al., Guo et al. published in 2009, a novel method to produce ZnAl LDH films on a pure aluminum sheet (purity > 99.5 wt. %) [337]. The authors proposed a one-step co-precipitation methodology based on the immersion of the Al sheets in a bath containing zinc nitrates and ammonium nitrate salts adjusted to a pH of 6.5 by means of a 1 wt. % ammonia. The obtained compact ZnAl LDH layer (see Fig. 14), showed not only a good adhesion performance but also remarkable corrosion performance with an impedance value of 16 MΩ after 120 h immersion in a solution of 3.5 % NaCl. This attests for the passive behavior of the layer and a large charge transfer resistance.

Relying on the same methodology, Tedim et al. prepared ZnAl LDH conversion coatings on AA2024-T3 substrate. It was also the first time that a corrosion inhibitor was intercalated within the LDH galleries and its release by anion exchange with chlorides was verified [48]. After the preparation of ZnAl LDH-NO_3, anion-exchange reaction in a vanadate containing solution was performed at pH 8-9 at 50°C > T. XRD patterns showed diffractions typically ascribed to Zn-Al LDH-NO_3 and LDH-VO_x nanocontainer powders. Moreover, the obtained surface revealed an uneven film structure, with micro-sized islands separated by a thin layer covering the remaining surface. This differentiated growth was attributed to a higher dissolution of aluminum matrix at sites where intermetallic particles existed [48]. EIS measurements and optical photographs

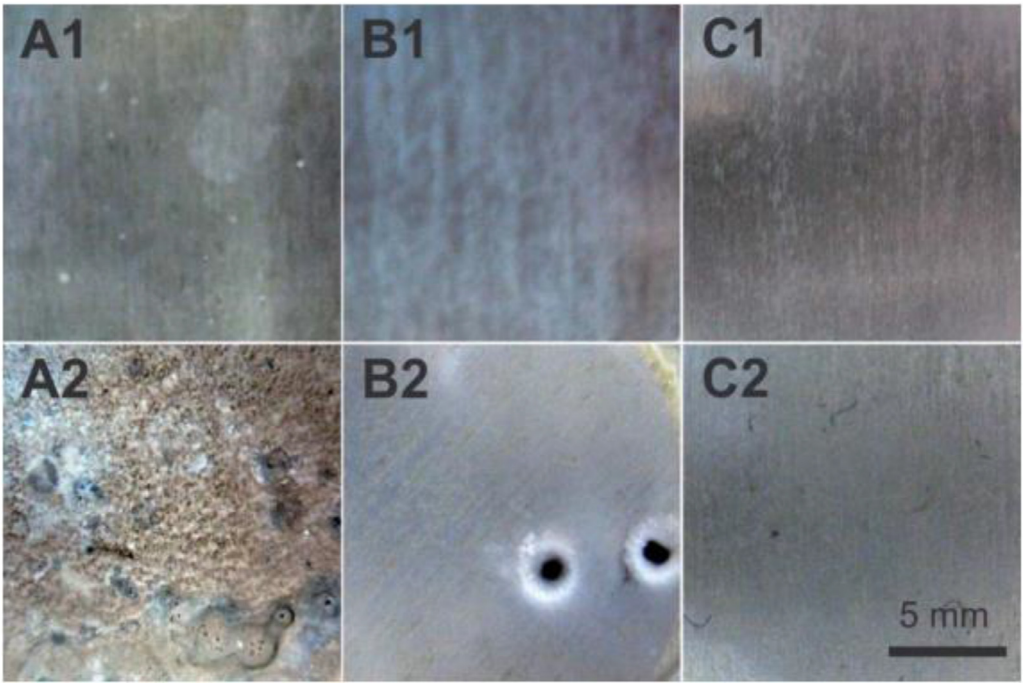

Fig. 15. Photographs acquired for AA2024 plates in the beginning (1) and after 1 month (2) of immersion in 0.05 M NaCl: (A) bare metal, (B) LDH–NO_3 and (C) LDH–V_2O_7. (Reprinted with permission from [48])

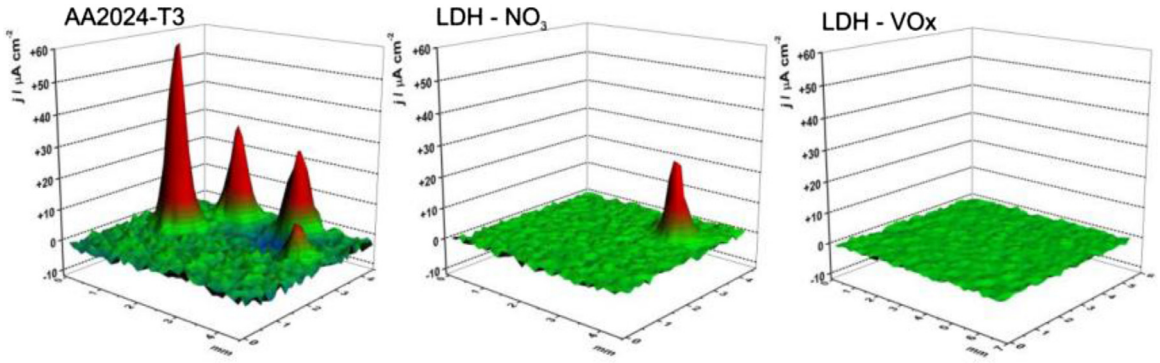

Fig. 16. 3D SVET maps of the different systems after 1 month of immersion in 0.05 M NaCl (Reprinted with permission from [84]).

(Fig. 15) showed that the protection of AA2024 substrate was significantly improved when LDHs were formed (Fig. 15).

Three other studies [79,84,338] followed to provide a comprehensive understanding of the influence of different parameters on the LDH growth and the LDH layer corrosion performance. The first was in respect to the effect of AA2024-T3 surface pre-treatments on the LDH growth. Different alkaline based pre-treatments were tested including existing industrial treatments [79]. The second study aimed at the optimization of the experimental synthesis conditions (the concentration of zinc nitrate and presence of corrosion inhibitor) for the fabrication of LDH films [338]. The results from these two studies [79,338] revealed that a compromise must be found between the stability of the native oxide film and the LDH formation to achieve a higher corrosion resistance, while the extent of surface coverage can be controlled by the concentration of reactants added into the synthesis bath. Finally, the authors provided an understanding of the mechanism of corrosion protection of these nanocontainer layers when intercalated with nitrate and vanadate, by using EIS and SVET (Fig. 16) as two main electrochemical investigation tools [84]. According to their investigation, the ZnAl LDH conversion coatings intercalated with NO_3^-, assume the role of a physical barrier against aggressive species (e.g. Cl^- and O_2), which includes as well as nano-trapping property of LDH. An additional protection mechanism was also associated to the presence of NO_3^- and Zn^{2+} (present in the LDH hydroxide layers), as both species promote corrosion inhibition effects. After intercalation with vanadate, the obtained LDH films demonstrated an even superior corrosion resistance, associated to the physical barrier nature of the LDH as well as to the capacity of the vanadate to be released and act as efficient corrosion inhibitor due to their oxidative power and formation of a protective layer at the surface, hence impeding the ORR reactions.

Several other approaches based on LDH-CCs for the corrosion protection of Al alloys were proposed since then [52,243,335,339]. Wang et al. described the synthesis of LDH coating by immersing Al substrates into a solution already containing pre-formed MgAl LDH particles for 36h at autoclave conditions (T = 100°C) [335]. The obtained LDH coated samples were subsequently modified by a further immersion in a solution containing 8-HQ at RT, pH 11 for 6h. The microstructure of the overall LDH coating intercalated with $8HQ^-$ was preserved and an efficient active anticorrosion layer was obtained. Zhang et al. [340] prepared ZnAl LDH film intercalated

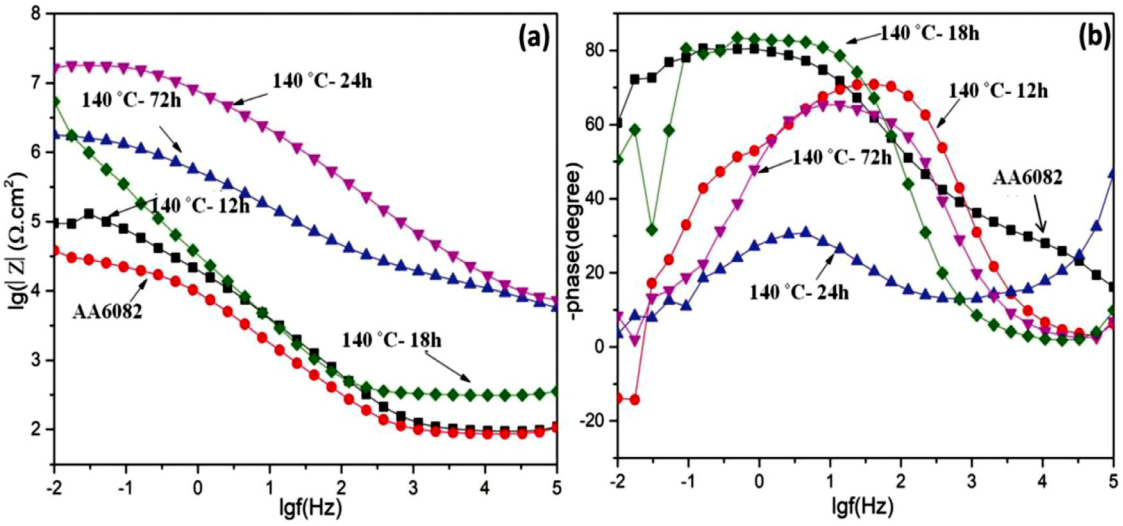

Fig. 17. Impedance a) and phase b) plots of the CaAl-LDH-coated specimens at various synthetic conditions in 0.1 M NaCl solution. (Reprinted with permission from [316]).

with vanadate, molybdate and MBT, on AA2024. Although it was stated that the respective anions were successfully intercalated between the LDH interlayers, the shift of the (003) and (006) XRD reflections was not clearly demonstrated. However, the electrochemical and SST tests showed an improved corrosion inhibition with all LDH films. The highest performance was recorded for ZnAl LDH-VO_3 and the lowest with ZnAl LDH-NO_3, accordingly with LDH–VO_3 > LDH–MBT > LDH–MoO_4 > LDH–NO_3. The same group stated that they managed to synthesize Ce-doped ZnAl-LDH film on AA2024 through urea hydrolysis [341]. The formed LDH films were afterwards loaded with $V_2O_7^{4-}$. The results of EIS measurements demonstrated a good corrosion resistance of the "double-doped" LDH films which was associated to a synergistic inhibition effect of the combination of released vanadate anions and dissolved Ce^{3+} from LDH structure. Nevertheless, no clear evidence of the Ce^{3+} cations insertion between the LDH galleries or within the hydroxide layers, was demonstrated. This implies that the Ce^{3+} could have simply been present/adsorbed on the surface of the LDH film and contributed to the overall corrosion inhibition.

Recently, Iqbal et al. reported for the first time the possibility to produce LDH thin films with Ca^{2+} and Al^{3+} cations on Al alloys [316]. The CaAl LDH conversion layers intercalated with nitrate were prepared on AA6083 substrate, by a one-step hydrothermal synthesis at 140 °C (under autoclave conditions) and a pH = 10. Different immersion times were tested with t= 24 h being the best condition for an optimized corrosion resistance. Indeed, the EIS measurements showed excellent barrier properties with an impedance value at 0.01 Hz close to 3 orders of magnitude higher (Fig. 17) in comparison to the bare substrate. The authors also highlighted that even enhanced corrosion resistance can be obtained with further intercalation with corrosion inhibitors.

The treatment of Al alloys with LDH-CC coatings can provide an active corrosion protection against aggressive environments and micro galvanic cells as a result of the presence of IMCs, but the role of LDH-CC can also be extended to hybrid multi-material assemblies that are responsible for accelerating corrosion as a result of a macro-galvanic effect. This possibility has been already shown by the use of LDH pigments [236], but a recent work described a methodology of implementing ZnAl LDH conversion coating as a pre-treatment before a hybrid friction spot joining of AA2024-T3 to CF-PPS (carbon-fiber reinforced polyphenylene sulfide) [342]. In trying to minimize the galvanic corrosion effect resulting from the direct contact of AA2024-T3 with the much noble CF-PPS, the AA2024-T3 part was subjected to a pre-treatment by ZnAl LDH incorporated with nitrate and vanadate (model corrosion inhibitor). The adhesion performance of the joints after LDH treatment was tested by the lap shear method (ASTM D 3163) and revealed an improvement close to 20 %. After being exposed to SST (ASTM B117-16), the overall mechanical performance of the joints treated with ZnAl-LDH (nitrate) was still well maintained and a good corrosion resistance was noted in comparison to the reference joints (non-treated with LDH). However, the joints treated with ZnAl LDH containing vanadate exhibited an unusual behavior. Indeed, in comparison to the many reported studies [44,48,92,286,287,332] of the superior inhibition performance of vanadate with Al alloys, the joints treated with ZnAl LDH vanadate demonstrated lower corrosion resistance and adhesion performance after SST. The authors justified this behavior to the unstable nature of vanadate speciation when subjected to a variation of pH or oxidation conditions. The fact remains, that for the first time it has been proven that LDH-NO_3 conversion films can be good candidates to improve corrosion resistance of hybrid joints without compromising their mechanical performance.

The corrosion protective property of LDH-CC can be expressed is several forms. In the above studies LDH-CC provided an active corrosion protection to Al alloys through the triggered release of corrosion inhibitors. However, LDH-CC can also be exploited as a support for further chemical modification to obtain a hydrophobic layer which will delay the ingress of water and aqueous species hence minimizing the occurrence of corrosion. Wang et al. proposed the fabrication of MgAl LDHs film growth by urea hydrolysis on a pure Al substrate [312]. The subsequent surface modification with hydrophobic compounds (sodium oleate, sodium laurate, and sodium stearate), led to the increase of the surface hydrophobicity of LDHs, delaying the formation of biofilms involved in biocorrosion. The performance of the treated LDH films was found to be as following; LDH-CC (without treatment) < LDH-CC with oleate < LDH-CC with laurate ≈ LDH-CC with stearate.

The above strategy was also demonstrated by Zhang et al. where LiAl LDH layers were grown on an AA2198-T851 and modified by the adsorption of a surfactant anion PFDTMS (1H,1H,2H,2H-perfluorodecyltrimethoxysilane) (Fig. 18 a). The investigation was supported by high contact angles (CA) measurements with water revealing a value of CA ~168° [46] (Fig. 18 b).

The same superhydrophobic properties were reproduced by treating MgAl- and ZnAl LDH-CC with stearic acid [47,343],

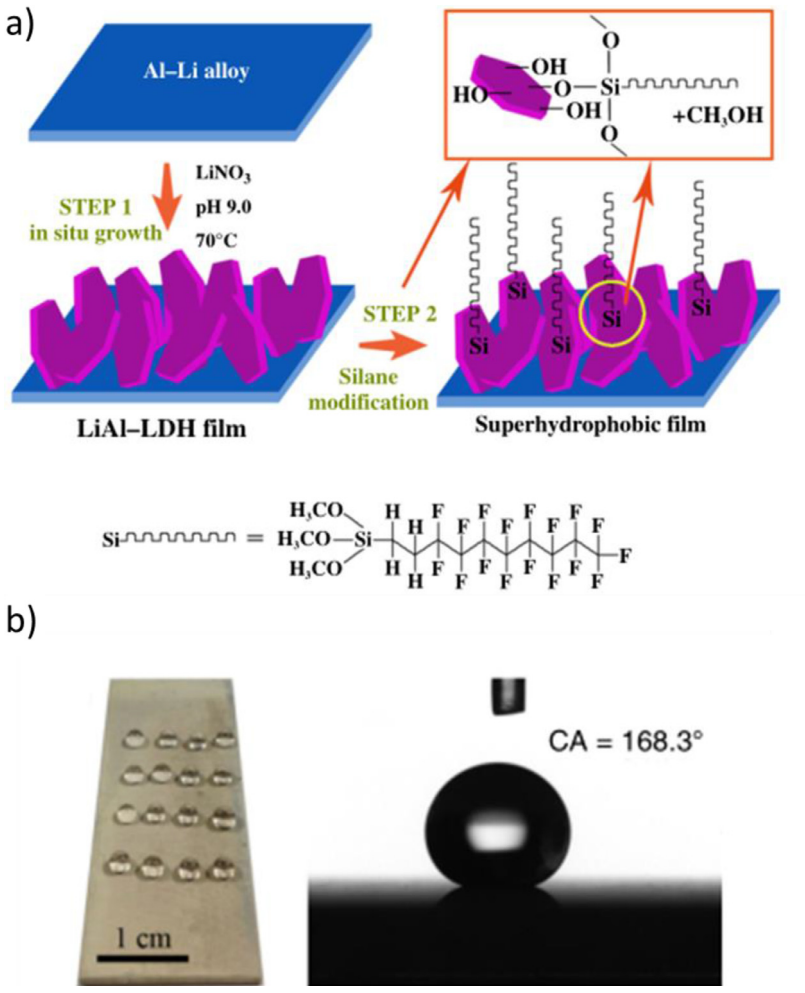

Fig. 18. Schematic illustration for the fabrication of superhydrophobic LiAl-LDH film on Al–Li alloy (a); photographs of water droplets on the surface of the Al substrate coated with LiAl LDH modified with PFDTMS (left) and results of the CA measurement (right) b). (Reprinted with permission from [46])

ZnAl LDH with laurate anions [313], MgAl and ZnMgAl LDH with F-triethoxy-1H,1H,2H,2H-tridecafluoro-n-octylsilane (FAS-13) [38,344]. In the case of laureate anions, hydrophobization was achieved by successful intercalation of this anion into the LDH galleries whereas for the others species namely PFDTMS [46], stearic acid [47] and (FAS-13) [38,344], it is believed that they were bonded onto the LDH film surface through electrostatic interaction or chemical reaction with the LDH hydroxyl group present at the surface [313]. Just recently, a new study showed the possibility to implement both hydrophobicity and active corrosion protection into an ZnAl LDH film grown on an Al (≥ 99.9 wt. %) substrate [345]. The ZnAl LDH film was prepared by co-precipitation and the resulting LDH coated Al panels were immersed first in a vanadate containing solution followed by a second immersion in a laurate-based solution. This resulted in a ZnAl LDH-CC co-intercalated with both laurates and vanadate. The electrochemical investigation using polarization and EIS revealed a superior corrosion resistance that was attributing to the superhydrophobicity from laurate, anion-exchange reaction from LDH allowing the trapping of aggressive chlorides and release of vanadate corrosion inhibitor.

Although hydrophobization treatments may contribute greatly to enhance the corrosion protection of Al alloys, the property of hydrophobicity can be useful only if applied as a last step on a multi-level coating scheme (last interface in contact with air). This is generally achieved by means of primers or top-coats. Moreover, the hydrophobic effect may be lost over long immersion times or upon mechanical defect. Therefore, the LDH aptitude of self-healing/active corrosion protection is much more relevant and should be additionally implemented.

The continuous improvement of LDH-CCs drove to the addition of an extra step, which is their implementation in frame of a multi-scheme protective system where LDH would play the role of the first “defensive line”, previously occupied by CCC. Therefore, attempts have been made to cover the LDH coated Al samples with an additional polymer coating and test the resulting corrosion resistance performance. Wu et al. fabricated vanadate intercalated MgAl LDH-CC on AA2024-T3 followed by the deposition of a sol-gel layer [287]. The hybrid system exhibited good adhesion (according to GBT9286-1998 standard) performance which meets the requirement for CCC replacements. More recently, Yasakau et al. reasserted the possibility to increase anticorrosion resistance by a bilayer system LDH/sol-gel. EIS and SVET investigations on an artificially defected LDH/sol-gel coated AA2024, revealed that the mechanism of corrosion protection is based on the ion-exchange concept, where the chlorides are captured and the corrosion inhibitors (vanadate) are released to act on the defected areas [346]. Moreover, the authors reiterated that the procedure used to pre-treat the AA2024 surface does have an influence on the LDH growth, a statement that supports that of Zheludkevich et al. [79]. A lab-based surface pre-treatment was compared to that of a conventional industrial pre-treatment. Although the lat-

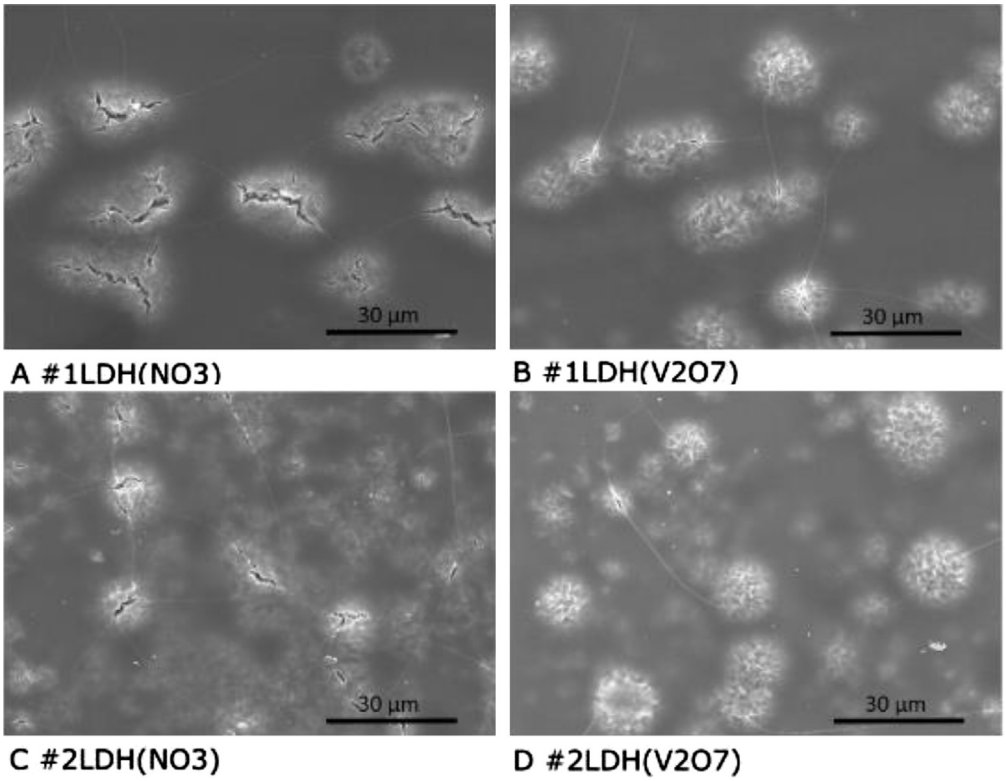

Fig. 19. SEM images of sol-gel coatings after immersion tests #1LDH(NO_3) (a), #2LDH(NO_3) (c), and #1LDH(V_2O_7) (b) and #2LDH(V_2O_7) (d). (#1 and #2 refer to the lab-based and industrial pre-treatments, respectively). (reprinted with permission from [346])

ter tends to result in a much stable and thicker Al oxide layer, it provides less dissolved Al for LDH formation. Therefore, the lab-based pre-treatment was found more favorable to the formation of a high coverage LDH film, which also means a high capacity of corrosion inhibitor storage. However, independently of the pre-treatment used, substantial damage was noted on the sol-gel coating above the LDH-NO_3 CC after immersion in a 0.5 M NaCl solution (Fig. 19 a and c). On the other hand, the LDH-V_2O_7 demonstrated a superior compatibility with the sol-gel coating (Fig. 19 b and d), which allowed them to act as efficient active corrosion protective systems.

As demonstrated with LDH pigments and LDH-CC on bare aluminum alloys, there are various ways to adapt and modify a system to achieve an active response. The intercalation of corrosion inhibitors into LDH-CC is generally classified as an extrinsic approach to corrosion protection [195]. Interestingly, intrinsic paths to improve corrosion resistance exploiting the properties of LDH nanocontainers are also possible. Yan et al. reported the observation of an intrinsic self-healing effect taking place by a dissolution/recrystallization of the LDH film [347]. After ZnAl LDH conversion layers were produced on AA6061 substrates (LDH-CC thickness = 8 µm), they were covered by an epoxy resin which was artificially scratched and immersed in a solution of 3.5 % NaCl. A restoration of the damaged LDH film and the recovering of the area of the scratch was witnessed after a certain period of time (thickness of the reconstructed LDH was close to 5 µm).

In a similar context, Visser et al. [86,315,348-357] proposed another original concept of self-healing protection that can also be regarded as intrinsic self-healing effect. Indeed, in an extrinsic approach, the Al substrate is already covered with the LDH-CC and is loaded with corrosion inhibitors that are released upon damage (Fig. 20). In the method proposed by Visser et al. [86,315,348–357], the LDH films are not readily fabricated on the Al substrate, but instead LDH film formation occurs as a targeted response to a damage caused in a polymer matrix (Fig. 20).

The Li-containing coatings were subjected to artificial defects and characterized by several electrochemical [352,355,357] and surface investigation [351,356] techniques. The authors showed that the Li from the coating can leach into the area of defect and promote the formation of an LiAl LDH conversion layer, hence providing a passive protection to the Al alloy (see Fig. 21). It was stated that the mechanism of formation of these LiAl LDH layers involved three main stages; (1) thinning of the Al native oxide layer, (2) anodic dissolution and LDH film formation and finally (3) continuous dissolution and growth of the LDH film.

This proposed mechanism is similar to the explanation provided by Buchheit et al. on the first studies carried out on LDH as conversion layers [11]. This prominent self-healing behavior by Li-leaching from organic coatings, has been reproduced in several studies and applied on different Al alloys (AA2024, AA7075, AA5083, and AA6014) [315].

Going through the various works published on LDH conversion coatings, it can be presumed that the topic remains novel and incomplete. The late accomplished studies on LDH-CC on bare Al alloys show a continuous improvement in terms of the mechanistic understanding [248,358] and the optimization of the LDH application [342,359]. A list of these works can be found in Table 5.

4.3.2. LDH-based sealing of anodic layers

Anodizing methods whether conventional or plasma based, are often employed for the pre-treatment of Al alloys as base before subsequent coverage with additional organic coatings. Indeed, the resulting anodized Al is porous (Fig. 22 a), which on one hand may enhance the adhesion to subsequent coating layers, but on the other hand may be an open access for aggressive elements into the interface of the Al alloy, leading to severe corrosion. In order to maintain the durability and prevent corrosion degradation

Table 5
Recapitulative of the studies achieved on LDH-CC on Al alloys a) without any additional surface treatment b) with hydrophobic properties and c) implemented in a multi-frame coating system.

a) LDH-CC without further modification

Al Alloy	LDH-CC		Intercaltion		Properties	Ref.
	Method	LDH type	Method	Anion		
AA1100, AA 2024-T3, AA 6061-T6, and AA 7075-T6	Co-precip. (25°C and 70°C, pH 11.5-13.5, 15-90 min)	LiAl/(OH)(CO_3)	Direct synthesis	OH^- CO_3^{2-}	Barrier protection / thick. : 0.62-1.49 µm	[8,10]
AA2024-T3	Co-precip. (90°C, 2-10 min)	LiAl/(OH)(CO_3)	Direct synthesis	OH^- CO_3^{2-}	Barrier protection/ thick.: undefined	[11]
Pure Aluminum (99,5%)	Hydrothermal co-precip. (120°C, pH 6.5, 6 h and 12 h)	ZnAl/NO_3			Barrier protection, good adhesion/ thick.: 10 µm	[337]
AA2024-T3	Co-precip. (<100°C, pH ~7, few hours)	ZnAl/NO_3	Anion-exchange	VO_x^{n-}	Barrier + Active corrosion protection and nanotrapping properties / thick.: undefined	[48,79,84,338]
AA5005	Hydrothermal co-precip. /autoclave (125°C, pH 9.5-10.5, 8 h)	MgAl/NO_3			Barrier protection + nanotrapping properties /thick.:12 µm	[243]
AA2024	Co-precip. (45°C, pH~7, 6 h)	ZnAl/NO_3	Anion-exchange	VO_3^- MoO_4^{2-}, MBT	Active corrosion protection /thick.: 5-20 nm	[52]
Al substrate (99.75 Al, 0.25 Fe in wt. %)	Hydrothermal co-precip./autoclave (100°C, pH~9, 36 h)	MgAl/NO_3	Anion-exchange	8HQ	Active corrosion protection /thick.: undefined	[335]
6N01 Al	Co-precip. (58-62°C, pH 9-10, 20 min)	LiAl/NO_3			Active corrosion protection/thick.: 100 nm	[339]
AA2024	Urea hydrolysis (70°C, 24 h)	ZnAl/NO_3	Direct growth + anion-exchange	Ce^{3+} dopping + $V_2O_7^{4-}$	Active corrosion protection/thick.: undefined	[341]
AA6082	Co-precip. (40-80°C, pH 6-7, 18-24 h)	ZnAl/NO_3			(Parameter study) Barrier protection/ thick.: 5 -50 µm (precess dependant)	[359]
AA6082	Hydrothermal co-precip./autoclave (140°C, pH 10, 12-72 h)	CaAl/NO_3			Barrier protection/ thick.: 9.5- 12 µm (time dependant)	[316]
AA2024-T3 (coupled with CF-PPS)	Co-precip. (95°C, pH 6.5, 30 min)	ZnAl/NO_3	Anion-exchange	VO_x^{n-}	Active corrosion protection/enhanced mechanical properties/ thick.: undefined	[342]

b) Hydrophobization of LDH-CC

Al Alloy	LDH-CC			Surface modification			Properties	Ref.
	Method	LDH type	CA (°)	Method	Specie	CA (°)		
Pure Al (99.99 wt. % Al)	Urea hydrolysis (70°C, 24 h)	MgAl/NO_3	~ 36	Surface treatment /adsorption	Oleate	114	Hydrophobicity, Antifouling, microbiologically influenced corrosion resistance/ thick.: undefined	[312]
					Laurate	129		
					Stearate	121		
2198-T851	Co-precip. (70°C, pH 10, 24 h)	LiAl/ NO_3		Surface treatment /adsorption	PFDTMS	168.3	Superhydrophob-icity/ thick.: ~50 µm	[46]
AA5005	Hydrothermal coprecip./autoc-lave (125°C, pH 10, 4 h)	MgAl/NO_3	~ 48.5	Surface treatment /adsorption	Stearic acid	138.5-153.5	Superhydrophobicity-anticorrosion/ thick.: ~13.3 µm	[47]
AA5052	Co-precip. (70°C, 3 h)	ZnAl/ NO_3	~70	Surface treatment /adsorption	Stearic acid	154	Superhydrophobicity anticorrosion/ thick.: undefined	[343]
Al (99.9 wt. % Al)	Co-precip. (85°C, pH 6.5, 12 h)	ZnAl/ NO_3	~ 36.6	Anion-exchange/ intercalation	Laurate	128	Superhydrophobicity-anticorrosion/ thick.: ~2 µm	[313]
AA6061	Co-precip. (90°C, pH 7-12, 24 h)	MgAl/NO_3		Surface treatment /adsorption	FAS-13	160	anti-icing, anticorrosion and mechanical robustness /thick: undefined	[38]
Al foil (99 wt.%)	Co-precip. (90°C, pH 7-12, 24h)	ZnMgAl/NO_3		Surface treatment /adsorption	FAS-13	159	corrosion inhibition and mechanical robustness /thick: undefined	[344]
Al (99.9 wt.%) plates	Co-precip. (85°C, pH 6.5, 12h)	ZnAl/NO_3		Anion-exchange/ intercalation	VO_x^{n-} + Laurate	150	Superhydrophobi and corrosion inhibition/thick: 4 µm	[345]

c) LDH-CC treated Al alloy + Polymer matrix

Al Alloy	LDH-CC		Intercaltion		Polymer coating	Properties	Ref.
	Method	LDH type	Method	Anion			
AA2024-T3	Urea hydrolysis (90°C,1 h)	MgAl/CO_3 thick. : 3.5 µm	Anion-exchange	VO_x^{n-}	Sol-gel/thick : 2.5 µm	Barrier/active corrosion protection, good adhesion.	[287]
AA2024-T3	Co-precip. (100°C, pH ~7, few hours)	ZnAl/ NO_3	Anion-exchange	$V_2O_7^{4-}$	Sol-gel/ thick: undefine-d	Barrier/active corrosion protection, good adhesion	[346]
Pure Al (99.5 wt.%) and AA6061	Co-precip. (90°C, pH 6.5, 24 h)	ZnAl/ NO_3Thick: 8 µm			Epoxy resin/ thick: undefine–d	Intrinsec self-healing by dissolution/recrystallization/ thick. of reconstructed LDH: 5 µm	[347]
AA2024, AA7075, AA5083, and AA6014	Precipitation mechanism promoted by corrosion reaction	LiAl/ (OH)(CO_3) LiAl/oxalate			Various coatings/ thick: 20-40 µm	Intrinsec self-healing by Li leaching and LDH formation / thick. of *in-situ* formed LDH: 0.1-1.5 µm	[86,315,351,353–357]

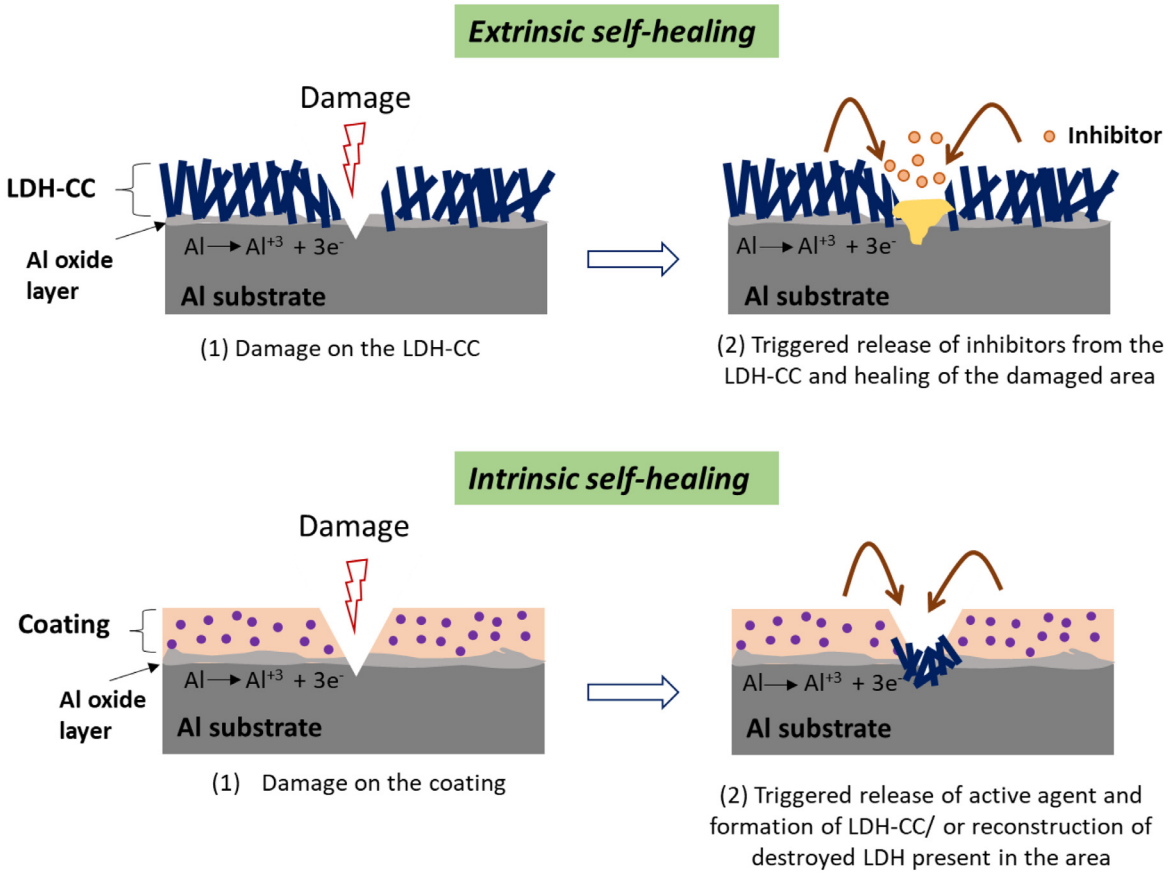

Fig. 20. Schematic illustration of the extrinsic and intrinsic approaches (according to [347] and [353]) to the LDH conversion coatings.

of the anodic layers, an additional post-sealing treatment needs to be performed [104,148,149,360]. Hot water sealing (HWS) is one of the most common sealing methods. The anodized Al parts are immersed in a hot boiling water (or steam) to allow the formation of boehmite, filling the pores of the anodic layer (Fig. 22 b) [361]. HWS improves the barrier properties of the anodic films but does not offer any active corrosion protection, due to the absence of corrosion inhibitors. Formally active compounds such as dichromate and nickel acetate use to be added by an impregnation process to confer an additional active protection [148]. However, due to their toxicity these were replaced by more suitable corrosion inhibitors [149,362] for example rare earth salts [149] (Fig. 22 c). Indeed, these corrosion inhibitors can be added during a HWS treatment or be trapped between the anodic layer and an organic coating [361] (Fig. 22 d).

Nevertheless, the direct addition of corrosion inhibitors into the pores of the anodic layer will lead to the manifestation of similar issues encountered with the organic coatings in Section 2.3, namely fast consumption of the inhibitor, possible interaction with the subsequent organic coating, degradation of the inhibitor ...etc.

This is where the LDH sealing could play a crucial role. In the following paragraphs the various advantages offered by the LDH-CC on enhancing the corrosion resistance of anodic films are reviewed.

4.3.2.1. Conventional anodizing. Conventional anodizing of Al alloys involves an electrochemical process where an electrical current is passed through an Al alloy sample, immersed in an acidic bath. A partial consumption of the Al alloy surface takes place and an anodic film is progressively formed toward the inner part of the metal alloy. The anodizing film generally consists of an inner barrier oxide layer (10–100 nm) and an outer porous layer, with pores that would exceed 100 μm in depth [363]. Hence, explaining why a post-sealing treatment is needed. The idea with LDH post-sealing is not only to seal these pores and sustain a barrier protection, but also to compensate the lack of active corrosion protection, by means of LDH nanocontainers loaded with corrosion inhibitors.

The earliest study on this specific topic was performed by Zhang et al. [240]. ZnAl LDH films were prepared by *in-situ* co-precipitation process on a porous anodic alumina/aluminum (PAO/Al) substrate. The process was followed by an anion-exchange reaction in order to intercalate laurate ions. The success of the intercalation with laurate anions was confirmed by the observation of a shift of the main LDH reflection (003) and (006) at lower angles. The modified LDH films demonstrated superhydrophobic properties which were associated with the micro- and nanoscale hierarchical structures. As stated earlier in this review, superhydrophobicity is a feature that provides corrosion protection but only in a passive manner, which means no self-healing properties are achieved.

To integrate self-healing properties into LDH films, corrosion inhibitors must be added. This is what Li et al. did in their work with vanadate loaded LDH film on anodized 2198 Al alloy [364]. The anodized samples were first subject to HWS (boiling water for 20min), followed by several hours immersion in a solution containing the precursor mixture ($Zn(NO_3)_2$ $6H_2O$ and NH_4-NO_3) at a pH close to neutral and T==45 °C.

The formation of the ZnAl LDH films was explained by the following equations:

$$NH_3 \cdot H_2O \rightarrow NH_4^+ + OH^- \quad (18)$$

$$Al_2O_3 + 2OH^- + 3H_2O \rightarrow 2Al(OH)_4^- \quad (19)$$

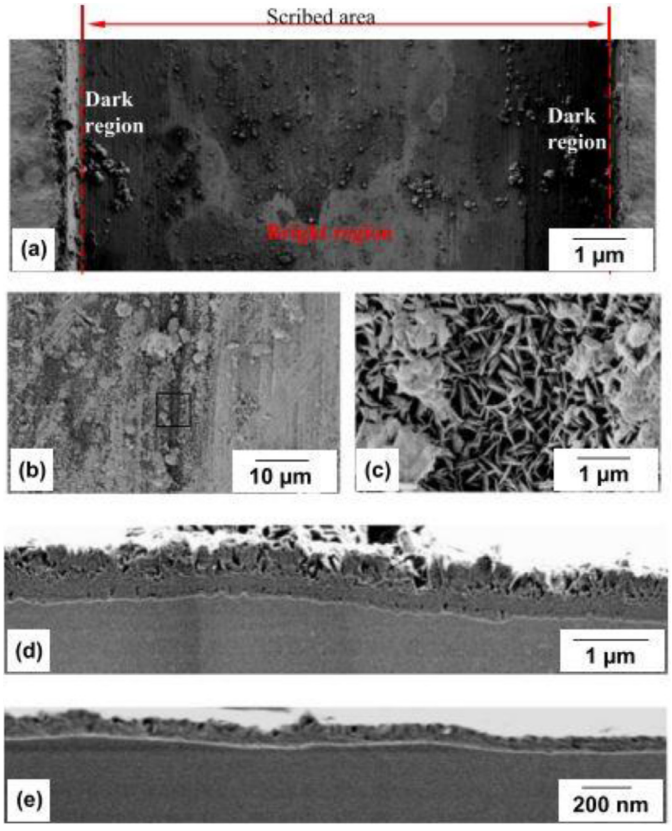

Fig. 21. Scanning electron micrographs of protective layers formed in scribed area after 168 h neutral salt spray testing with a primer coating pigmented with lithium oxalate: planar views (a)–(c) and cross-sectional views (d)–(e). (Reprinted with permission from [350])

$$Zn^{2+} + 4OH^{-} \rightarrow [Zn(OH)_4]^{2-} \quad (20)$$

$$Al(OH)_4^{-} + [Zn(OH)_4]^{2-} + NO^{3-} + H_2O \rightarrow ZnAl\ LDH \quad (21)$$

These equations represent the mechanism of LDH formation claimed previously by other studies [11,235]. The last step consisted of immersing the readily formed LDH coated samples, in to a solution containing $NaVO_3$ at a pH = 8.8, T= 45°C for 2 h.

The LDH films on AA2198 demonstrated enhanced corrosion protection which could be explained by the sealing of the pores, reducing the penetration of corrosive ions; and the release of vanadate ions providing a long-lasting protection. This research group also prepared LDH film with different cations Mg^{2+}, Co^{2+}, Zn^{2+} and Ni^{2+} on the same anodized AA2198 [365]. The obtained LDH films displayed different morphologies, with ZnAl LDH and NiAl LDH showing a more compact and best adhesion performance to the anodized layer. However, after hydrophobization treatment with PFDTMS, it has been found that the superhydrophobic properties were more evident with the samples treated with the Mg- and Co-Al LDH films. This was justified by the more porous structure of these two LDH films and their capacity to trap a larger amount of air. These statement were supported by the following CA values performed after PFDTMS treatment: MgAl LDH, CA=168.8°; CoAl LDH, CA=169.6°; NiAl LDH, CA=165.8° and ZnAl, CA=164.2°. Indeed, Mg- and Co-Al LDH films show higher water contact angles in comparison to the compact Ni- and ZnAl LDH layers (Fig. 23).

Kuznetsov et al. applied the concept on tartaric sulphuric anodized (TSA) AA2024 [244] (Fig. 24 a). The bilayer system was investigated by SEM and glow discharge optical emission spectroscopy (GDOES) and the results have shown that the LDH covers the surface and fills the pores of the anodic layer. It was clearly demonstrated that the active sealing enhances the overall corrosion performance and ensures an effective healing of artificial defects, which was clearly demonstrated by salt spray test according to the ISO 9227 standard (Fig. 24 b).

In an analogue work, Mata et al. suggested the fabrication of LiAl LDH on TSA anodized AA2024 instead of ZnAl LDH films [44]. The authors performed a screening of some important synthesis parameters such as temperature and pH to identify the most suitable conditions to grow LiAl LDH with improved structural and corrosion performance. At the end of this investigation, the authors claimed that LiAl LDH intercalated with vanadate can be prepared at low temperatures such as 55°C and 25°C and the resulting coating has shown efficient corrosion protection guarantied both

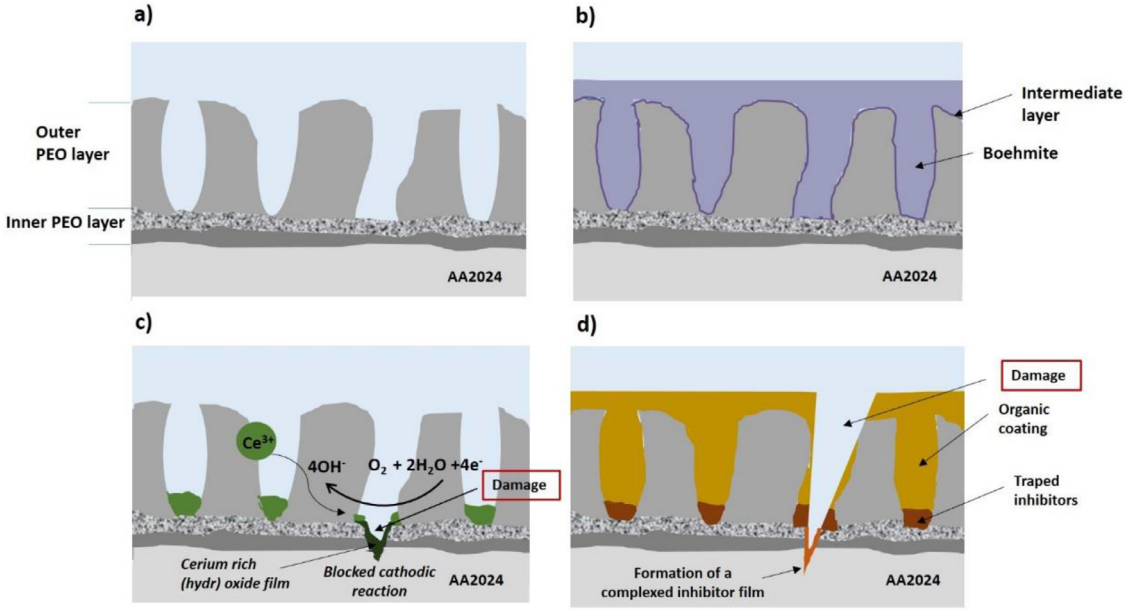

Fig. 22. Schemes representing (a) an anodized AA2024 without sealing, (b) with hot water/steam sealing, (c) with REMS (cerium) sealing and (d) with organic coating and inhibitors sealing. (Reprinted with permission from [361]).

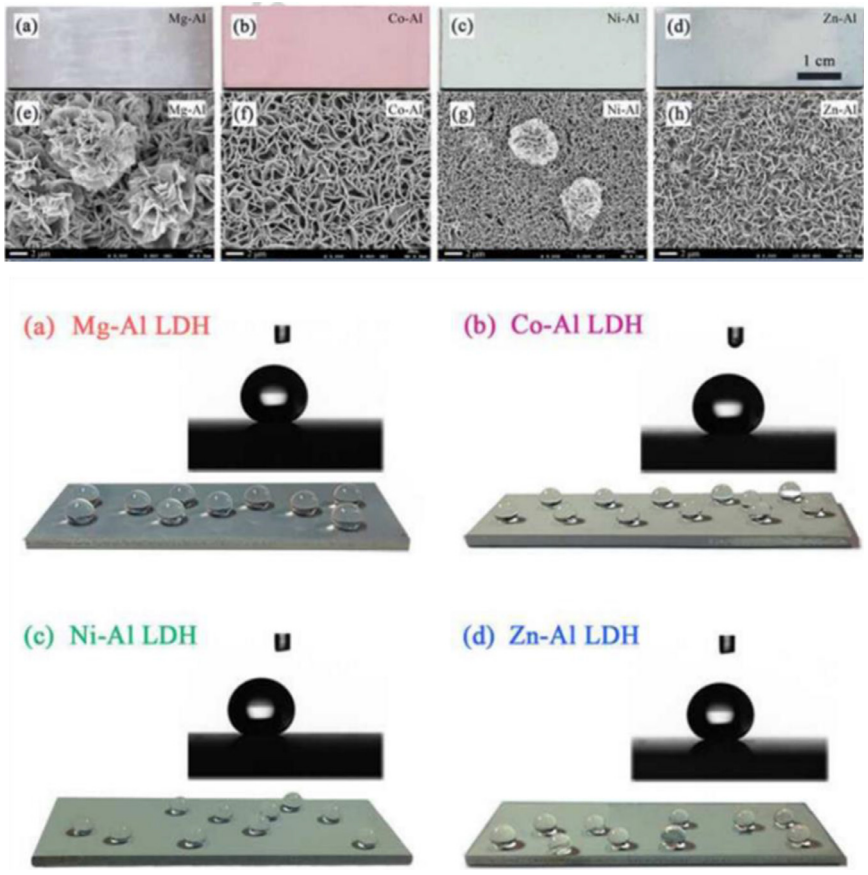

Fig. 23. Photographs of Mg-Al (a), Co-Al (b), Ni-Al (c), Zn-Al LDH (d) films with their corresponding SEM morphologies of (e)-(h) after surface modification with PFDTMS. (Reprinted with permission from [365])

by a barrier and active self-healing effect. These results demonstrate the superiority of LiAl LDH coatings over the conventional hot water sealing since they can be prepared at lower temperature and still demonstrate good corrosion resistance. Liu et al. compared the performance of anodized 2Al2 alloy when treated with NiCeAl- and ZnCeAl LDH films [366]. It was revealed that due to their strong interlayer interaction and compact structure, NiCeAl LDH containers can host more vanadate inhibitors, hence demonstrating a higher corrosion resistance in comparison to ZnCeAl LDH. This work highlights the influence of the divalent cations on the LDH structure in promoting corrosion protection. In the same perspective, MgCeAl LDH-CC were prepared on HWS anodized AA6082 [367]. EIS measurements showed enhanced corrosion resistance with the implementation of the Ce the LDH interlayers, even after 1200h. This concept was subsequently improved with an addition superhydrophobic treatment with 1H, 1H, 2H, 2H perfluorododecyl trichlorosilane (PFDTS) [368]. In the latter study, the AA6082 was first anodized using a hydrosulfuric acid solution. The obtained anodic layer was further treated with a MgCeAl LDH-CC followed by a dipping in a PFDTS based solution. The final CA of the PFDTS treated LDH was estimated to be close to 155.6°. The results of the electrochemical investigation revealed a long-lasting corrosion resistance that also goes beyond 1200 h.

4.3.2.2. Plasma electrolytic oxidation (PEO). Another possible application is the formation of LDH on the surface of plasma electrolytic oxidation (PEO) coated aluminum surfaces. PEO is an advanced anodizing process where ceramic-like coatings are formed at high voltages in low-concentrated eco-friendly alkaline electrolytes with visible short-lived micro discharges over the alloy surface [369]. The oxide layers developed by PEO are hard, well-adherent to the substrate and improve both corrosion and wear properties of the Al alloys [370–372]. However, similarly to conventional anodizing, PEO coatings always show a porous structure that can compromise the properties of the coating. In order to address this issue, several attempts have been made including selection of optimized current/voltage regimes and post-treatments [371,373–375]. Nevertheless, none of these attempts promote active protection to the ceramic layers nor does it prevent the porosity.

Serdechnova et al. have shown that ZnAl LDH layer *in-situ* grown and loaded with vanadate as corrosion inhibitor on a phosphate/silicon based-PEO covered AA2024 aluminum alloy, allows to achieve “smart” active corrosion protection (Fig. 25 a and b) [314]. The synthesis of the LDH films was carried out by simple co-precipitation method with the same conditions employed by Kuznetsov et al. [244]. EIS and SVET results have demonstrated self-healing ability for the specimen containing vanadate inhibitor.

The possibility to use LDH nanocontainers as a post-sealing treatment has generated a lot of interest, and more studies have been performed in order to understand the factors/parameters of both the PEO and LDH preparation process that could influence the LDH growth. For instance, in an attempt to prepare NiAl LDH film on AA6061, Dou et al. [376] noticed that LDH would preferably grow on the γ-Al_2O_3 rather than the α-Al_2O_3 phases composing the PEO coatings. To support their argument, the authors first noted that LDH formation dominated in areas where the molten alumina had a higher cooling rate, and the latter areas are claimed to be mainly composed of the γ-Al_2O_3 phase. Secondly, they claimed that the A1-O-A1bond energy of α-Al_2O_3 is greater than that of γ-Al_2O_3 which means that Al is unlikely to be dissolved from the α-Al_2O_3. To further prove their point, XRD and FT-

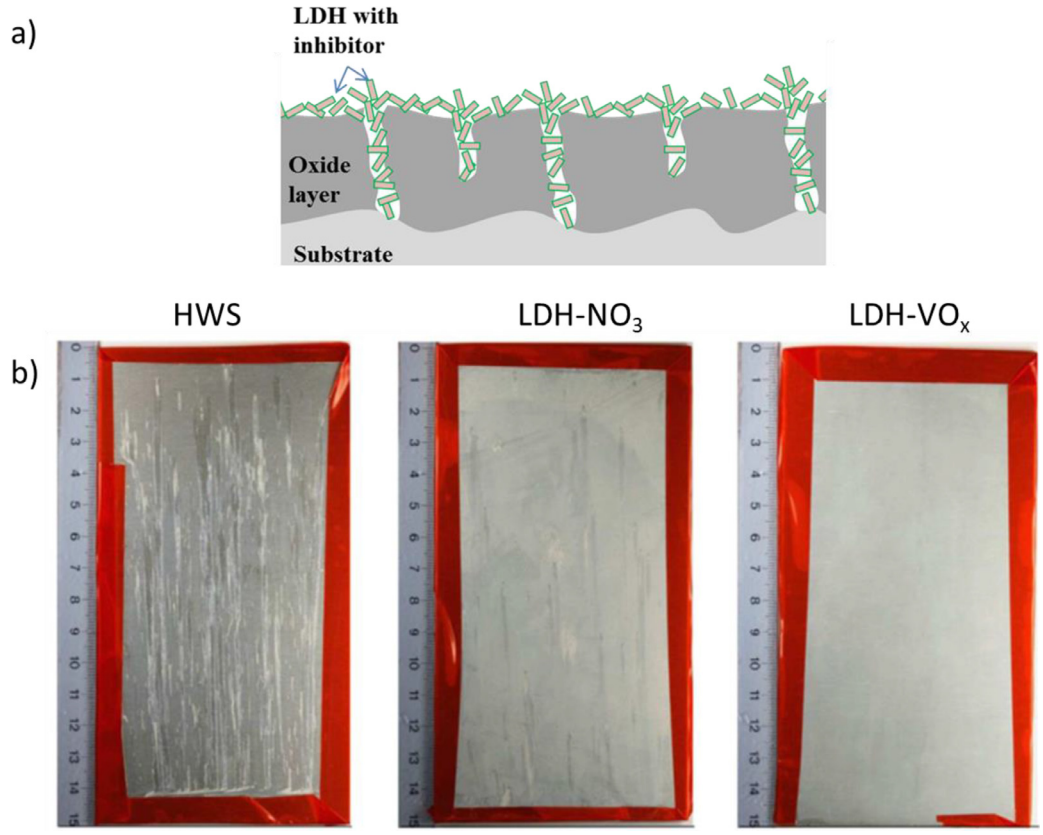

Fig. 24. Schematic representation of anodized layer sealed with LDH loaded with inhibitor (a) and Photographs of samples HWS, LDH-NO_3 and LDH-VO_x after 168 h exposure to salt spray test according to ISO 9227 (b). (Reprinted with permission from [244]).

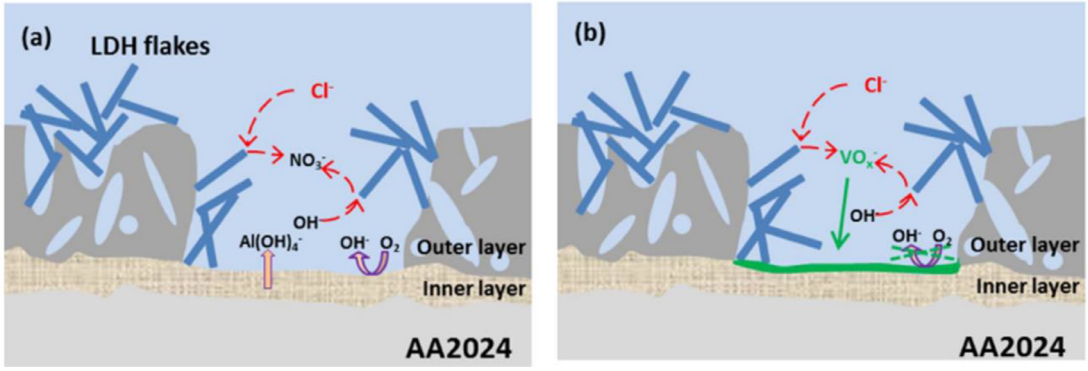

Fig. 25. The possible mechanism of active corrosion protection of PEO sample with LDH-NO_3 (a) and PEO sample with LDH-VO_x (b).(Reprinted with permission from [314]).

IR measurements were achieved on α-Al_2O_3 and γ-Al_2O_3 powders before and after they were subjected to LDH growth. The (003) and (006) XRD reflections associated with the NiAl LDH were much more intense for the LDH formed on γ-Al_2O_3 then on α-Al_2O_3. The FT-IR also showed stronger absorption peaks for NiAl-LDH on γ- Al_2O_3 in comparison to NiAl LDH formed on α-Al_2O_3.

Mohedano et al. conducted a detailed investigation on the influence of PEO voltage on the LDH growth [377]. Four voltages were selected (350 V, 400 V, 450 V and 500 V) and the higher the voltage, the thicker was the resulting PEO coating. Using SEM, XRD and GDEOS, the authors demonstrated that LDH growth was very limited in the case of PEO coatings obtained at higher voltages. Although the thicker PEO coatings demonstrated better corrosion performance, they could not be supported by the active corrosion protection provided by vanadate loaded LDH nanocontainers. It was also argued that not only the α-Al_2O_3 phase is unfavorable to LDH growth but γ-Al_2O_3 phase rendered the dissolution impossible as well. In other words, no recrystallization would allow the formation of LDH [378]. However, the results of this study did not reveal a complete explanation in respect to the relation between PEO parameters and LDH growth. Therefore, the same group of researchers published another study dedicated to the understanding of the influence of the PEO phase composition, prepared on AA2024, on the in-situ LDH growth [80]. The main conclusions drawn from the investigation are the following: a) both crystalline α-Al_2O_3 and γ-Al_2O_3 phases are unfavorable to LDH growth, while natural amorphous Al_2O_3 and the PEO inner layer would facilitate the LDH growth, b) the tortuosity of the PEO layer together with

the accessibility to $Al(OH)^{-}_{4}$ (see Eqs. (16) and (18)) are the limiting factors for LDH formation. Therefore, for optimized results, a compromise needs to be found between these conditions.

In a different study, Zhang et al. [379] questioned the influence of the elements composing the PEO coating rather than its morphology. It was found that, LDH films produced on the PEO coating formed in a $NaAlO_2$ electrolyte were more uniformly distributed and dense in comparison to the ones prepared on a Na_2SiO_4 based PEO. Moreover, the removal of the Si enriched surface by polishing the PEO outer layer, also contributed positively to the LDH-CC formation. In other words, the presence of silicon impedes the nucleation and growth of LDH layers.

Recently, a systematic study was carried out by del Olmo et al. [380]. Several preparation parameters for both PEO and LDH were tested to obtain an optimized LDH treated PEO coating on AA1050-H18 substrate. The investigation showed that a continuous and well-defined LDH layer can be obtained when the thickness of PEO coatings is ~1 µm. This is due to an easy access to $Al(OH)^{2+}$ cations. Moreover, the corrosion resistance evaluation of the LDH treated PEO coatings revealed that the ZnAl LDH intercalated with NO_3^- alone, does not contribute in enhancing the corrosion protection of the PEO coated substrate. The only way to reinforce the corrosion protection, is by loading the LDH nanocontainers with efficient corrosion inhibitors such as vanadate.

The above studies [80,379,380] summarized a few conditions that need to be met in order to be able to grow LDH on a PEO coated Al alloy. However, it is important to resolve situation where LDH growth on certain PEO coatings remains challenging. A potential answer would be to find a new source for Al^{3+} cations. In a very recent work, the formation of a xerogel layer was added between the steps of PEO treatment and LDH post-treatment, aiming at creating a new source for Al^{3+} [20]. The PEO coating on AA2024 was prepared at constant voltage mode with 450 V, 10 min and 0.5 A, and these chosen conditions were qualified as unsuitable for LDH growth [80,377]. However, after the addition of the xerogel layer seconded by an LDH treatment, a homogeneous and compact layer of LDH was formed over the xerogel modified PEO coating. The xerogel formation relies on the dissolution of the metal salt dominated by hydrolysis followed by condensation reactions:

- Aluminum oxide gel formation:

$$Al\ (NO_3)_3 \cdot 9H_2O \rightleftharpoons [Al\ (H_2O)_6]^{3+} + 3NO_3^- \quad (22)$$

$$[Al(H_2O)_6]^{3+} \rightleftharpoons [Al(H_2O)_6](OH)_a^{(3-a)+} \underset{-H_2O}{\rightarrow} Al_xO_y(OH)_z \cdot nH_2O \quad (23)$$

- Hydrolysis reaction

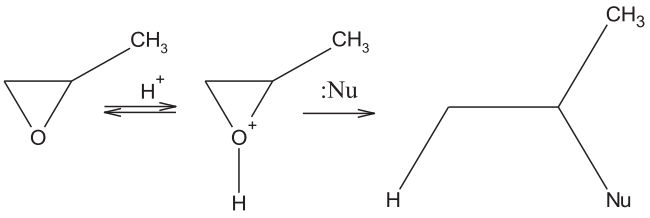

(24)

Nucleophile $(Nu) = NO_3^-,\ H_2O$

After formation of the xerogel layer on the PEO coated AA2024, the ZnAl LDH-NO_3 synthesis can take place according to:

$$Al_xO_y(OH)_z.nH_2O + H_2O + OH^- \rightarrow xAl(OH)_4^- \quad (25)$$

$$Zn^{2+} + OH^- \rightarrow Zn(OH)^+ \quad (23)$$

$$Zn(OH)^+ + xAl(OH)_4^- + NO_3^- + H_2O \rightarrow \boldsymbol{LDH - NO_3} \quad (26)$$

Although a slight corrosion improvement was observed with the samples treated with ZnAl LDH intercalated with vanadate, the performance was not significantly better in comparison to other LDH treated coatings [44,314,377]. However, this groundwork allows to broaden the possibilities of LDH growth on different treated surfaces.

All relevant studies associated with the LDH treatment of conventional anodized and PEO treated Al alloys were summarized in Table 6.

5. Implementation of LDH in industry

LDH presents a number of attractive features e.g. anion-exchange, insertion of various elements into the structure, calcination/rehydration, thermostability, surface modification etc., that found use in various applications such as catalysis, energy and corrosion protection, as discussed in this review paper. Another important advantage of LDH is that they are easy to manipulate, cost-effective and conform to REACH regulations. These factors make their implementation into industrial applications very feasible. It is important to point out that LDH in form of slurry/powder is already being produced in large scales by several companies. For example, SASOL GmbH have a list of products such as the trademark products PLURAL® (based on MgAl LDH) which are produced through a patented [381] metal alcoholate route [382]. Their product is largely applied as a catalyst support for the heterogeneous catalysis industry. SINWON chemical Co., LTD., produced a series of non-toxic and heavy metal free LDH pigment (mainly MgAl LDHs), that are commercialized as neutralizing agents for Polyolefin, heat stabilizers for halogenated polymers (e.g. PVC), heat-retaining agent for agricultural films and flame retardant [383].

In the context of corrosion protection, LDH is still in the process of development. However, there are a few companies that have dedicated their R&D to focus in this area of expertise. For instance, KISUMA Chemicals [384], a world leader in the production of hydrotalcites, possesses a branch specifically devoted to the development and optimization of LDH pigments for corrosion protection. They aim mostly is to improve the barrier properties of polymers and provide better encapsulation solutions [384]. Another company, SMALLMATEK Lda. [385], produces and performs research on LDH additives mainly for the purpose of corrosion protection. Their pigments can be incorporated into coatings and integrated in a multi-level corrosion protective framework.

The latter examples are not the only ones, BASF Coating GmbH has also shown interest in the development of LDH particles for corrosion protection. The company has been collaborating with research groups and exploring ways to use these pigments, especially on automotive coatings [17,54,386]. More recently, AkzoNobel Coatings GmbH has proposed a novel alternative to chromate-based coatings that is based on lithium technology. The concept has been discussed earlier in the section of LDH as functional coatings for bare Al alloys [315,353,356]. The idea is to provide a self-healing property to a coating by a triggered (e.g. scratch) leaching of Li salts from a polymer matrix which would react with the interface (e.g. dissolved Al) and form a LDH protective layer on the area of the damage. This patented method is commercially available for the corrosion protection of aeronautical parts [387,388].

Since the first reports on the use of LDH for corrosion protection [9–11] till recently, important progress has been made in terms of process parameters, morphology and implementation in multi-level corrosion protective systems. In this review only case studies on Al alloys have been cited, however the use of LDH has been applied successfully to various metal substrates such as zinc [81,248], steel [53,246,389,390], iron and Mg alloys [38,245,391–

Table 6
Overview of the LDH treatment performed on conventional anodized and PEO treated Al alloys.

Al Alloy	Anodizing treatment	LDH treatment		Intercalation/ surface Modification		Properties	Ref.
		Method	Type	Method	Anion		
Conventional anodizing							
Pure Al (99.5 .wt %)	Anodizing in H_2SO_4/thick.: undefined	Co-precip. (45°C, pH 6.5, 36 h)	ZnAl/ NO_3	Anion exchange	Laurate	Sealing, Superhydrophobicity and anticorrosion/LDH thick.: 0.27–0.30 μm	[240]
AA2198	Anodizing in H_2SO_4 /thick: undefined	Co-precip. (45°C, pH ~7, few h)	ZnAl/ NO_3	Anion exchange	VO_3^-	Sealing, active corrosion protection	[364]
AA2198	Anodizing in H_2SO_4 /thick: undefined	Co-precip. (45°C, pH ~7, few h)	Zn-, Mg-, Ni- and CoAl/ NO_3	Surface treatmnet/ adsorption	PFDTMS	Sealing and Superhydrophobocity	[365]
AA2024-T3	TSA anodizing/ thick:3 μm	Co-precip. (95°C, pH 6.5, 30 min)	ZnAl/ NO_3	Anion exchange	VO_x^{n-}	Sealing and active corrosion protection	[244]
AA2024-T3	TSA anodizing/ thick:3 μm	Co-precip. (25-95°C, pH 9-12, 30 min)	LiAl/ NO_3 LiAl/ (OH) (CO_3)	Anion exchange	VO_x^{n-}	Sealing and active corrosion protection/ LDH thick.: 1–2.2 μm	[44]
2Al2	Anodizing in oxalic acid/thick ~ 3 μm	Co-precip. (80°C, pH 9.3 ± 0.2, 6 h)	ZnAl/ NO_3 NiAl/ NO_3	Anion exchange	Ce^{3+}/ Ce^{4+} dopping + VO_4^{3-}	Sealing and active corrosion protection/ LDH thick.: 3–10 nm	[366]
AA6083	Anodizing in H_2SO_4 + HWS	Co-precip. (80°, 18-24h)	MgAl/NO_3		Ce^{3+} /Ce^{+4} dopping	Sealing and active corrosion protection/ anodic+LDH thick: 28.6-33.3 μm	[367]
AA6083	Anodizing in H_2SO_4	Co-precip. (40°C, 2h)	MgAl/NO_3	Ion-exchange	PFDTS	Sealing, active corrosion protection and superhydrophobicity/ anodic+LDH: 32 ±3.5 μm.	[368]
Plasma electrolytic oxidation							
AA2024-T3	PEO (Na_2SiO_3 +$Na_2H_2P_2O_7$ +NaOH) /thick: 3-6 μm	Co-precip. (95°C, pH 6.5,30 min)	ZnAl/ NO_3	Anion exchange	VO_x^{n-}	Sealing and active corrosion protection	[314]
AA6061	PEO (Na $_2SiO_3$ + $(NaPO_3)_6$+ Na_2WO_4 +KOH)/ thick ~ 20 μm	Co-precip. (80°C, pH 7, 1-48 h)	NiAl/ NO_3			(Parameter study) γ-Al_2O_3 more favorable to LDH growth than α-Al_2O_3	[376]
AA2024	PEO (Na $_2SiO_3$ +$Na_2H_2P_2O_7$ +NaOH) /thick: 1-6 μm	Co-precip. (95°C, pH 6.5,30 min)	ZnAl/ NO_3	Anion exchange	VO_x^{n-}	(Parameter study) Thicker PEO coatings decrease probability of LDH growth.	[377]
AA2024	PEO (Na $_2SiO_3$ + $Na_2H_2P_2O_7$ or Na_3PO_4 +NaOH) /thick: 1-50 μm	Co-precip. (95°C, pH 6.5,30 min)	ZnAl/ NO_3			(Parameter study) α-Al_2O_3 and γ-Al_2O_3 unfavorable to LDH growth.	[80]
AA2024	PEO (Na_2SiO_3 + KOH) or ($NaAlO_2$ + KOH)/ thick: undefined	Co-precip. (70°C, pH 6.4, 0.16 -24 h)	ZnAl/ NO_3			(Parameter study) $NaAlO_2$ electrolyte more favorable to LDH growth.	[379]
AA1050-H18	Flash PEO (various electrolytes)/ thick: 1-2.5 μm	Co-precip. (95°C, pH 6.5, 30-60 min)	ZnAl/ NO_3			(Parameter study) Low porosity of flash PEO Well defined LDH for PEO with thick ~ 1 μm	[380]
AA2024	PEO (Na $_2SiO_3$ +Na_3PO_4 +KOH) /thick: 50 μm	1) Xerogel formation/thick:330nm 2) LDH: co-precip. (95°C, pH 6.5, 30 min)	ZnAl/ NO_3	Anion exchange	VO_x^{n-}	New source for LDH formation. Sealing and active corrosion protection	[20]

395]. This is an important feature of LDH since it could be advantageous for a wide range of industrial applications.

Nevertheless, there is still room for improvement when it comes to operating conditions, such as processing time and temperature, stability in various conditions (e.g. different pH ranges) and coating compatibility and adhesion performance. These are just a few points among others to overcome, but this was the case for most innovation technologies at the first stage of its development. A summary of the LDH (in form of pigments and conversion coatings) properties and advantages is provided in Table 7.

Table 7
Overview of the LDH pigments and LDH-CC properties and advantages

Properties	LDH pigments	Ref.	LDH-CC	Ref.
Synthesis /processing	- Possibility for preparation at 60°C > T and reduced synthesis and ageing time. - Requires no additional accelerators. - Diversity of preparation methods. - Possible formation of unwanted products but may be avoided by optimizing processing condition. - Waste highly dependent on the precursors used for LDH preparation, but overall non-toxic. (See below) - Interestingly LDH pigments are used to recycle waste and minimize sludges generated from other industrial processes.	[242,396–399]	- Possibility of preparation at RT and with reduces processing time depending on the precursors. - Requires no additional accelerators. - Unwanted products can be easily avoided. - Waste highly dependent on the precursors but overall is minimal and non-toxic	[338, 359]
pH stability	- LDH release mechanism can be induced by anion exchange at basic medium or by dissolution in acid medium. However, the dissolution is not always desired and depends on the composition of the hydroxide layers cations and the interlayer anions. - The optimum pH range of obtaining LDH can be interpreted as the optimum domain of existence/stability of LDH, which can be summarized for various LDH types as: - pH 4.5 < LDH stability < pH 11.5	[400,401]	- Similarly, to the LDH pigments, the risk of dissolution in acidic environments may compromise their corrosion protection abilities. - Not much studies have been performed in investigating the pH influence on LDH -CC performance.	[402]
Compatibility	- This parameter can be related to the pH stability of LDH pigments and their ability to mix well with organic coatings. Several LDH surface modifications were proposed to overcome this problematic and good results were achieved. - Non-compatibility of LDH pigments may impede their good functionality. - Compatibility also depends on the concentration used in the organic coating. Reported concentration from 2 to 15 % of LDH pigment in polymer coatings were used	[15,17,54–56,286,300,304–306,308–310]	- The reported studies on subsequent addition of organic coating on LDH-CC do not show any incompatibility issues. - The surface modifications achieved on LDH-CC to obtain hydrophobic properties is an indication that this pathway can be followed to promote further compatibility with subsequent organic coatings.	[287,312,343,344,346]
Adhesion/risk of disbonding	- The risk of disbonding due to the addition of LDH pigments into an organic coating was often pointed out. This is also related to the above compatibility factor. However, the risk has been minimized with the recent development in this field.	[18, 286]	- The adhesion tests performed on LDH-CC with or without subsequent addition of organic coatings demonstrated reasonable results. - Moreover, as mentioned above, improving the compatibility by LDH-CC surface modification can enhance adhesion and minimize the risk of disbonding. - The combination of anodized Al alloy and LDH-CC can ensure further strengthening of the adhesion properties.	[287,337,346]

(*continued on next page*)

Table 7 (*continued*)

Properties	LDH pigments	Ref.	LDH-CC	Ref.
Corrosion protection mechanism	- Active corrosion protection/Self-healing through inhibitor release or reconstruction - Corrosion sensing - Aggressive anions trapping (eg. Cl^-, SO_4^{2-}) - Some studies reported comparable to better corrosion resistance from LDH pigments in comparison to Cr(VI) pigments.	[15,18,34, 35,83,238, 289,299]	- Active corrosion protection/Self-healing through inhibitor release or reconstruction - Corrosion sensing - Aggressive anions trapping (eg. Cl^-, SO_4^{2-}) - Barrier protection - Post treatment /sealing - Hydrophobicity - LDH-CC corrosion resistance performance was reported to be comparable to better than CCC.	[8,9,20,46, 48,80,240, 244,312,313, 315,338,355, 356,364-367,377,380, 387]
Toxicity	- Some of the LDH pigments used for corrosion protection applications are also considered for drug delivery therefore they were cleared for any risk of toxicity. However, more studies should be performed in this direction.	[403,404]	- The toxicity data available for LDH pigments are also applicable for LDH-CC	
Applicability to metals	- Aluminum alloys, magnesium alloys, zinc and different steels	[12,13,299, 389,395, 405–413]	- Aluminum alloys, magnesium alloys, zinc and electrogalvanized stainless steel	[10,48,81, 244–246,248, 314,390, 414–416]
Cost and availability	- Depending on the precursors used to synthesis LDH pigments, they can be cost effective and widely available. A few types of LDH pigments are also readily available in nature. - The energy consumption required for LDH synthesized can be minimized by an optimization of the synthesis parameters (e.g. lowering the temperature) - Only low amounts of LDH pigments is needed to provide corrosion protection	[18,54,55]	- The cost- effectiveness of LDH-CC is dependent on the starting precursors and the synthesis process parameters. - Lower concentration of cation in addition to inhibitors used for LDH-CC synthesis have proven to provide efficient corrosion inhibition. - Optimized LDH synthesis parameters have also shown promising results in terms of corrosion protection.	[44,338,354, 355,359]

6. Conclusions and outlook

Throughout the different sections of this review, layered double hydroxides have shown promising results in the area of corrosion protection. Their aptitude to demonstrate sensing, nanotrapping, barrier and active corrosion protection properties make them potential alternatives to the traditional chromate-based coating. LDH can either be used as pigments or as conversion coatings for the corrosion protection of Al alloys. This means that their use can be adjusted according to the desired outcome. They can be used to compensate the lack of active corrosion protection of a barrier coating (e.g. organic coating) or serve as the first functional protective layer of an Al alloy. Indeed, remarkable results have been obtained on the latter applications with a continuous improvement.

LDH has already filled a few requirements to be considered as future replacement to Cr(VI)-based coatings. Indeed, in addition to the proven anti-corrosion performance, LDH has the advantage to be environmentally friendly, cost effective, accessible and applicable to a wide range of metal substrates. Nonetheless, LDH is not the only emerging alternative to chromate and, therefore, need to fit into other requirements such as processing parameters, compatibility with other coatings and adhesion performance. These factors can be overcome by further optimization of the LDHs both in form of pigments and conversion coatings. It is important to perform more systematic studies on environmentally friendly inhibitors that could be intercalated, since they are the main feature for active corrosion protection funtionality. These studies should include modelling approaches to build a data base that would facilitate the access to the synthesis parameters and anion-exchange, which would help to obtain the best outcome in terms of active corrosion protection. The other point is to test LDH in a multi-level protective frame. The simulation of a real multi-layer coating system would be important to anticipate issues related to adhesion/disbonding or blistering caused by lack of compatibility.

Declaration of Competing Interest

No competing interests can be declared.

Acknowledgements

This work was the result of the participation of several projects namely the European FP7 project “PROAIR” (PIAPP-GA-2013-612415), the European project MULTISURF and FUNCOAT in frame of the H2020-MSCA-RISE, grant agreement No 645676 and No 823942, respectively.

M.S. and M.L.Z. are also thankful to I2B fond for financial support of this work in frame of MUFfin project as well as the ACTICOAT project (Era.Net RUS Plus Call 2017, Project 477).

This work was also financed by Portugal 2020 through European Regional Development Fund (ERDF) in the frame of Operational Competitiveness and Internationalization Programme (POCI), in the scope of the project MAGICOAT POCI-01-0145-FEDER-016597 / PTDC/CTM-BIO/2170/2014 and in the scope of the project CICECO-Aveiro Institute of Materials, POCI-01-0145-FEDER-007679 (FCT Ref. UID/CTM/50011/2013), and co-financed by national funds through the FCT/MEC.

Data availability

No datasets were generated or analyzed during the current study.

ASTM B117-16	Standard Practice for Operating Salt Spray (Fog) Apparatus
ASTM D3163	Standard Test Method for Determining Strength of Adhesively Bonded Rigid Plastic Lap-Shear Joints in Shear by Tension Loading
ASTM D4585-99	Standard Practice for Testing Water Resistance of Coatings Using Controlled Condensation
ASTM D714-56	Standard Method of Evaluating Degree of Blistering of Paint
GBT9286-1998	Paints and varnishes-Cross cut test for films
ISO 9227	Corrosion tests in artificial atmospheres — Salt spray tests

References

[1] S.L. Suib, Zeolitic and layered materials, Chem. Rev 93 (1993) 803–826, doi:10.1021/cr00018a009.
[2] D. Levin, S.L. Soled, J.Y. Ying, Chimie douce synthesis of nanostructured layered materials, ASC 622 (1996) 237–249, doi:10.1021/bk-1996-0622.ch016.
[3] E.G. David, R.C. Slade, Structural aspects of layered double hydroxides, in: Layered Double Hydroxides, Springer, Berlin, Heidelberg, 2006, pp. 1–87, doi:10.1007/430_005.
[4] X. Duan, D.G. Evans eds., Layered Double Hydroxides, 119, Springer Science & Business Media, 2006.
[5] G. Centi, S. Perathoner, Catalysis by layered materials: A review, Micropor. Mesopor. Mat 107 (2008) 3–15, doi:10.1016/j.micromeso.2007.03.011.
[6] F. Annabi-Bergaya, Layered clay minerals. Basic research and innovative composite applications, Micropor. Mesopor.Mat. 107 (2008) 141–148, doi:10.1016/j.micromeso.2007.05.064.
[7] D.E.L. Vieira, D. Sokol, A. Smalenskaite, A. Kareiva, M.G.S. Ferreira, J.M. Vieira, A.N. Salak, Cast iron corrosion protection with chemically modified MgAl layered double hydroxides synthesized using a novel approach, Surf. Coat. Technol 375 (2019) 158–163, doi:10.1016/j.surfcoat.2019.07.028.
[8] R.G. Buchheit, M.D. Bode, G.E. Stoner, Corrosion-resistant, chromate-free talc coatings for aluminum, Corrosion 50 (1994) 205–214, doi:10.5006/1.3293512.
[9] R.G. Buchheit, S.B. Mamidipally, P. Schmutz, H. Guan, Active corrosion protection in Ce-modified hydrotalcite conversion coatings, Corrosion 58 (2002), doi:10.5006/1.3277303.
[10] R.B. Leggat, W. Zhang, R.G. Buchheit, S.R. Taylor, Performance of hydrotalcite conversion treatments on AA2024-T3 when used in a coating system, Corrosion 58 (2002) 322–328, doi:10.5006/1.3287681.
[11] W. Zhang, R.G. Buchheit, Hydrotalcite coating formation on Al-Cu-Mg alloys from oxidizing bath chemistries, Corrosion 58 (2002) 591–600, doi:10.5006/1.3277650.
[12] H.N. McMurray, G. Williams, Inhibition of filiform corrosion on organic-coated aluminum alloy by hydrotalcite-like anion-exchange pigments, Corrosion 60 (2004) 219–228, doi:10.5006/1.3287724.
[13] G. Williams, H.N. McMurray, Inhibition of filiform corrosion on polymer coated AA2024-T3 by hydrotalcite-like pigments incorporating organic anions, Electrochem. Solid-State Lett 7 (2004) B13–B15, doi:10.1149/1.1691529.
[14] M. Kendig, M. Hon, A hydrotalcite-like pigment containing an organic anion corrosion inhibitor, Electrochem. Solid-State Lett 8 (2005) B10–B11, doi:10.1149/1.1857743.
[15] M.L. Zheludkevich, S.K. Poznyak, L.M. Rodrigues, D. Raps, T. Hack, L.F. Dick, T. Nunes, M.G.S. Ferreira, Active protection coatings with layered double hydroxide nanocontainers of corrosion inhibitor, Corros. Sci 52 (2010) 602–611, doi:10.1016/j.corsci.2009.10.020.
[16] J. Tedim, S.K. Poznyak, A. Kuznetsova, D. Raps, T. Hack, M.L. Zheludkevich, M.G.S. Ferreira, Enhancement of active corrosion protection via combination of inhibitor-loaded nanocontainers, ACS Appl. Mater. Inter 2 (2010) 1528–1535, doi:10.1021/am100174t.
[17] T. Stimpfling, F. Leroux, H. Hintze-Bruening, Organo-modified layered double hydroxide in coating formulation to protect AA2024 from corrosion, Colloids. Surfaces. A 458 (2014) 147–154, doi:10.1016/j.colsurfa.2014.01.042.
[18] R. Subasri, K.S. Raju, D.S. Reddy, A. Jyothirmayi, V.S. Ijeri, O. Prakash, S.P. Gaydos, Environmentally friendly Zn–Al layered double hydroxide (LDH)-based sol–gel corrosion protection coatings on AA 2024-T3, J. Coat. Technol. Res. 16 (2019) 1447–1463, doi:10.1007/s11998-019-00229-y.
[19] M.A. Zadeh, J. Tedim, M.L. Zheludkevich, S. Van der Zwaag, S.J. Garcia, Synergetic active corrosion protection of AA2024-T3 by 2D-anionic and 3D-cationic nanocontainers loaded with Ce and mercaptobenzothiazole, Corros. Sci 135 (2018) 35–45, doi:10.1016/j.corsci.2018.02.018.
[20] A.C. Bouali, E.A. Straumal, M. Serdechnova, D.C.F. Wieland, M. Starykevich, C. Blawert, M.L. Zheludkevich, Layered double hydroxide based active corrosion protective sealing of plasma electrolytic oxidation/sol-gel composite coating on AA2024, Appl. Surf. Sci 494 (2019) 829–840, doi:10.1016/j.apsusc.2019.07.117.
[21] W.F. Foshag, The chemical composition of hydrotalcite and the hydrotalcite group of minerals, Proc. U. S. Natl. 58 (1920) 147–153.
[22] S.J. Mills, A.G. Christy, R.T. Schmitt, The creation of neotypes for hydrotalcite, Mineral. Mag 80 (2016) 1023–1029, doi:10.1180/minmag.2016.080.040.
[23] T. Stanimirova, Hydrotalcite polytypes from Snarum, Norway, Ann. Univ. Sofia, Faculty Geol. 94 (2001) 73–80.
[24] C. Frondel, Constitution and polymorphism of the pyroaurite and sjogrenite groups, Am. Mineral. J. Earth Planetary Mater. 26 (1941) 295–315.

[25] R. Allmann, The crystal structure of pyroaurite, Acta. Crys. B 24 (1968) 972–977, doi:10.1107/S0567740868003511.
[26] H.F.W. Taylor, Crystal structures of some double hydroxide minerals, Mineral. Mag 39 (1973) 377–389, doi:10.1180/minmag.1973.039.304.01.
[27] H.F.W. Taylor, Segregation and cation-ordering in sjögrenite and pyroaurite, Mineral. Mag 37 (1969) 338–342, doi:10.1180/minmag.1969.037.287.04.
[28] H.F.W. Taylor, The rapid formation of crystalline double hydroxy salts and other compounds by controlled hydrolysis, Clay. Miner 19 (1984) 591–603, doi:10.1180/claymin.1984.019.4.06.
[29] G. Mishra, B. Dash, S. Pandey, Layered double hydroxides: A brief review from fundamentals to application as evolving biomaterials, Appl. Clay. Sci. 153 (2018) 172–186, doi:10.1016/j.clay.2017.12.021.
[30] A. Legrouri, M. Badreddine, A. Barroug, A. De Roy, J.P. Besse, Influence of pH on the synthesis of the Zn–Al–nitrate layered double hydroxide and the exchange of nitrate by phosphate ions, J. Mater. Sci. Lett. 18 (1999) 1077–1079, doi:10.1023/A:1006647505203.
[31] X. Xie, X. Ren, J. Li, X. Hu, Z. Wang, Preparation of small particle sized ZnAl-hydrotalcite-like compounds by ultrasonic crystallization, J. Nat. Gas Chem 15 (2006) 100–104, doi:10.1016/S1003-9953(06)60015-7.
[32] S.P.V. Mahajanam, R.G. Buchheit, Characterization of inhibitor release from Zn-Al-[V10O28] 6− hydrotalcite pigments and corrosion protection from hydrotalcite-pigmented epoxy coatings, Corrosion 64 (2008) 230–240, doi:10.5006/1.3278468.
[33] M.S. Yarger, E.M. Steinmiller, K.S. Choi, Electrochemical synthesis of Zn− Al layered double hydroxide (LDH) films, Inorg. Chem 47 (2008) 5859–5865, doi:10.1021/ic800193j.
[34] S.K. Poznyak, J. Tedim, L.M. Rodrigues, A.N. Salak, M.L. Zheludkevich, L.F.P. Dick, M.G.S. Ferreira, Novel inorganic host layered double hydroxides intercalated with guest organic inhibitors for anticorrosion applications, ACS Appl. Mater. Inter 1 (2009) 2353–2362, doi:10.1021/am900495r.
[35] J. Tedim, A. Kuznetsova, A.N. Salak, F. Montemor, D. Snihirova, M. Pilz, M.L. Zheludkevich, M.G.S. Ferreira, Zn–Al layered double hydroxides as chloride nanotraps in active protective coatings, Corros. Sci 55 (2012) 1–4, doi:10.1016/j.corsci.2011.10.003.
[36] E. Lopez-Salinas, Y. Ono, Intercalation chemistry of a Mg Al layered double hydroxide ion-exchanged with complex MCl2− 4 (M Ni, Co) ions from organic media, Micropor. Mater 1 (1993) 33–42, doi:10.1016/0927-6513(93)80006-G.
[37] N. Iyi, Y. Ebina, T. Sasaki, Water-swellable MgAl− LDH (layered double hydroxide) hybrids: synthesis, characterization, and film preparation, Langmuir 24 (2008) 5591–5598, doi:10.1021/la800302w.
[38] F. Wang, Z. Guo, Insitu growth of durable superhydrophobic Mg–Al layered double hydroxides nanoplatelets on aluminum alloys for corrosion resistance, J. Alloy. Comp. 767 (2018) 382–391, doi:10.1016/j.jallcom.2018.07.086.
[39] F. Prinetto, G. Ghiotti, P. Graffin, D. Tichit, Synthesis and characterization of sol–gel Mg/Al and Ni/Al layered double hydroxides and comparison with co-precipitated samples, Micropor. Mesopor. Mat. 39 (2000) 229–247, doi:10.1016/S1387-1811(00)00197-9.
[40] O.R.M. Neto, N.F. Ribeiro, C.A. Perez, M. Schmal, M.M. Souza, Incorporation of cerium ions by sonication in Ni–Mg–Al layered double hydroxides, Appl. Clay. Sci. 48 (2010) 542–546, doi:10.1016/j.clay.2010.02.015.
[41] M. Li, J.P. Cheng, J.H. Fang, Y. Yang, F. Liu, X.B. Zhang, NiAl-layered double hydroxide/reduced graphene oxide composite: microwave-assisted synthesis and supercapacitive properties, Electrochim. Acta 134 (2014) 309–318, doi:10.1016/j.electacta.2014.04.141.
[42] F.L. Theiss, G.A. Ayoko, R.L. Frost, Synthesis of layered double hydroxides containing Mg2+, Zn2+, Ca2+ and Al3+ layer cations by co-precipitation methods—A review, Appl. Surf. Sci 383 (2016) 200–213, doi:10.1016/j.apsusc.2016.04.150.
[43] E. Scavetta, B. Ballarin, M. Gazzano, D. Tonelli, D, (2009). Electrochemical behaviour of thin films of Co/Al layered double hydroxide prepared by electrodeposition, Electrochim. Acta 54 (2009) 1027–1033, doi:10.1016/j.electacta.2008.07.078.
[44] D. Mata, M. Serdechnova, M. Mohedano, C.L. Mendis, S.V. Lamaka, J. Tedim, T. Hack, S. Nixon, M.L. Zheludkevich, Hierarchically organized Li–Al-LDH nano-flakes: a low-temperature approach to seal porous anodic oxide on aluminum alloys, RSC. Adv 7 (2017) 35357–35367, doi:10.1039/C7RA05593E.
[45] T. Takei, A. Miura, N. Kumada, Soft-chemical synthesis and catalytic activity of Ni-Al and Co-Al layered double hydroxides (LDHs) intercalated with anions with different charge density, J. Asian Ceram. Soc. 2 (2014) 289–296, doi:10.1016/j.jascer.2014.06.002.
[46] Y. Zhang, J. Liu, Y. Li, M. Yu, S. Li, B. Xue, A facile approach to superhydrophobic LiAl-layered double hydroxide film on Al–Li alloy substrate, J. Coat. Technol. Res. 12 (2015) 595–601, doi:10.1007/s11998-015-9660-9.
[47] F. Zhang, C.L. Zhang, L. Song, R.C. Zeng, L.Y. Cui, H.Z. Cui, Corrosion resistance of superhydrophobic Mg–Al layered double hydroxide coatings on aluminum alloys, Acta. Metall. Sin. Engl 28 (2015) 1373–1381, doi:10.1007/s40195-015-0335-4.
[48] J. Tedim, M.L. Zheludkevich, A.N. Salak, A. Lisenkov, M.G.S. Ferreira, M. G. S., Nanostructured LDH-container layer with active protection functionality, J. Mater. Chem. 21 (39) (2011) 15464–15470, doi:10.1039/C1JM12463C.
[49] A.I. Khan, D. O'Hare, Intercalation chemistry of layered double hydroxides: recent developments and applications, J. Mater. Chem. 12 (2002) 3191–3198, doi:10.1039/B204076J.
[50] M. Serdechnova, A.N. Salak, F.S. Barbosa, D.E. Vieira, J. Tedim, M.L. Zheludkevich, M.G.S. Ferreira, Interlayer intercalation and arrangement of 2-mercaptobenzothiazolate and 1, 2, 3-benzotriazolate anions in layered double hydroxides: In situ X-ray diffraction study, J. Solid. State. Chem. 233 (2016) 158–165, doi:10.1016/j.jssc.2015.10.023.
[51] J. Carneiro, A.F. Caetano, A. Kuznetsova, F. Maia, A.N. Salak, J. Tedim, N. Scharnagl, M.L. Zheludkevich, M.G.S. Ferreira, Polyelectrolyte-modified layered double hydroxide nanocontainers as vehicles for combined inhibitors, RSC Adv. 5 (2015) 39916–39929, doi:10.1039/C5RA03741G.
[52] Y. Zhang, J. Liu, Y. Li, M. Yu, S. Li, B. Xue, Fabrication of inhibitor anion-intercalated layered double hydroxide host films on aluminum alloy 2024 and their anticorrosion properties, J. Coat. Technol. Res. 12 (2015) 293–302, doi:10.1007/s11998-014-9644-1.
[53] V. Shkirskiy, P. Keil, H. Hintze-Bruening, F. Leroux, P. Vialat, G. Lefèvre, K. Ogle, P. Volovitch, Factors affecting MoO42−inhibitor release from Zn2Al based layered double hydroxide and their implication in protecting hot dip galvanized steel by means of organic coatings, ACS Appl. Mater. Inter 7 (2015) 25180–25192, doi:10.1021/acsami.5b06702.
[54] T. Stimpfling, F. Leroux, H. Hintze-Bruening, Phosphate-based organic molecules interleaved with layered double hydroxide: unraveling the roles of host cations and the guest-inhibiting effect in aluminum corrosion protection, Eur. J. Inorg. Chem 2012 (2012) 5396–5404, doi:10.1002/ejic.201200504.
[55] T. Stimpfling, F. Leroux, H. Hintze-Bruening, Unraveling EDTA corrosion inhibition when interleaved into Layered Double Hydroxide epoxy filler system coated onto aluminum AA 2024, Appl. Clay. Sci. 83 (2013) 32–41, doi:10.1016/j.clay.2013.08.005.
[56] T. Stimpfling, P. Vialat, H. Hintze-Bruening, P. Keil, V. Shkirskiy, P. Volovitch, K. Ogle, F. Leroux, Amino acid interleaved layered double hydroxides as promising hybrid materials for AA2024 corrosion inhibition, Eur. J. Inorg. Chem 2016 (2016) 2006–2016, doi:10.1002/ejic.201501161.
[57] D.G. Evans, X. Duan, Preparation of layered double hydroxides and their applications as additives in polymers, as precursors to magnetic materials and in biology and medicine, ChemComm 5 (2016) 485–496, doi:10.1039/B510313B.
[58] A. Gomes, D. Cocke, D. Tran, A. Baksi, et al., Layered double hydroxides in energy research: advantages and challenges, in: A. Jha, et al. (Eds.), Energy Technology, Springer, Cham, 2015, doi:10.1007/978-3-319-48220-0_34.
[59] B. Li, J. He, D.G. Evans, X. Duan, Inorganic layered double hydroxides as a drug delivery system—intercalation and in vitro release of fenbufen, Appl. Clay. Sci 27 (2004) 199–207, doi:10.1016/j.clay.2004.07.002.
[60] K. Zhang, Z.P. Xu, J. Lu, Z.Y. Tang, H.J. Zhao, D.A. Good, M.Q. Wei, Potential for layered double hydroxides-based, innovative drug delivery systems, Int. J. Mol. Sci 15 (2014) 7409–7428, doi:10.3390/ijms15057409.
[61] H. Hirahara, Y. Sawai, S. Aisawa, S. Takahashi, Y. Umetsu, E. Narita, Synthesis and antacid property of Mg-Fe layered double hydroxide, J. Clay Sci. Soc. Jpn. (in Japanese) 42 (2002) 70–76, doi:10.11362/jcssjnendokagaku1961.42.70.
[62] X. Bi, H. Zhang, L. Dou, Layered double hydroxide-based nanocarriers for drug delivery, Pharmaceutics 6 (2014) 298–332, doi:10.3390/pharmaceutics6020298.
[63] X. Guo, F. Zhang, D.G. Evans, X. Duan, Layered double hydroxide films: synthesis, properties and applications, ChemComm 46 (2010) 5197–5210, doi:10.1039/C0CC00313A.
[64] K. Yan, Y. Liu, Y. Lu, J. Chai, L. Sun, Catalytic application of layered double hydroxide-derived catalysts for the conversion of biomass-derived molecules, Catal. Sci. Technol 7 (2017) 1622–1645 https://doi.org/https://doi.org/, doi:10.1039/C7CY00274B.
[65] S. Nishimura, A. Takagaki, K. Ebitani, Characterization, synthesis and catalysis of hydrotalcite-related materials for highly efficient materials transformations, Green. Chem 15 (2013) 2026–2042, doi:10.1039/C3GC40405F.
[66] K.H. Goh, T.T. Lim, Z. Dong, Application of layered double hydroxides for removal of oxyanions: a review, Water. Res 42 (2008) 1343–1368, doi:10.1016/j.watres.2007.10.043.
[67] M. Zubair, M. Daud, G. McKay, F. Shehzad, M.A. Al-Harthi, Recent progress in layered double hydroxides (LDH)-containing hybrids as adsorbents for water remediation, Appl.Clay Sci. 143 (2017) 279–292, doi:10.1016/j.clay.2017.04.002.
[68] C. Mousty, F. Leroux, LDHs as electrode materials for electrochemical detection and energy storage: supercapacitor, battery and (bio)-sensor, Recent. Pat. Nanotech 6 (2012) 174–192, doi:10.2174/187221012803531556.
[69] J. Zhao, J. Chen, S. Xu, M. Shao, Q. Zhang, F. Wei, X. Duan, Hierarchical NiMn layered double hydroxide/carbon nanotubes architecture with superb energy density for flexible supercapacitors, Adv. Funct. Mater 24 (2014) 2938–2946, doi:10.1002/adfm.201303638.
[70] M. Shao, R. Zhang, Z. Li, M. Wei, D.G. Evans, X. Duan, Layered double hydroxides toward electrochemical energy storage and conversion: design, synthesis and applications, ChemComm 51 (2015) 15880–15893, doi:10.1039/C5CC07296D.
[71] X. Long, Z. Wang, S. Xiao, Y. An, S. Yang, Transition metal based layered double hydroxides tailored for energy conversion and storage, Mater. Today 19 (2016) 213–226, doi:10.1016/j.mattod.2015.10.006.
[72] R. Patel, J.T. Park, M. Patel, J.K. Dash, E.B. Gowd, R. Karpoormath, J.H. Kim, Transition-metal-based layered double hydroxides tailored for energy conversion and storage, J. Mater. Chem. A 6 (2018) 12–29, doi:10.1039/C7TA09370E.
[73] M.S. Reisch, Confronting the looming hexavalent chromium ban, Chem. Eng. News 95 (2017) 28–29.
[74] E. Abdullayev, R. Price, D. Shchukin, Y. Lvov, Halloysite tubes as nanocontainers for anticorrosion coating with benzotriazole, ACS Appl. Mater. Inter 1 (2009) 1437–1443, doi:10.1021/am9002028.

[75] C. Avila-Gonzalez, R. Cruz-Silva, C. Menchaca, S. Sepulveda-Guzman, J. Uruchurtu, Use of silica tubes as nanocontainers for corrosion inhibitor storage, J. Nanotechnol 2011 (2011) 1–9, doi:10.1155/2011/461313.

[76] A.C. Balaskas, I.A. Kartsonakis, L.A. Tziveleka, G.C. Kordas, Improvement of anti-corrosive properties of epoxy-coated AA 2024-T3 with TiO2 nanocontainers loaded with 8-hydroxyquinoline, Prog. Org. Coat 74 (2012) 418–426, doi:10.1016/j.porgcoat.2012.01.005.

[77] M.L. Zheludkevich, J. Tedim, M.G.S. Ferreira, "Smart" coatings for active corrosion protection based on multi-functional micro and nanocontainers, Electrochim. Acta 82 (2012) 314–323, doi:10.1016/j.electacta.2012.04.095.

[78] G. Williams, H.N. McMurray, M.J. Loveridge, Inhibition of corrosion-driven organic coating disbondment on galvanised steel by smart release group II and Zn (II)-exchanged bentonite pigments, Electrochim. Acta 55 (2010) 1740–1748, doi:10.1016/j.electacta.2009.10.059.

[79] J. Tedim, M.L. Zheludkevich, A.C. Bastos, A.N. Salak, J. Carneiro, F. Maia, A.D. Lisenkov, A.B. Oliveira, M.G.S. Ferreira, Effect of surface treatment on the performance of LDH conversion films, ECS Electrochem. Lett 3 (2014) C4–C8, doi:10.1149/2.005401eel.

[80] M. Serdechnova, M. Mohedano, A.C. Bouali, D. Höche, B. Kuznetsov, S. Karpushenkov, C. Blawert, M.L. Zheludkevich, Role of phase composition of PEO coatings on AA2024 for in-situ LDH growth, Coatings 7 (2017) 190, doi:10.3390/coatings7110190.

[81] A. Mikhailau, H. Maltanava, S.K. Poznyak, A.N. Salak, M.L. Zheludkevich, K. Yasakau, M.G.S. Ferreira, One-step synthesis and growth mechanism of nitrate intercalated ZnAl LDH conversion coatings on zinc, ChemComm 55 (2019) 6878–6881, doi:10.1039/C9CC02571E.

[82] F.P. de Sá, B.N. Cunha, L.M. Nunes, Effect of pH on the adsorption of Sunset Yellow FCF food dye into a layered double hydroxide (CaAl-LDH-NO3), Chem. Eng. J 215 (2013) 122–127, doi:10.1016/j.cej.2012.11.024.

[83] R.G. Buchheit, H. Guan, S. Mahajanam, F. Wong, Active corrosion protection and corrosion sensing in chromate-free organic coatings, Prog. Org. Coat 47 (2013) 174–182, doi:10.1016/j.porgcoat.2003.08.003.

[84] J. Tedim, A.C. Bastos, S. Kallip, M.L. Zheludkevich, M.G.S. Ferreira, Corrosion protection of AA2024-T3 by LDH conversion films. Analysis of SVET results, Electrochim. Acta. 210 (2016) 215–224, doi:10.1016/j.electacta.2016.05.134.

[85] G. Williams, H.N. McMurray, Anion-exchange inhibition of filiform corrosion on organic coated AA2024-T3 aluminum alloy by hydrotalcite-like pigments, Electrochem. Solid State Lett 6 (2003) B9–B11, doi:10.1149/1.1539771.

[86] P. Visser, A. Lutz, J.M.C. Mol, H. Terryn, Study of the formation of a protective layer in a defect from lithium-leaching organic coatings, Prog. Org. Coat 99 (2016) 80–90, doi:10.1016/j.porgcoat.2016.04.028.

[87] P. Pokorny, P. Tej, P. Szelag, Chromate conversion coatings and their current application, Metalurgija 55 (2016) 253–256.

[88] G.S. Frankel, R.L. McCreery, Inhibition of Al alloy corrosion by chromates, J. Electrochem. Soc. 10 (2001) 34–39.

[89] M.A. Zadeh, S. Van Der Zwaag, S.J. Garcia, Routes to extrinsic and intrinsic self-healing corrosion protective sol-gel coatings: a review, Self-Healing Mater. 1 (2013) 1–18, doi:10.2478/shm-2013-0001.

[90] M.L. Zheludkevich, A.E. Hughes, Delivery systems for self healing protective coatings, in: Active Protective Coatings, Springer, Dordrecht, 2016, pp. 157–199, doi:10.1007/978-94-017-7540-3_8.

[91] M.W. Kendig, R.G. Buchheit, Corrosion inhibition of aluminum and aluminum alloys by soluble chromates, chromate coatings, and chromate-free coatings, Corrosion 59 (2003) 379–400, doi:10.5006/1.3277570.

[92] B.L. Hurley, R.L. McCreery, Raman spectroscopy of monolayers formed from chromate corrosion inhibitor on copper surfaces, J. Electrochem. Soc. 150 (2003) B367–B373, doi:10.1149/1.1586923.

[93] L. Xia, R.L. McCreery, Chemistry of a chromate conversion coating on aluminum alloy AA2024-T3 probed by vibrational spectroscopy, J. Electrochem. Soc. 145 (1998) 3083–3089, doi:10.1149/1.1838768.

[94] H. Stuenzi, W. Marty, Early stages of the hydrolysis of chromium (III) in aqueous solution. 1. Characterization of a tetrameric species, Inorg. Chem. 22 (1983) 2145–2150, doi:10.1021/ic00157a012.

[95] O. Gharbi, S. Thomas, C. Smith, N. Birbilis, Chromate replacement: what does the future hold? NPJ Mater. Degrad 2 (2018) 1–8, doi:10.1038/s41529-018-0034-5.

[96] T.K. Shruthi, G.M. Swain, Detection of H2O2 from the Reduction of Dissolved Oxygen on TCP-Coated AA2024-T3: Impact on the Transient Formation of Cr (VI), J. Electrochem. Soc. 166 (2019) C3284–C3289, doi:10.1149/2.0361911jes.

[97] Y. Liu, Z. Feng, X. Zhou, G.E. Thompson, P. Skeldon, S.B. Lyon, D. Graham, Corrosion inhibition of pure aluminium and AA2014-T6 alloy by strontium chromate at low concentration, Surf, Interface. Anal. 48 (2016) 804–808, doi:10.1002/sia.5845.

[98] Y. Xie, S. Holmgren, D.M. Andrews, M.S. Wolfe, Evaluating the impact of the US National Toxicology Program: a case study on hexavalent chromium, Environ. Health. Perspect 125 (2017) 181–188, doi:10.1289/EHP21.

[99] U.S. Department of Health and Human Services, 14th Report on Carcinogens on November 3, 2016.

[100] R.J. Taylor, A.E. Hughes, The development of a chromium-free conversion coating for aluminium alloys, [Conference Material]. 1994. http://hdl.handle.net/102.100.100/238648?index=1.

[101] T. Harvey, Cerium-based conversion coatings on aluminium alloys: a process review, Corros. Eng. Sci. Techn. 48 (2013) 248–269, doi:10.1179/1743278213Y.0000000089.

[102] M. Becker, Chromate-free chemical conversion coatings for aluminum alloys, Corros. Rev. 37 (2019) 321–342, doi:10.1515/corrrev-2019-0032.

[103] R.L. Twite, G.P. Bierwagen, Review of alternatives to chromate for corrosion protection of aluminum aerospace alloys, Prog. Org. Coat 33 (1998) 91–100, doi:10.1016/S0300-9440(98)00015-0.

[104] F. Pearlstein, V.S. Agarwala, Trivalent chromium solutions for applying chemical conversion coatings to aluminum alloys or for sealing anodized aluminum, Plating Surf. Finish 81 (1994) 50–55.

[105] J.T. Qi, T. Hashimoto, J.R. Walton, X. Zhou, P. Skeldon, G.E. Thompson, Trivalent chromium conversion coating formation on aluminium, Surf. Coat. Technol 280 (2015) 317–329, doi:10.1016/j.surfcoat.2015.09.024.

[106] J. Qi, L. Gao, Y. Liu, B. Liu, T. Hashimoto, Z. Wang, G.E. Thompson, Chromate formed in a trivalent chromium conversion coating on aluminum, J. Electrochem. Soc. 164 (2017) C442–C449 //doi.org/, doi:10.1149/2.0021709jes.

[107] L. Li, D.Y. Kim, G.M. Swain, Transient formation of chromate in trivalent chromium process (TCP) coatings on AA2024 as probed by Raman spectroscopy, J. Electrochem. Soc. 159 (2012) C326–C333, doi:10.1149/2.019208jes.

[108] J. Qi, J. Walton, G.E. Thompson, S.P. Albu, J. Carr, Spectroscopic studies of chromium VI formed in the trivalent chromium conversion coatings on aluminum, J. Electrochem. Soc. 163 (2016) C357–C363, doi:10.1149/2.0531607jes.

[109] Henkel-adhesives.com, BONDERITE M-CR T 5900 AERO, https://www.henkel-adhesives.com/mx/en/product/surface-treatments/bonderite_m-cr_t5900aero.html. (Accessed 19th July 2020).

[110] Atotech, BluCr® – the first trivalent chromium hard chrome plating process in the market. https://www.atotech.com/products/general-metal-finishing/wear-resistance/functional-chrome-coatings/blucr/. (Accessed 19th July 2020)

[111] M. Ely, J. Światowska, A. Seyeux, S. Zanna, P. Marcus, Role of post-treatment in improved corrosion behavior of trivalent chromium protection (TCP) coating deposited on aluminum alloy 2024-T3, J. Electrochem. Soc. 164 (2017) C276–C284, doi:10.1149/2.0431706jes.

[112] T.S.N. Sankara Narayanan, Surface pretretament by phosphate conversion coatings-A review, Rev. Adv. Mater. Sci 9 (2005) 130–177.

[113] A.S. Akhtar, D. Susac, P.C. Wong, K.A.R. Mitchell, The effect of pH and role of Ni2+ in zinc phosphating of 2024-Al alloy: Part II: Microscopic studies with SEM and SAM, Appl. Surf. Sci. 253 (2006), doi:10.1016/j.apsusc.2005.12.105.

[114] A.S. Akhtar, K. Wong, K. Mitchell, The effect of pH and role of Ni2+ in zinc phosphating of 2024-Al alloy: Part I: Macroscopic studies with XPS and SEM, Appl. Surf. Sci 253 (2006) 493–501, doi:10.1016/j.apsusc.2005.12.100.

[115] S. Zhang, Study on phosphating treatment of aluminum alloy: role of yttrium oxide, J. Rare Earths 27 (2009) 469–473, doi:10.1016/S1002-0721(08)60271-9.

[116] B. Cheng, S. Ramamurthy, N.S. McIntyre, Characterization of phosphate films on aluminum surfaces, J. Mater. Eng. Perform. 6 (1997) 405–412, doi:10.1007/s11665-997-0108-y.

[117] D. Susac, X. Sun, R.Y. Li, K.C. Wong, P.C. Wong, K.A.R. Mitchell, R. Champaneria, Microstructural effects on the initiation of zinc phosphate coatings on 2024-T3 aluminum alloy, Appl. Surf. Sci 239 (2004) 45–59, doi:10.1016/j.apsusc.2004.04.038.

[118] K. Ogle, A. Tomandl, N. Meddahi, M. Wolpers, The alkaline stability of phosphate coatings I: ICP atomic emission spectroelectrochemistry, Corros. Sci 46 (2004) 979–995, doi:10.1016/S0010-938X(03)00182-3.

[119] A. Tomandl, M. Wolpers, K. Ogle, The alkaline stability of phosphate coatings II: in situ Raman spectroscopy, Corros. Sci 46 (2004) 997–1011, doi:10.1016/S0010-938X(03)00183-5.

[120] S. Ucaroglu, I. Talinli, Recovery and safer disposal of phosphate coating sludge by solidification/stabilization, J. Environ. Manage 105 (2012) 131–137, doi:10.1016/j.jenvman.2012.03.029.

[121] B.R.W. Hinton, D.R. Arnott, N.E. Ryan, Cerium conversion coatings for the corrosion protection of aluminum, Mater. Forum 9 (1986) 162–173.

[122] B.R.W. Hinton, Corrosion inhibition with rare earth metal salts, J. Alloy. Compd. 180 (1992) 15–25, doi:10.1016/0925-8388(92)90359-H.

[123] B.R.W. Hinton, D.R. Arnott, N.E. Ryan, The inhibition of aluminium alloy corrosion by cerous cations, Metals forum 7 (1984) 211–217.

[124] M.J. O'Keefe, S. Geng, S. Joshi, Cerium-based conversion coatings as alternatives to hex chrome: Rare-earth compounds provide resistance against corrosion for aluminum alloys in military applications, Met. Finish 105 (2007) 25–28, doi:10.1016/S0026-0576(07)80547-2.

[125] A.E. Hughes, D. Ho, M. Forsyth, B.R.W. Hinton, Towards replacement of chromate inhibitors by rare earth systems, Corros. Rev 25 (2007) 591–606, doi:10.1515/CORRREV.2007.25.5-6.591.

[126] D. Bekhiti, J. Creus, N. Mesrati, A. Abdi, H. Messaoudi, Improvement of the corrosion behavior of aluminum alloy 6061-T6 with yttrium and lanthanum conversion coatings, Materiali Tehnol. 52 (2018) 329–334, doi:10.17222/mit.2017.160.

[127] R.S. Gharabagh, A.S. Rouhaghdam, Corrosion of environmentally friendly lanthanum conversion coating on AA2024-T3 aluminum alloy, Prot. Met. Phys. Chem. Surf 50 (2014) 88–93, doi:10.1134/S2070205114010183.

[128] A. Pardo, M.C. Merino, R. Arrabal, F. Viejo, M. Carboneras, A.E. Coy, Improvement of corrosion behavior of aluminum alloy/silicon carbide composites with lanthanum surface treatments, Corrosion 62 (2006) 141–151, doi:10.5006/1.3278259.

[129] D. Arnott, B.R.W. Hinton, N. Ryan, Cationic film-forming inhibitors for the corrosion protection of AA 7075 aluminum alloy in chloride solutions, Mater. Perform 26 (1987) 42–47, doi:10.5006/1.3278259.

[130] K.A. Yasakau, M.L. Zheludkevich, S.V. Lamaka, M.G.S. Ferreira, Mechanism of

corrosion inhibition of AA2024 by rare-earth compounds, J. Phys. Chem. B. 110 (2006) 5515–5528, doi:10.1021/jp0560664.
[131] R. Catubig, A.E. Hughes, I.S. Cole, B.R.W. Hinton, M. Forsyth, The use of cerium and praseodymium mercaptoacetate as thiol-containing inhibitors for AA2024-T3, Corros. Sci 81 (2014) 45–53, doi:10.1016/j.corsci.2013.12.001.
[132] O. Lopez-Garrity, G.S. Frankel, Corrosion inhibition of aluminum alloy 2024-T3 by praseodymium chloride, Corrosion 70 (2014) 928–941, doi:10.5006/1244.
[133] T.A. Markley, A.E. Hughes, T.C. Ang, G.B. Deacon, P. Junk, M. Forsyth, Influence of praseodymium: synergistic corrosion inhibition in mixed rare-earth diphenyl phosphate systems, Electrochem. Solid State Lett 10 (2007) C72–C75, doi:10.1149/1.2790724.
[134] R.N. Miller, Non-toxic corrosion resistant conversion coating for aluminum and aluminum alloys and the process for making the same. U.S. Patent No. 5,221,371. 22 Jun. 1993.
[135] B. Valdez, S. Kiyota, M. Stoytcheva, R. Zlatev, J.M. Bastidas, Cerium-based conversion coatings to improve the corrosion resistance of aluminium alloy 6061-T6, Corros. Sci 87 (2014), doi:10.1016/j.corsci.2014.06.023.
[136] D.K. Heller, W.G. Fahrenholtz, M.J. O'Keefe, The effect of post-treatment time and temperature on cerium-based conversion coatings on Al 2024-T3, Corros. Sci 52 (2010) 360–368, doi:10.1016/j.corsci.2009.09.023.
[137] N. Birbilis, R.G. Buchheit, D.L. Ho, M. Forsyth, Inhibition of AA2024-T3 on a phase-by-phase basis using an environmentally benign inhibitor, cerium dibutyl phosphate, Electrochem. Solid State Lett 8 (2005) C180–C183, doi:10.1149/1.2073672.
[138] W.G. Fahrenholtz, M.J. O'Keefe, H. Zhou, J.T. Grant, Characterization of cerium-based conversion coatings for corrosion protection of aluminum alloys, Surf. Coat. Technol 155 (2002) 208–213, doi:10.1016/S0257-8972(02)00062-2.
[139] M. Dabalà, L. Armelao, A. Buchberger, I. Calliari, Cerium-based conversion layers on aluminum alloys, Appl. Surf. Sci 172 (2001) 312–322, doi:10.1016/S0169-4332(00)00873-4.
[140] M.L. Zheludkevich, R. Serra, M.F. Montemor, K.A. Yasakau, I.M. Salvado, M.G.S. Ferreira, Nanostructured sol–gel coatings doped with cerium nitrate as pre-treatments for AA2024-T3: corrosion protection performance, Electrochim. Acta 51 (2005) 208–217, doi:10.1016/j.electacta.2005.04.021.
[141] J. Carneiro, J. Tedim, S.C. Fernandes, C.S.R. Freire, A.J.D. Silvestre, A. Gandini, M.G.S. Ferreira, M.L. Zheludkevich, Chitosan-based self-healing protective coatings doped with cerium nitrate for corrosion protection of aluminum alloy 2024, Prog. Org. Coat. 75 (2012) 8–13, doi:10.1016/j.porgcoat.2012.02.012.
[142] L.S. Kasten, J.T. Grant, N. Grebasch, N. Voevodin, F.E. Arnold, M.S. Donley, An XPS study of cerium dopants in sol–gel coatings for aluminum 2024-T3, Surf. Coat. Tenchnol 140 (2001) 11–15, doi:10.1016/S0257-8972(01)01004-0.
[143] H. Wang, R. Akid, Encapsulated cerium nitrate inhibitors to provide high-performance anti-corrosion sol–gel coatings on mild steel, Corros. Sci 50 (2008) 1142–1148, doi:10.1016/j.corsci.2007.11.019.
[144] K.A. Yasakau, S. Kallip, M.L. Zheludkevich, M.G.S. Ferreira, Active corrosion protection of AA2024 by sol–gel coatings with cerium molybdate nanowires, Electrochim. Acta 112 (2013) 236–246, doi:10.1016/j.electacta.2013.08.126.
[145] M.F. Montemor, D.V. Snihirova, M.G. Taryba, S.V. Lamaka, I.A. Kartsonakis, A.C. Balaskas, G.C. Kordas, J. Tedim, A. Kuznetsov, M.L. Zheludkevich, M.G.S. Ferreira, Evaluation of self-healing ability in protective coatings modified with combinations of layered double hydroxides and cerium molibdate nanocontainers filled with corrosion inhibitors, Electrochim. Acta 60 (2012) 31–40, doi:10.1016/j.electacta.2011.10.078.
[146] R. Noiville, O. Jaubert, M. Gressier, J.P. Bonino, P.L. Taberna, B. Fori, M.J. Menu, corrosion inhibitor release from silica and boehmite nanocontainers, Mater. Sci. Eng 229 (2018) 144–154, doi:10.1016/j.mseb.2017.12.026.
[147] A. Carangelo, M. Curioni, A. Acquesta, T. Monetta, F. Bellucci, Application of EIS to in situ characterization of hydrothermal sealing of anodized aluminum alloys: Comparison between hexavalent chromium-based sealing, hot water sealing and cerium-based sealing, J. Electrochem. Soc. 163 (2016) C619–C626, doi:10.1149/2.0231610jes.
[148] F. Mansfeld, C. Chen, C.B. Breslin, D. Dull, Sealing of anodized aluminum alloys with rare earth metal salt solutions, J. Electrochem. Soc. 145 (1998) 2792–2798, doi:10.1149/1.1838716.
[149] A. Carangelo, M. Curioni, A. Acquesta, T. Monetta, F. Bellucci, Cerium-based sealing of anodic films on AA2024T3: effect of pore morphology on anticorrosion performance, J. Electrochem. Soc. 163 (2016) C907–C916, doi:10.1149/2.1001614jes.
[150] F.H. Scholes, C. Soste, A.E. Hughes, S.G. Hardin, P.R. Curtis, The role of hydrogen peroxide in the deposition of cerium-based conversion coatings, Appl. Surf. Sci 253 (2006) 1770–1780, doi:10.1016/j.apsusc.2006.03.010.
[151] S.A. Hayes, P. Yu, T.J. O'Keefe, M.J. O'Keefe, J.O. Stoffer, The phase stability of cerium species in aqueous systems: I. E-pH diagram for the system, J. Electrochm.Soc. 149 (2002) C623, doi:10.1149/1.1516775.
[152] A. Kolics, A.S. Besing, P. Baradlai, A. Wieckowski, Cerium deposition on aluminum alloy 2024-T3 in acidic NaCl solutions, J. Electrochm. Soc. 150 (2003) B512–B516, doi:10.1149/1.1615995.
[153] J. Li, B. Hurley, R.G. Buchheit, The effect of CeCl3 as an inhibitor on the localized corrosion of AA2024-T3 as a function of temperature, J. Electrochem. Soc. 163 (2016) C845–C852, doi:10.1149/2.0561614jes.
[154] A.E. Hughes, J.M.C. Mol, I.S. Cole, The cost and availability of rare earth-based corrosion inhibitors, in: Proceedings of the Rare Earth-Based Corrosion Inhibitors, Woodhead Publishing, 2014, pp. 291–305, doi:10.1533/9780857093585.291.
[155] N. Haque, A.E. Hughes, S. Lim, C. Vernon, Rare earth elements: Overview of mining, mineralogy, uses, sustainability and environmental impact, Resources 3 (2014) 614–635, doi:10.3390/resources3040614.
[156] J.D. Wilson, Whatever happened to the rare earths weapon? Critical materials and international security in Asia, Asian Security 14 (2018) 358–373, doi:10.1080/14799855.2017.1397977.
[157] I. Milošev, G.S. Frankel, Review- conversion coatings based on zirconium and/or Titanium, J. Electrochem. Soc. 165 (2018) C127–C144, doi:10.1149/2.0371803jes.
[158] Henkel.com. Aluminum Chrome-free Conversion. Corrosion Protection with Eco-friendly Conversion Coatings; Available from: https://www.bonderite.com/en/technologies/light-metal-finishing/chrome-free-conversion-coatings.html. (Accessed 19th July 2020)
[159] H. Zhang, X. Zhang, X. Zhao, Y. Tang, Y. Zuo, Preparation of Ti–Zr-based conversion coating on 5052 aluminum alloy, and its corrosion resistance and antifouling performance, Coatings 8 (2018) 397–406, doi:10.3390/coatings8110397.
[160] M.A. Smit, J.A. Hunter, J.D.B. Sharman, G.M. Scamans, J.M. Sykes, Effects of thermal and mechanical treatments on a titanium-based conversion coating for aluminium alloys, Corros. Sci 46 (2004) 1713–1727, doi:10.1016/j.corsci.2003.10.009.
[161] O. Lunder, C. Simensen, Y. Yu, K. Nisancioglu, Formation and characterisation of Ti–Zr based conversion layers on AA6060 aluminium, Surf. Coat. Technol 184 (2004) 278–290, doi:10.1016/j.surfcoat.2003.11.003.
[162] A. Yi, W. Li, J. Du, S. Mu, Preparation and properties of chrome-free colored Ti/Zr based conversion coating on aluminum alloy, Appl. Surf. Sci 258 (2012) 5960–5964, doi:10.1016/j.apsusc.2011.12.045.
[163] J. Cerezo, I. Vandendael, R. Posner, J.W.H. De Wit, J.M.C. Mol, H. Terryn, The effect of surface pre-conditioning treatments on the local composition of Zr-based conversion coatings formed on aluminium alloys, Appl. Surf. Sci 366 (2016) 339–347, doi:10.1016/j.apsusc.2016.01.106.
[164] J. Cerezo, P. Taheri, I. Vandendael, R. Posner, K. Lill, J.H.W. De Wit, J.M.C. Mol, H. Terryn, Influence of surface hydroxyls on the formation of Zr-based conversion coatings on AA6014 aluminum alloy, Surf. Coat. Technol 254 (2014) 277–283, doi:10.1016/j.surfcoat.2014.06.030.
[165] M. Doerre, L. Hibbitts, G. Patrick, N.K. Akafuah, Advances in automotive conversion coatings during pretreatment of the body structure: a review, Coatings 8 (2018) 405–420, doi:10.3390/coatings8110405.
[166] L. Li, A.L. Desouza, G.M. Swain, In situ pH measurement during the formation of conversion coatings on an aluminum alloy (AA2024), Analyst 138 (2013) 4398–4402, doi:10.1039/C3AN00663H.
[167] Q.P. Li, Z.Q. Yan, Q. Xu, B. Zhang, S. Sun, J.G. Liu, C.W. Yan, A high-performance Ti-Zr based chromium-free conversion coating on 2024 aluminum alloy, Int. J. Electrochem. Sci 11 (2016) 10675–10689, doi:10.20964/2016.12.39.
[168] I. Schoukens, I. Vandendael, J. De Strycker, A.A. Saleh, H. Terryn, I. De Graeve, Effect of surface composition and microstructure of aluminised steel on the formation of a titanium-based conversion layer, Surf. Coat. Technol. 235 (2013) 628–636, doi:10.1016/j.surfcoat.2013.08.041.
[169] I. Milošev, B. Volarič, Conversion coatings based on rare earth nitrates and chlorides for corrosion protection of aluminum alloy 7075-T6, Corrosion 73 (2017) 822–843, doi:10.5006/2353.
[170] X. Zhong, X. Wu, Y. Jia, Y. Liu, Self-repairing vanadium–zirconium composite conversion coating for aluminum alloys, Appl. Surf. Sci 280 (2013) 489–493, doi:10.1016/j.apsusc.2013.05.015.
[171] G. Yoganandan, K.P. Premkumar, J.N. Balaraju, Evaluation of corrosion resistance and self-healing behavior of zirconium–cerium conversion coating developed on AA2024 alloy, Surf. Coat. Technol 270 (2015) 249–258, doi:10.1016/j.surfcoat.2015.02.049.
[172] C. Cai, X.Q. Liu, X. Tan, G.D. Li, H. Wang, J.M. Li, J.F. Li, A Zr-and Cr (III)-containing conversion coating on Al alloy 2024-T3 and its self-repairing behavior, Mater. Corros. 68 (2017) 338–346, doi:10.1002/maco.201609067.
[173] S. Le Manchet, D. Verchère, J. Landoulsi, Effects of organic and inorganic treatment agents on the formation of conversion layer on hot-dip galvanized steel: An X-ray photoelectron spectroscopy study, Thin Solid Films 520 (2012) 2009–2016, doi:10.1016/j.tsf.2011.09.064.
[174] S. Le Manchet, J. Landoulsi, C. Richard, D. Verchère, Study of a chromium-free treatment on Hot-Dip Galvanized steel: Electrochemical behaviour and performance in a saline medium, Surf. Coat. Technol 205 (2010) 475–482, doi:10.1016/j.surfcoat.2010.07.009.
[175] H. Yu, B. Chen, H. Wu, X. Sun, B. Li, Improved electrochemical performance of trivalent-chrome coating on Al 6063 alloy via urea and thiourea addition, Electrochim. Acta 54 (2008) 720–726, doi:10.1016/j.electacta.2008.06.069.
[176] H.C. Yu, X.Y. Huang, F.H. Lei, X.C. Tan, Y.Y. Han, Preparation and electrochemical properties of Cr (III)–Ti-based coatings on 6063 Al alloy, Surf. Coat.Technol 218 (2013) 137–141, doi:10.1016/j.surfcoat.2012.12.042.
[177] W.K. Chen, C.Y. Bai, C.M. Liu, C.S. Lin, M.D. Ger, The effect of chromic sulfate concentration and immersion time on the structures and anticorrosive performance of the Cr (III) conversion coatings on aluminum alloys, Appl. Surf. Sci 256 (2010) 4924–4929, doi:10.1016/j.apsusc.2010.03.003.
[178] V. Moutarlier, M.P. Gigandet, J. Pagetti, B. Normand, Influence of oxalic acid addition to chromic acid on the anodising of Al 2024 alloy, Surf. Coat.Technol 182 (2004) 117–123, doi:10.1016/S0257-8972(03)00875-2.
[179] Y. Guo, G.S. Frankel, Active corrosion inhibition of AA2024-T3 by trivalent chrome process treatment, Corrosion 68 (2012) 45001–45002, doi:10.5006/0010-9312-68-4-3.

[180] Y. Guo, G.S. Frankel, Characterization of trivalent chromium process coating on AA2024-T3, Surf. Coat. Technol 206 (2012) 3895–3902, doi:10.1016/j.surfcoat.2012.03.046.
[181] W.H. Kok, X. Sun, L. Shi, K.C. Wong, K.A.R. Mitchell, T. Foster, Formation of zinc phosphate coatings on AA6061 aluminum alloy, J. Mater. Sci. 36 (2001) 3941–3946, doi:10.1023/A:1017970205276.
[182] I. Van Roy, H. Terryn, G. Goeminne, Study of the formation of zinc phosphate layers on AA5754 aluminium alloy, Transactions of the IMF 76 (1998) 19–23, doi:10.1080/00202967.1998.11871185.
[183] X. Sun, D. Susac, R. Li, K.C. Wong, T. Foster, K.A.R. Mitchell, Some observations for effects of copper on zinc phosphate conversion coatings on aluminum surfaces, Surf. Coat. Technol 155 (2002) 46–50, doi:10.1016/S0257-8972(02)00027-0.
[184] B.L. Lin, Y.Y. Xu, B. Tian, Effect of phosphating technologies on corrosion resistance of phosphate coatings on 6063 Aluminum Alloy, in: Proceedings of the Advanced Materials Research, Trans Tech Publications Ltd, 2012, pp. 2079–2082, doi:10.4028/www.scientific.net/AMR.399-401.2079.
[185] M. Bethencourt, F.J. Botana, M.A. Cauqui, M. Marcos, M.A. Rodrıguez, J.M. Rodrıguez-Izquierdo, Protection against corrosion in marine environments of AA5083 Al–Mg alloy by lanthanide chlorides, J. Alloy. Compd. 250 (1997) 455–460, doi:10.1016/S0925-8388(96)02826-5.
[186] M. Dabalà, E. Ramous, M. Magrini, Corrosion resistance of cerium-based chemical conversion coatings on AA5083 aluminium alloy, Mater. Corros 55 (2004) 381–386, doi:10.1002/maco.200303744.
[187] A. Butler, B. Hinton, G. McAdam, A.E. Hughes, S.G. Hardin, T.G. Harvey, T. Nikpour, A. Stonham, S.J. Harris, C.C. Figgures, S. Church, D. Dixon, P.C. Morgan, C. Bowden, Testing repairs of conversion-coated aluminium alloys, ATB Metallurgie 43 (2003) 273–277 http://hdl.handle.net/102.100.100/192492?index=1.
[188] A.E. Hughes, T.W. Turney, K.J.H. Nelson, U.S. Patent No. 6,206,982. Washington, DC: U.S. Patent and Trademark Office. 2001.
[189] J. Stoffer, T. O' Keefe, X. Lin, E. Morris, P. Yu, S. Hayes, Surface characterization of cerium based conversion coatings, in: Proceedings of the 40th Structures, Structural Dynamics, and Materials Conference and Exhibit, 1999, p. 1293, doi:10.2514/6.1999-1293.
[190] L.E. Palomino, P.H. Suegama, I.V. Aoki, Z. Pászti, H.G. de Melo, Investigation of the corrosion behaviour of a bilayer cerium-silane pre-treatment on Al 2024-T3 in 0.1 M NaCl, Electrochim, Acta 52 (2007) 7496–7505, doi:10.1016/j.electacta.2007.03.002.
[191] H. Hasannejad, M. Aliofkhazraei, A. Shanaghi, T. Shahrabi, A.R. Sabour, Nanostructural and electrochemical characteristics of cerium oxide thin films deposited on AA5083-H321 aluminum alloy substrates by dip immersion and sol–gel methods, Thin Solid Films 517 (2009) 4792–4799, doi:10.1016/j.tsf.2009.03.046.
[192] D.K. Heller, W.G. Fahrenholtz, M.J. O'Keefe, Effect of phosphate source on post-treatment of cerium-based conversion coatings on Al 2024-T3, J. Electrochem. Soc. 156 (2009) C400–C406, doi:10.1149/1.3224005.
[193] F.O. George, P. Skeldon, G.E. Thompson, Formation of zirconium-based conversion coatings on aluminium and Al–Cu alloys, Corros. Sci 65 (2012) 231–237, doi:10.1016/j.corsci.2012.08.031.
[194] W. Zhan, X. Qian, B. Gui, L. Liu, X. Liu, Z. Li, L. Hu, Preparation and corrosion resistance of titanium–zirconium–cerium based conversion coating on 6061 aluminum alloy, Mater. Corros 71 (2020) 419–429, doi:10.1002/maco.201911193.
[195] M. AbdolahZadeh, S. van der Zwaag, S. Garcia, Self-healing corrosion-protective sol–gel coatings based on extrinsic and intrinsic healing approaches, Self-healing Materials, Springer, 2016, doi:10.1007/12_2015_339.
[196] J.B. Cambon, J. Esteban, F. Ansart, J.P. Bonino, V. Turq, S.H. Santagneli, C.V. Santili, S.H. Pulcinelli, Effect of cerium on structure modifications of a hybrid sol–gel coating, its mechanical properties and anti-corrosion behavior, Mater. Res. Bull 47 (2012) 3170–3176, doi:10.1016/j.materresbull.2012.08.034.
[197] V. Palanivel, Y. Huang, W.J. van Ooij, Effects of addition of corrosion inhibitors to silane films on the performance of AA2024-T3 in a 0.5 M NaCl solution, Prog. Org. Coat. 53 (2005) 153–168, doi:10.1016/j.porgcoat.2003.07.008.
[198] K.A. Yasakau, M.L. Zheludkevich, O.V. Karavai, M.G.S. Ferreira, Influence of inhibitor addition on the corrosion protection performance of sol–gel coatings on AA2024, Prog. Org. Coat 63 (2008) 352–361 https://doi.org/https://doi.org/, doi:10.1016/j.porgcoat.2007.12.002.
[199] V. Moutarlier, B. Neveu, M.P. Gigandet, Evolution of corrosion protection for sol–gel coatings doped with inorganic inhibitors, Surf. Coat. Technol 202 (2008) 2052–2058, doi:10.1016/j.surfcoat.2007.08.040.
[200] J. Mardel, S.J. Garcia, P.A. Corrigan, T. Markley, A.E. Hughes, T.H. Muster, D. Laud, T.G. Harvey, A.M. Glenn, S.G.Hardin P.A.White, X.Zhou C.Luo, G.E. Thompson, J.M.C. Mol, The characterisation and performance of Ce (dbp) 3-inhibited epoxy coatings, Prog. Org. Coat 70 (2011) 91–101, doi:10.1016/j.porgcoat.2010.10.009.
[201] M. Abuín, A. Serrano, J. Llopis, M.A. García, N. Carmona, Silica doped with lanthanum sol–gel thin films for corrosion protection, Thin Solid Films 520 (2012) 5267–5271, doi:10.1016/j.tsf.2012.03.046.
[202] D. Raps, T. Hack, J. Wehr, M.L. Zheludkevich, A.C. Bastos, M.G.S. Ferreira, O. Nuyken, Electrochemical study of inhibitor-containing organic–inorganic hybrid coatings on AA2024, Corros. Sci 51 (2009) 1012–1021, doi:10.1016/j.corsci.2009.02.018.
[203] M. Kadkhodie, A. Shanaghi, H. Moradi, Improving of Corrosion Behavior of Al 7075 by Applied Titania–Benzotriazole Nanostructured Coating with Sol Gel Method, Prot. Met. Phys. Chem. Surf 53 (2017) 1040–1049, doi:10.1134/S2070205117060120.
[204] M.S. Sharifiyan, A. Shanaghi, H. Moradi, P.K. Chu, Effects of high concentration of Benzotriazole on corrosion behavior of nanostructured titania-alumina composite coating deposited on Al 2024 by sol-gel method, Surf. Coat. Technol 321 (2017) 36–44, doi:10.1016/j.surfcoat.2017.04.041.
[205] A.R. Simbar, A. Shanaghi, H. Moradi, P.K. Chu, Corrosion behavior of functionally graded and self-healing nanostructured TiO2–Al2O3-Benzotriazole coatings deposited on AA 2024-T3 by the sol-gel method, Mater. Chem. Phys 240 (2020) 122233, doi:10.1016/j.matchemphys.2019.122233.
[206] M. Quinet, B. Neveu, V. Moutarlier, P. Audebert, L. Ricq, Corrosion protection of sol–gel coatings doped with an organic corrosion inhibitor: chloranil, Prog. Org. Coat 58 (2007) 46–53, doi:10.1016/j.porgcoat.2006.11.007.
[207] D. Battocchi, A.M. Simoes, D.E. Tallman, G.P. Bierwagen, Electrochemical behaviour of a Mg-rich primer in the protection of Al alloys, Corros. Sci 48 (2006) 1292–1306, doi:10.1016/j.corsci.2005.04.008.
[208] A.D. King, J.R. Scully, Sacrificial anode-based galvanic and barrier corrosion protection of 2024-T351 by a Mg-rich primer and development of test methods for remaining life assessment, Corrosion 67 (2011) 055004-1-055004-22https://doi.org/, doi:10.5006/1.3590330.
[209] M.E. Nanna, G.P. Bierwagen, Mg-rich coatings, a new paradigm for Cr-free corrosion protection of Al aerospace alloys, JCT Res. 1 (2004) 69–80, doi:10.1007/s11998-004-0001-7.
[210] S.S. Pathak, S.K. Mendon, M.D. Blanton, J.W. Rawlins, Magnesium-based sacrificial anode cathodic protection coatings (Mg-rich primers) for aluminum alloys, Metals 2 (2012) 353–376, doi:10.3390/met2030353.
[211] A.D. King, B. Kannan, J.R. Scully, Environmental degradation of a Mg-rich primer in selected field and laboratory environments: part 1—without a topcoat, Corrosion 70 (2014) 512–535, doi:10.5006/0988.
[212] A.D. King, B. Kannan, J.R. Scully, Environmental degradation of a Mg-rich primer in selected field and laboratory environments: part 2—primer and topcoat, Corrosion 70 (2014) 536–557, doi:10.5006/0989.
[213] M. Serdechnova, V.L. Ivanov, M.R.M. Domingues, D.V. Evtuguin, M.G.S. Ferreira, M.L. Zheludkevich, Photodegradation of 2-mercaptobenzothiazole and 1, 2, 3-benzotriazole corrosion inhibitors in aqueous solutions and organic solvents, Phys. Chem. Chem. Phys 16 (2014) 25152–25160, doi:10.1039/C4CP03867C.
[214] D. Grigoriev, E. Shchukina, D.G. Shchukin, Nanocontainers for self-healing coatings, Adv. Mater. Inter 4 (2017) 1600318, doi:10.1002/admi.201600318.
[215] E. Shchukina, H. Wang, D.G. Shchukin, Nanocontainer-based self-healing coatings: current progress and future perspectives, ChemComm 55 (2019) 3859–3867, doi:10.1039/C8CC09982K.
[216] D. Borisova, H. Möhwald, D.G. Shchukin, Mesoporous silica nanoparticles for active corrosion protection, ACS Nano 5 (2011) 1939–1946, doi:10.1021/nn102871v.
[217] T. Chen, J.J. Fu, pH-responsive nanovalves based on hollow mesoporous silica spheres for controlled release of corrosion inhibitor, Nanotechnology 23 (2012) 235605, doi:10.1088/0957-4484/23/23/235605.
[218] F. Maia, J. Tedim, A.D. Lisenkov, A.N. Salak, M.L. Zheludkevich, M.G.S. Ferreira, Silica nanocontainers for active corrosion protection, Nanoscale 4 (2012) 1287–1298, doi:10.1039/C2NR11536K.
[219] M. Saremi, M. Yeganeh, Application of mesoporous silica nanocontainers as smart host of corrosion inhibitor in polypyrrole coatings, Corros. Sci 86 (2014) 159–170, doi:10.1016/j.corsci.2014.05.007.
[220] E.V. Skorb, D. Fix, D.V. Andreeva, H. Möhwald, D.G. Shchukin, Surface-modified mesoporous SiO2 containers for corrosion protection, Adv. Funct. Mater 19 (2019) 2373–2379, doi:10.1002/adfm.200801804.
[221] I. Recloux, M. Mouanga, M.E. Druart, Y. Paint, M.G. Olivier, Silica mesoporous thin films as containers for benzotriazole for corrosion protection of 2024 aluminium alloys, Appl. Surf. Sci 346 (2015) 124–133, doi:10.1016/j.apsusc.2015.03.191.
[222] E. Shchukina, D. Shchukin, D. Grigoriev, Effect of inhibitor-loaded halloysites and mesoporous silica nanocontainers on corrosion protection of powder coatings, Prog. Org. Coat 102 (2017) 60–65, doi:10.1016/j.porgcoat.2016.04.031.
[223] G.L. Li, M. Schenderlein, Y. Men, H. Möhwald, D.G. Shchukin, Monodisperse polymeric core–shell nanocontainers for organic self-healing anticorrosion coatings, Adv. Mater. Inter 1 (2014) 1300019, doi:10.1002/admi.201300019.
[224] A. Lutz, O. van den Berg, J. Van Damme, K. Verheyen, E. Bauters, I. De Graeve, F.E. Du Prez, H. Terryn, A shape-recovery polymer coating for the corrosion protection of metallic surfaces, ACS Appl. Mater. Inter 7 (2015) 175–183, doi:10.1021/am505621x.
[225] F. Maia, K.A. Yasakau, J. Carneiro, S. Kallip, J. Tedim, T. Henriques, A. Cabral, J. Venâncio, M.L. Zheludkevich, M.G.S. Ferreira, Corrosion protection of AA2024 by sol–gel coatings modified with MBT-loaded polyurea microcapsule, Chem. Eng. J 283 (2016) 1108–1117, doi:10.1016/j.cej.2015.07.087.
[226] N.P. Tavandashti, M. Ghorbani, A. Shojaei, J.M.C. Mol, H. Terryn, K. Baert, Y. Gonzalez-Garcia, Inhibitor-loaded conducting polymer capsules for active corrosion protection of coating defects, Corros. Sci 112 (2016) 138–149, doi:10.1016/j.corsci.2016.07.003.
[227] D. Fix, D.V. Andreeva, Y.M. Lvov, D.G. Shchukin, H. Möhwald, Application of inhibitor-loaded halloysite nanotubes in active anti-corrosive coatings, Adv. Funct. Mater 19 (2009) 1720–1727, doi:10.1002/adfm.200800946.
[228] D.G. Shchukin, S.V. Lamaka, K.A. Yasakau, M.L. Zheludkevich, M.G.S. Ferreira,

H. Möhwald, Active anticorrosion coatings with halloysite nanocontainers, J. Phys. Chem. C 112 (2008) 958–964, doi:10.1021/jp076188r.
[229] N. Gray, D.G. Lumsdon, S. Hillier, Effect of pH on the cation exchange capacity of some halloysite nanotubes, Clay. Miner 51 (2016) 373–383, doi:10.1180/claymin.2016.051.3.04.
[230] I.A. Kartsonakis, I.L. Danilidis, G.S. Pappas, G.C. Kordas, Encapsulation and release of corrosion inhibitors into titania nanocontainers, J. Nanosci. Nanotechnol. 10 (2010) 5912–5920, doi:10.1166/jnn.2010.2571.
[231] E.D. Mekeridis, I.A. Kartsonakis, G.C. Kordas, Multilayer organic–inorganic coating incorporating TiO2 nanocontainers loaded with inhibitors for corrosion protection of AA2024-T3, Prg. Org. Coat 73 (2012) 142–148, doi:10.1016/j.porgcoat.2011.10.005.
[232] S.A.S. Dias, S.V. Lamaka, T.C. Diamantino, M.G.S. Ferreira, Synergistic protection against corrosion of AA2024-T3 by sol-gel coating modified with La and Mo-enriched zeolites, J. Electrochem. Soc. 161 (2014) C215–C222, doi:10.1149/2.064404jes.
[233] S.A.S. Dias, A. Marques, S.V. Lamaka, A. Simões, T.C. Diamantino, M.G.S. Ferreira, The role of Ce (III)-enriched zeolites on the corrosion protection of AA2024-T3, Electrochim. Acta 112 (2013) 549–556, doi:10.1016/j.electacta.2013.09.026.
[234] E.L. Ferrer, A.P. Rollon, H.D. Mendoza, U. Lafont, S.J. Garcia, Double-doped zeolites for corrosion protection of aluminium alloys, Micropor. Mesopor. Mat 188 (2014) 8–15, doi:10.1016/j.micromeso.2014.01.004.
[235] S. Bohm, H.N. McMurray, D.A. Worsley, S.M. Powell, Novel environment friendly corrosion inhibitor pigments based on naturally occurring clay minerals, Mater. Corros 52 (2001) 896–903 https://doi.org/12<896::AID-MACO896>3.0.CO;2-8, doi:10.1002/1521-4176(200112)52.
[236] M. Serdechnova, S. Kallip, M.G.S. Ferreira, M.L. Zheludkevich, Active self-healing coating for galvanically coupled multi-material assemblies, Electrochem. Comm 41 (2014) 51–54, doi:10.1016/j.elecom.2014.01.023.
[237] A. Ghazi, E. Ghasemi, M. Mahdavian, B. Ramezanzadeh, M. Rostami, The application of benzimidazole and zinc cations intercalated sodium montmorillonite as smart ion exchange inhibiting pigments in the epoxy ester coating, Corros. Sci 94 (2015) 207–217, doi:10.1016/j.corsci.2015.02.007.
[238] G. Williams, H.N. McMurray, Inhibition of filiform corrosion on organic-coated AA2024-T3 by smart-release cation and anion-exchange pigments, Electrochim. Acta 69 (2012) 287–294, doi:10.1016/j.electacta.2012.03.002.
[239] D. Li, F. Wang, X. Yu, J. Wang, Q. Liu, P. Yang, H. Yang, M. Zhang, Anticorrosion organic coating with layered double hydroxide loaded with corrosion inhibitor of tungstate, Prog. Org. Coat 71 (2011) 302–309, doi:10.1016/j.porgcoat.2011.03.023.
[240] F. Zhang, L. Zhao, H. Chen, S. Xu, D.G. Evans, X. Duan, Corrosion resistance of superhydrophobic layered double hydroxide films on aluminum, Angew. Chem 120 (2008) 2500–2503, doi:10.1002/ange.200704694.
[241] N. Iyi, Y. Ebina, T. Sasaki, Synthesis and characterization of water-swellable LDH (layered double hydroxide) hybrids containing sulfonate-type intercalant, J. Mater. Chem. 21 (2011) 8085–8095, doi:10.1039/C1JM10733J.
[242] Q. Wang, D. O'Hare, Recent advances in the synthesis and application of layered double hydroxide (LDH) nanosheets, Chem. Rev 112 (2012) 4124–4155, doi:10.1021/cr200434v.
[243] F. Zhang, C.L. Zhang, S. Liang, R.C. Zeng, Z.G. Liu, H.Z. Cui, Corrosion of in-situ grown MgAl-LDH coating on aluminum alloy, Trans. Nonferrous Met. Soc 25 (2015) 3498–3504, doi:10.1016/S1003-6326(15)63987-5.
[244] B. Kuznetsov, M. Serdechnova, J. Tedim, M. Starykevich, S. Kallip, M.P. Oliveira, T. Hack, S. Nixon, M.G.S. Ferreira, M.L. Zheludkevich, Sealing of tartaric sulfuric (TSA) anodized AA2024 with nanostructured LDH layers, Rsc Adv. 6 (2016) 13942–13952, doi:10.1039/C5RA27286F.
[245] T.N. Shulha, M. Serdechnova, S.V. Lamaka, D.C.F. Wieland, K.N. Lapko, M.L. Zheludkevich, Chelating agent-assisted in situ LDH growth on the surface of magnesium alloy, Scientific Rep. 8 (2018) 1–10, doi:10.1038/s41598-018-34751-7.
[246] K. Hoshino, S. Furuya, R.G. Buchheit, Effect of NO3− intercalation on corrosion resistance of conversion coated Zn-Al-CO3 LDHs on electrogalvanized steel, J. Electrochem. Soc. 165 (2018) C461 https://orcid.org/0000-0002-1793-4593.
[247] K. Lin, X. Luo, X. Pan, C. Zhang, Y. Liu, Enhanced corrosion resistance of LiAl-layered double hydroxide (LDH) coating modified with a Schiff base salt on aluminum alloy by one step in-situ synthesis at low temperature, Appl. Surf. Sci 463 (2019) 1085–1096, doi:10.1016/j.apsusc.2018.09.034.
[248] A.C. Bouali, M.H. Iuzviuk, M. Serdechnova, K.A. Yasakau, D.F. Wieland, G. Dovzhenko, H. Maltananva, I.A. Zobkalo, M.G.S. Ferreira, M.L. Zheludkevich, Zn-Al LDH growth on AA2024 and zinc and their intercalation with chloride: Comparison of crystal structure and kinetics, Appl. Surf. Sci 501 (2020) 144027, doi:10.1016/j.apsusc.2019.144027.
[249] J. Li, K. Lin, X. Luo, H. Zhang, Y.F. Cheng, X. Li, Y. Liu, Enhanced corrosion protection property of Li-Al layered double hydroxides (LDHs) film modified by 2-guanidinosuccinic acid with excellent self-repairing and self-antibacterial properties, Appl. Surf. Sci 480 (2019) 384–394, doi:10.1016/j.apsusc.2019.02.164.
[250] R.P. Wijitwongwan, S.G. Intasa-ard, M. Ogawa, Preparation of layered double hydroxides toward precisely designed hierarchical organization, ChemEng 3 (2019) 68, doi:10.3390/chemengineering3030068.
[251] T. Lopez, P. Bosch, E. Ramos, R. Gomez, O. Novaro, D. Acosta, F. Figueras, Synthesis and characterization of sol– gel hydrotalcites, Structure Texture, Langmuir 12 (1996) 189–192, doi:10.1021/la940703s.
[252] M. Jitianu, D.C. Gunness, D.E. Aboagye, M. Zaharescu, A. Jitianu, Nanosized Ni–Al layered double hydroxides—Structural characterization, Mater. Res. Bull. 48 (2013) 1864–1873, doi:10.1016/j.materresbull.2013.01.030.
[253] T. Hibino, H. Ohya, Synthesis of crystalline layered double hydroxides: Precipitation by using urea hydrolysis and subsequent hydrothermal reactions in aqueous solutions, Appl. Clay Sci 45 (2019) 123–132, doi:10.1016/j.clay.2009.04.013.
[254] L.B. Staal, S.S.C. Pushparaj, C. Forano, V. Prevot, D.B. Ravnsbæk, M. Bjerring, U.G. Nielsen, Competitive reactions during synthesis of zinc aluminum layered double hydroxides by thermal hydrolysis of urea, J. Mater. Chem. A. 5 (2017) 21795–21806, doi:10.1039/C7TA05761J.
[255] M. Adachi-Pagano, C. Forano, J.-P. Besse, Synthesis of Al-rich hydrotalcite-like compounds by using the urea hydrolysis reaction—control of size and morphology, J. Mater. Chem. 13 (2003) 1988–1993, doi:10.1039/B302747N.
[256] J. Liu, J. Song, H. Xiao, L. Zhang, Y. Qin, D. Liu, W. Hou, N. Du, Synthesis and thermal properties of ZnAl layered double hydroxide by urea hydrolysis, Powder Technol 253 (2014) 41–45, doi:10.1016/j.powtec.2013.11.007.
[257] Z.P. Xu, G.Q. Lu, Hydrothermal synthesis of layered double hydroxides (LDHs) from mixed MgO and Al2O3: LDH formation mechanism, Chem. Mater 17 (2005) 1055–1062, doi:10.1021/cm048085g.
[258] Q. Wang, S.V.Y. Tang, E. Lester, D. O'Hare, Synthesis of ultrafine layered double hydroxide (LDHs) nanoplates using a continuous-flow hydrothermal reactor, Nanoscale 5 (2013) 114–117, doi:10.1039/C2NR32568C.
[259] F.L. Theiss, S.J. Palmer, G.A. Ayoko, R.L. Frost, Sulfate intercalated layered double hydroxides prepared by the reformation effect, J. Therm. Anal. Calorim. 107 (2012) 1123–1128, doi:10.1007/s10973-011-1369-0.
[260] J. Qu, X. He, X. Li, Z. Ai, Y. Li, Q. Zhang, X. Liu, Precursor preparation of Zn–Al layered double hydroxide by ball milling for enhancing adsorption and photocatalytic decoloration of methyl orange, Rsc Adv. 7 (2017) 31466–31474, doi:10.1039/C7RA05316A.
[261] J. Qu, X. He, B. Wang, L. Zhong, L. Wan, X. Li, S. Song, Q. Zhang, Synthesis of Li–Al layered double hydroxides via a mechanochemical route, Appl. Clay. Sci 120 (2016) 24–27, doi:10.1016/j.clay.2015.11.017.
[262] J. Qu, L. Sha, C. Wu, Q. Zhang, Applications of mechanochemically prepared layered double hydroxides as adsorbents and catalysts: A mini-review, Nanomaterials 9 (2019) 80, doi:10.3390/nano9010080.
[263] X. Wang, E.N. Kalali, W. Xing, D.Y. Wang, CO2 induced synthesis of Zn-Al layered double hydroxide nanostructures towards efficiently reducing fire hazards of polymeric materials, Nano. Adv 3 (2018) 12–17, doi:10.22180/na221.
[264] F.Z. Mahjoubi, A. Khalidi, M. Abdennouri, N. Barka, Zn–Al layered double hydroxides intercalated with carbonate, nitrate, chloride and sulphate ions: Synthesis, characterisation and dye removal properties, J. Taibah. Univ. Sci. 11 (2017) 90–100, doi:10.1016/j.jtusci.2015.10.007.
[265] A. Jaiswal, R. Mani, S. Banerjee, R.K. Gautam, M.C. Chattopadhyaya, Synthesis of novel nano-layered double hydroxide by urea hydrolysis method and their application in removal of chromium (VI) from aqueous solution: kinetic, thermodynamic and equilibrium studies, J. Mol. Liq. 202 (2015) 52–61, doi:10.1016/j.molliq.2014.12.004.
[266] P. Benito, F.M. Labajos, V. Rives, Uniform fast growth of hydrotalcite-like compounds, Crys. Growth. Des 6 (2006) 1961–1966, doi:10.1021/cg0506222.
[267] Y. Kim, E.S. Cho, S. Park, S. Kim, One-pot microwave-assisted synthesis of reduced graphene oxide/nickel cobalt double hydroxide composites and their electrochemical behavior, J. Ind. Eng. Chem. 33 (2016) 108–114, doi:10.1016/j.jiec.2015.09.023.
[268] P. Benito, M. Herrero, F.M. Labajos, V. Rives, Effect of post-synthesis microwave–hydrothermal treatment on the properties of layered double hydroxides and related materials, Appl. Clay. Sci 48 (2010) 218–227, doi:10.1016/j.clay.2009.11.051.
[269] E. Perez-Barrado, P. Salagre, L.F. Marsal, M. Aguilo, Y. Cesteros, F. Diaz, J. Pallarès, F. Cucinotta, L. Marchese, M.C. Pujol, Ultrasound-assisted reconstruction and delamination studies on CaAl layered double hydroxides, Appl. Surf. Sci 118 (2015) 116–123, doi:10.1016/j.clay.2015.08.043.
[270] M. Szabados, R. Mészáros, S. Erdei, Z. Kónya, A. Kukovecz, P. Sipos, I. Pálinkó, Ultrasonically-enhanced mechanochemical synthesis of CaAl-layered double hydroxides intercalated by a variety of inorganic anions, Ultrason. Sonochem 31 (2016) 409–416, doi:10.1016/j.ultsonch.2016.01.026.
[271] A.N. Salak, D.E. Vieira, I.M. Lukienko, Y.O. Shapovalov, A.V. Fedorchenko, E.L. Fertman, Y.G. Pashkevich, R.Y. Babkin, A.D. Shilin, V.V. Rubanik, M.G.S. Ferreira, J.M. Vieira, High-power ultrasonic synthesis and magnetic-field-assisted arrangement of nanosized crystallites of cobalt-containing layered double hydroxides, ChemEng 3 (2019) 62, doi:10.3390/chemengineering3030062.
[272] D. Sokol, D.E. Vieira, A. Zarkov, M.G.S. Ferreira, A. Beganskiene, V.V. Rubanik, A.D. Shilin, A. Kareiva, A.N. Salak, Sonication accelerated formation of Mg-Al-phosphate layered double hydroxide via sol-gel prepared mixed metal oxides, Sci. Rep 9 (2019) 1–9, doi:10.1038/s41598-019-46910-5.
[273] F. Geng, H. Xin, Y. Matsushita, R. Ma, M. Tanaka, F. Izumi, N. Iyi, T. Sasaki, New layered rare-earth hydroxides with anion-exchange properties, Chem. Eur. J 14 (2008) 9255–9260, doi:10.1002/chem.200800127.
[274] R.M.M. Santos, J. Tronto, V. Briois, C.V. Santilli, Thermal decomposition and recovery properties of ZnAl–CO 3 layered double hydroxide for anionic dye adsorption: insight into the aggregative nucleation and growth mechanism of the LDH memory effect, J. Mater. Chem A. 5 (2007) 9998–10009, doi:10.1039/C7TA00834A.
[275] V.R. Magri, A. Duarte, G.F. Perotti, V.R. Constantino, Investigation of thermal behavior of layered double hydroxides intercalated with carboxymethyl-

cellulose aiming bio-carbon based nanocomposites, ChemEng 3 (2019) 55, doi:10.3390/chemengineering3020055.
[276] G. Mascolo, M.C. Mascolo, On the synthesis of layered double hydroxides (LDHs) by reconstruction method based on the “memory effect”, Micropor. Mesopor. Mat 214 (2015) 246–248, doi:10.1016/j.micromeso.2015.03.024.
[277] S.V. Prasanna, P.V. Kamath, Anion-exchange reactions of layered double hydroxides: interplay between coulombic and H-bonding interactions, Ind. Eng. Chem. Res 48 (2019) 6315–6320, doi:10.1021/ie9004332.
[278] S. Miyata, Physico-chemical properties of synthetic hydrotalcites in relation to composition, Clays Clay Miner 28 (1980) 50–56, doi:10.1346/CCMN.1980.0280107.
[279] S. Miyata, Anion-exchange properties of hydrotalcite-like compounds, Clays Clay Miner 31 (1983) 305–311, doi:10.1346/CCMN.1983.0310409.
[280] D.G. Costa, A.B. Rocha, W.F. Souza, S.S.X. Chiaro, A.A. Leitão, Comparative Structural, thermodynamic and electronic analyses of ZnAlAn− hydrotalcite-like compounds (An− Cl−, F−, Br−, OH−, CO32− or NO3−): An ab initio study, Appl. Clay. Sci 56 (2012) 16–22, doi:10.1016/j.clay.2011.11.014.
[281] A. Hayashi, H. Nakayama, Intercalation reaction of carbonate MgAl-layered double hydroxide using alcohol as solvent, Chem. Lett 40 (2011) 276–278, doi:10.1246/cl.2011.276.
[282] H.C.B. Hansen, R.M. Taylor, The use of glycerol intercalates in the exchange of CO 3 2− with SO 4 2−, NO 3− or Cl− in pyroaurite-type compounds, Clay. Miner. 26 (1991) 311–327, doi:10.1180/claymin.1991.026.3.02.
[283] T. Hibino, Anion selectivity of layered double hydroxides: effects of crystallinity and charge density, Eur. J. Inorg. Chem 2018 (2018) 722–730, doi:10.1002/ejic.201701067.
[284] M. Meyn, K. Beneke, G. Lagaly, Anion-exchange reactions of layered double hydroxides, Inorg. Chem 29 (1990) 5201–5207, doi:10.1021/ic00351a013.
[285] L. Palin, M. Milanesio, W. van Beek, E. Conterosito, Understanding the ion exchange process in LDH nanomaterials by fast in situ XRPD and PCA-assisted kinetic analysis, J. Nanomater 2019 (2019) 1–9, doi:10.1155/2019/4612493.
[286] J.M. Vega, N. Granizo, D. De La Fuente, J. Simancas, M. Morcillo, Corrosion inhibition of aluminum by coatings formulated with Al–Zn–vanadate hydrotalcite, Prog. Org. Coat 70 (2011) 213–219, doi:10.1016/j.porgcoat.2010.08.014.
[287] J. Wu, D. Peng, Y. He, X. Du, Z. Zhang, B. Zhang, X. Li, Y. Huang, In situ formation of decavanadate-intercalated layered double hydroxide films on AA2024 and their anti-corrosive properties when combined with hybrid sol gel films, Materials 10 (2017) 426, doi:10.3390/ma10040426.
[288] Y. Dong, F. Wang, Q. Zhou, Protective behaviors of 2-mercaptobenzothiazole intercalated Zn–Al-layered double hydroxide coating, J. Coat. Technol. Res. 11 (2014) 793–803, doi:10.1007/s11998-014-9568-9.
[289] F. Wong, R.G. Buchheit, Utilizing the structural memory effect of layered double hydroxides for sensing water uptake in organic coatings, Prg. Org. Coat. 2004 51 (2004) 91–102, doi:10.1016/j.porgcoat.2004.07.001.
[290] M.L. Zheludkevich, D. Raps, A.C. Bastos, T. Hack, M.G.S. Ferreira, Self-Healing Coatings with Multi-Level Protection Based on Active Nanocontainers, Conference Paper, NanoSpain, Portugal, 2018.
[291] N.K. Akafuah, S. Poozesh, A. Salaimeh, G. Patrick, K. Lawler, K. Saito, Evolution of the automotive body coating process—A review, Coatings 6 (2016) 24, doi:10.3390/coatings6020024.
[292] J. Sinko, Challenges of chromate inhibitor pigments replacement in organic coatings, Prog. Org. Coat 42 (2001) 267–282, doi:10.1016/S0300-9440(01)00202-8.
[293] M.L. Zheludkevich, S. Kallip, M. Serdechnova, Protection of multimaterial assemblies, Phy. Sci. Rev 1 (2016) 1–19, doi:10.1515/psr-2015-0012.
[294] Z. Chang, D. Evans, X. Duan, P. Boutinaud, M. De Roy, C. Forano, Preparation and characterization of rare earth-containing layered double hydroxides, J. Phys. Chem. Solids. 67 (2006) 1054–1057, doi:10.1016/j.jpcs.2006.01.025.
[295] M. Kaneyoshi, W. Jones, Layered double hydroxide intercalate of metal-chelate complex—a novel precursor for the formation of a mixed metal oxide. molecular crystals and liquid crystals science and technology. section A, Mol. Cryst. Liq. Cryst. 356 (2001) 459–468, doi:10.1016/j.jpcs.2006.01.025.
[296] T. Posati, F. Costantino, L. Latterini, M. Nocchetti, M. Paolantoni, L. Tarpani, New insights on the incorporation of lanthanide ions into nanosized layered double hydroxides, Inorg. Chem 51 (2012) 13229–13236, doi:10.1021/ic301584g.
[297] T. Ye, W. Huang, L. Zeng, M. Li, J. Shi, CeO2-x platelet from monometallic cerium layered double hydroxides and its photocatalytic reduction of CO2, Appl. Cat B 210 (2017) 141–148, doi:10.1016/j.apcatb.2017.03.051.
[298] J. Liu, Y. Zhang, M. Yu, S. Li, B. Xue, X. Yin, Influence of embedded ZnAlCe-NO3− layered double hydroxides on the anticorrosion properties of sol–gel coatings for aluminum alloy, Prog. Inorg. Coat 81 (2015) 93–100, doi:10.1016/j.porgcoat.2014.12.015.
[299] S.P.V. Mahajanam, R.G. Buchheit, Characterization of Zn-Al-V 10 O 28 6−; corrosion-inhibiting hydrotalcite pigments in epoxy resins, in: RG Buchheit, RG Kelly, NA Missert, BA Shaw (Eds.), Corrosion and Protection of Light Metal Alloys, 2004, pp. 270–282.
[300] K.G. Omdeo, V.R. Ajay, K. Krishnan, V.K. Abitha, N. Samarth, T. Sabu, S. Mishra, in: Surface modification of synthesized layered double hydroxide [LDH] for methylene blue dye removal in textile industry via photocatalytic activity under visible light, 2017, pp. 135–147. Trans Tech Publications Ltd. 10.4028/www.scientific.net/JNanoR.46.135.
[301] J.M. Oh, S.J. Choi, G.E. Lee, S.H. Han, J.H. Choy, Inorganic drug-delivery nanovehicle conjugated with cancer-cell-specific ligand, Adv. Funct. Mater 19 (2009) 1617–1624, doi:10.1002/adfm.200801127.
[302] H. Hu, K.M. Xiu, S.L. Xu, W.T. Yang, F.J. Xu, Functionalized layered double hydroxide nanoparticles conjugated with disulfide-linked polycation brushes for advanced gene delivery, Bioconjugate Chem 24 (2013) 968–978, doi:10.1021/bc300683y.
[303] C.I. Ezeh, X. Huang, X. Yang, C.G. Sun, J. Wang, Sonochemical surface functionalization of exfoliated LDH: Effect on textural properties, CO2 adsorption, cyclic regeneration capacities and subsequent gas uptake for simultaneous methanol synthesis, Ultrason. Sonochem 39 (2017) 330–343, doi:10.1016/j.ultsonch.2017.04.041.
[304] S. Elbasuney, Surface engineering of layered double hydroxide (LDH) nanoparticles for polymer flame retardancy, Powder Technol 277 (2015) 63–73, doi:10.1016/j.powtec.2015.02.044.
[305] J. Hu, M. Gan, L. Ma, Z. Li, J. Yan, J. Zhang, Synthesis and anticorrosive properties of polymer–clay nanocomposites via chemical grafting of polyaniline onto Zn-Al layered double hydroxides, Surf. Coat. Technol 240 (2014) 55–62, doi:10.1016/j.surfcoat.2013.12.012.
[306] P. Du, C. Liu, S. Qiu, G. Liu, H. Zhao, Surface modification of Mg/Al layered double hydroxide by camphorsulfonic acid doped polyaniline and its applications for anticorrosive coating, Surf. Topogr. Metrol. Prop 6 (2018) 034012 10.1088/2051-672X/aac8a6.
[307] S. Swarup, C.K. Schoff, A survey of surfactants in coatings technology, Prog. Org. Coat 23 (1993) 1–22, doi:10.1016/0033-0655(93)80002-R.
[308] S.G.R. Emad, X. Zhou, S. Morsch, S.B. Lyon, Y. Liu, D. Graham, S.R. Gibbon, How pigment volume concentration (PVC) and particle connectivity affect leaching of corrosion inhibitive species from coatings, Prog. Org. Coat 134 (2019) 360–372, doi:10.1016/j.porgcoat.2019.05.008.
[309] S.G.R. Emad, S. Morsch, T. Hashimoto, Y. Liu, S.R. Gibbon, S.B. Lyon, X. Zhou, Leaching from coatings pigmented with strontium aluminium polyphosphate inhibitor pigment-evidence for a cluster-percolation model, Prog. Org. Coat 137 (2019) 105340, doi:10.1016/j.porgcoat.2019.105340.
[310] S.G.R. Emad, X. Zhou, S.B. Lyon, G.E. Thompson, Y. Liu, G. Smyth, S.R. Gibbon, Influence of volume concentration of active inhibitor on microstructure and leaching behaviour of a model primer, Prog. Org. Coat 102 (2017) 71–81, doi:10.1016/j.porgcoat.2016.04.039.
[311] A.E. Hughes, A. Trinchi, F.F. Chen, Y.S. Yang, I.S. Cole, S. Sellaiyan, J. Carr, P.D. Lee, G.E. Thompson, T.Q. Xiao, The application of multiscale quasi 4D CT to the study of SrCrO4 distributions and the development of porous networks in epoxy-based primer coatings, Prog. Org. Coat 77 (2014) 1946–1956, doi:10.1016/j.porgcoat.2014.07.001.
[312] Y. Wang, D. Zhang, Z. Lu, Hydrophobic Mg–Al layered double hydroxide film on aluminum: Fabrication and microbiologically influenced corrosion resistance properties, Colloids Surf. A Physicochem. Eng. Asp 474 (2015) 44–51, doi:10.1016/j.colsurfa.2015.03.005.
[313] Y. Cao, D. Zheng, X. Li, J. Lin, C. Wang, S. Dong, C. Lin, Enhanced corrosion resistance of superhydrophobic layered double hydroxide films with long-term stability on Al substrate, ACS Appl. Mater. Interfaces. 10 (18), 15150-15162. https://doi.org/ 10.1021/acsami.8b02280.
[314] M. Serdechnova, M. Mohedano, B. Kuznetsov, C.L. Mendis, M. Starykevich, S. Karpushenkov, J. Tedim, M.G.S. Ferreira, C. Blawert, M.L. Zheludkevich, PEO coatings with active protection based on in-situ formed LDH-nanocontainers, J .Electrochem. Soc 164 (2016) C36–C45, doi:10.1149/2.0301702jes.
[315] P. Visser, H. Terryn, J.M.C. Mol, Active corrosion protection of various aluminium alloys by lithium-leaching coatings, Surf. Interface. Anal 51 (2019) 1276–1287, doi:10.1002/sia.6638.
[316] M.A. Iqbal, L. Sun, A.M. LaChance, H. Ding, M. Fedel, In situ growth of a CaAl-NO 3−-layered double hydroxide film directly on an aluminum alloy for corrosion resistance, Dalton. Trans 49 (2020) 3956–3964, doi:10.1039/C9DT01773A.
[317] M.H. Iuzviuk, A.C. Bouali, M. Serdechnova, K.A. Yasakau, D.C.F. Wieland, G. Dovzhenko, A. Mikhailau, C. Blawert, I.A. Zobkaloa, M.G.S. Ferreirac, M.L. Zheludkevich, In-situ kinetics studies of Zn-Al LDH intercalation with corrosion related species, Phys. Chem. Chem. Phys. 22 (2020) 17574–17586, doi:10.1039/D0CP01765E.
[318] X. Chen, Y. Lei, W. Yang, Fabrication of free-standing layer-by-layer films of layered double hydroxide nanosheets and polyelectrolytes, Chem. Lett 37 (2008) 1050–1051, doi:10.1246/cl.2008.1050.
[319] T. Yui, T. Kameyama, T. Sasaki, T. Torimoto, K. Takagi, Pyrene-to-porphyrin excited singlet energy transfer in LBL-deposited LDH nanosheets, J. Porphyr. Phthalocyanines. 11 (2007) 428–433, doi:10.1142/S1088424607000485.
[320] L. Li, R. Ma, Y. Ebina, N. Iyi, T. Sasaki, Positively charged nanosheets derived via total delamination of layered double hydroxides, Chem. Mater 17 (2005) 4386–4391, doi:10.1021/cm0510460.
[321] J. Han, X. Xu, X. Rao, M. Wei, D.G. Evans, X. Duan, Layer-by-layer assembly of layered double hydroxide/cobalt phthalocyanine ultrathin film and its application for sensors, J. Mater. Chem. 21 (2011) 2126–2130, doi:10.1039/C0JM02430A.
[322] R. Roto, A. Yamagishi, G. Villemure, Electrochemical quartz crystal microbalance study of mass transport in thin film of a redox active Ni–Al–Cl layered double hydroxide, J. Electroanal. Chem. 572 (2004) 101–108, doi:10.1016/j.jelechem.2004.06.005.
[323] L. Wang, C. Li, M. Liu, D.G. Evans, X. Duan, Large continuous, transparent and oriented self-supporting films of layered double hydroxides with tunable chemical composition, ChemComm (2007) 123–125, doi:10.1039/B613687G.
[324] J. Lee, S. Rhee, D.Y. Jung, Orientation-controlled assembly and solvothermal ion-exchange of layered double hydroxide nanocrystals, ChemComm (2003) 2740–2741, doi:10.1039/B308269E.

[325] J.H. Lee, S.W. Rhee, D.Y. Jung, Solvothermal ion exchange of aliphatic dicarboxylates into the gallery space of layered double hydroxides immobilized on Si substrates, Chem. Mater 16 (2004) 3774–3779, doi:10.1021/cm049357i.
[326] Y. Kuang, L. Zhao, S. Zhang, F. Zhang, M. Dong, S. Xu, Morphologies, preparations and applications of layered double hydroxide micro-/nanostructures, Materials 3 (2010) 5220–5235, doi:10.3390/ma3125220.
[327] X. Duan, J. Lu, D.G. Evans, Assembly chemistry of anion-intercalated layered materials, in: Proceedings of the Modern inorganic synthetic chemistry, Elsevier, 2011, pp. 375–404, doi:10.1016/B978-0-444-53599-3.10017-4.
[328] I. Gualandi, M. Monti, E. Scavetta, D. Tonelli, V. Prevot, C. Mousty, Electrodeposition of layered double hydroxides on platinum: insights into the reactions sequence, Electrochim. Acta 152 (2015) 75–83, doi:10.1016/j.electacta.2014.11.096.
[329] E. Scavetta, B. Ballarin, M. Giorgetti, I. Carpani, F. Cogo, D. Tonelli, Electrodes modified by one-step electrosynthesis of Ni/Al-NO~ 3 double layered hydroxide, J. New Mat. Electrochem. Systems. 7 (2004) 43–50.
[330] C. Obayashi, M. Ishizaka, T. Konishi, H. Yamada, K. Katakura, Preparation of the electrochemically precipitated Mn-Al LDHs and their electrochemical behaviors, Electrochemistry 80 (2012) 879–882, doi:10.5796/electrochemistry.80.879.
[331] S. Yoon, J.Y. Yun, J.H. Lim, B. Yoo, Enhanced electrocatalytic properties of electrodeposited amorphous cobalt-nickel hydroxide nanosheets on nickel foam by the formation of nickel nanocones for the oxygen evolution reaction, J. Alloy. Compd. 693 (2017) 964–969, doi:10.1016/j.jallcom.2016.09.247.
[332] M. Iannuzzi, G.S. Frankel, Mechanisms of corrosion inhibition of AA2024-T3 by vanadates, Corros. Sci 49 (2007) 2371–2391, doi:10.1016/j.corsci.2006.10.027.
[333] M. Iannuzzi, J. Kovac, G.S. Frankel, A study of the mechanisms of corrosion inhibition of AA2024-T3 by vanadates using the split cell technique, Electrochim. Acta. 52 (2007) 4032–4042, doi:10.1016/j.electacta.2006.11.019.
[334] C.S. Neves, A.C. Bastos, A.N. Salak, M. Starykevich, D. Rocha, M.L. Zheludkevich, A. Cunha, A. Almeida, J. Tedim, M.G.S. Ferreira, Layered double hydroxide clusters as precursors of novel multifunctional layers: A bottom-up approach, Coatings 9 (2019) 328, doi:10.3390/coatings9050328.
[335] L. Wang, Q. Zong, W. Sun, Z. Yang, G. Liu, Chemical modification of hydrotalcite coating for enhanced corrosion resistance, Corros. Sci. 93 (2015) 256–266, doi:10.1016/j.corsci.2015.01.033.
[336] A.N. Salak, J. Tedim, A.I. Kuznetsova, M.L. Zheludkevich, M.G.S. Ferreira, Anion exchange in Zn–Al layered double hydroxides: in situ X-ray diffraction study, Chem. Phys. Lett 495 (2010) 73–76, doi:10.1016/j.cplett.2010.06.041.
[337] X. Guo, S. Xu, L. Zhao, W. Lu, F. Zhang, D.G. Evans, X. Duan, One-step hydrothermal crystallization of a layered double hydroxide/alumina bilayer film on aluminum and its corrosion resistance properties, Langmuir 25 (2009) 9894–9897, doi:10.1021/la901012w.
[338] J. Tedim, M.L. Zheludkevich, A.C. Bastos, A.N. Salak, A.D. Lisenkov, M.G.S. Ferreira, Influence of preparation conditions of layered double hydroxide conversion films on corrosion protection, Electrochim. Acta 117 (2014) 164–171, doi:10.1016/j.electacta.2013.11.111.
[339] C. Zhang, X. Luo, X. Pan, L. Liao, X. Wu, Y. Liu, Self-healing Li-Al layered double hydroxide conversion coating modified with aspartic acid for 6N01 Al alloy, Appl. Surf. Sci 394 (2017) 275–281, doi:10.1016/j.apsusc.2016.10.034.
[340] F. Zhang, M. Sun, S. Xu, L. Zhao, B. Zhang, Fabrication of oriented layered double hydroxide films by spin coating and their use in corrosion protection, Chem. Eng. J 141 (2008) 362–367, doi:10.1016/j.cej.2008.03.016.
[341] Y. Zhang, Y. Li, Y. Ren, H. Wang, F. Chen, Double-doped LDH films on aluminum alloys for active protection, Mater. Lett 192 (2017) 33–35, doi:10.1016/j.matlet.2017.01.038.
[342] A.C. Bouali, N.M. André, M.R. Silva Campos, M. Serdechnova, J.F. dos Santos, S.T. Amancio-Filho, M.L. Zheludkevich, Influence of LDH conversion coatings on the adhesion and corrosion protection of friction spot-joined AA2024-T3/CF-PPS, J. Mater. Sci. Technol 67 (2020) 197–210, doi:10.1016/j.jmst.2020.06.038.
[343] M.I.C. Malta, M.R.S. Vieira, R.G.C. Silva, L.M.C. Silva, E.G. Araújo, S.H. Maciel, S.L. Urtiga Filho, Superhydrophobic Surfaces on 5052 Aluminum Alloy Obtained from LDH film modified with stearic acid for enhanced corrosion protection, Mater. Res 22 (2019) 1–8, doi:10.1590/1980-5373-mr-2018-0882.
[344] F. Wang, Z. Guo, Facile synthesis of superhydrophobic three-metal-component layered double hydroxide films on aluminum foils for highly improved corrosion inhibition, J. New. Chem. 43 (2019) 2289–2298, doi:10.1039/C8NJ05732J.
[345] Y. Cao, D. Zheng, J. Luo, F. Zhang, C. Wang, S. Dong, Y. Ma, Z. Liang, C. Lin, Enhanced corrosion protection by Al surface immobilization of in-situ grown layered double hydroxide films co-intercalated with inhibitors and low surface energy species, Corros. Sci 164 (2020) 108340, doi:10.1016/j.corsci.2019.108340.
[346] K.A. Yasakau, A. Kuznetsova, S. Kallip, M. Starykevich, J. Tedim, M.G.S. Ferreira, M.L. Zheludkevich, A novel bilayer system comprising LDH conversion layer and sol-gel coating for active corrosion protection of AA2024, Corros. Sci 143 (2018) 299–313, doi:10.1016/j.corsci.2018.08.039.
[347] T. Yan, S. Xu, Q. Peng, L. Zhao, X. Zhao, X. Lei, F. Zhang, Self-healing of layered double hydroxide film by dissolution/recrystallization for corrosion protection of aluminum, J. Electrochem. Soc. 160 (2013) C480–C486, doi:10.1149/2.053310jes.
[348] J.S. Laird, P. Visser, S. Ranade, A.E. Hughes, H. Terryn, J.M.C. Mol, Li leaching from Lithium Carbonate-primer: An emerging perspective of transport pathway development, Prog. Org. Coat 134 (2019) 103–118, doi:10.1016/j.porgcoat.2019.04.062.
[349] Y. Liu, P. Visser, X. Zhou, S.B. Lyon, T. Hashimoto, M. Curioni, D. Graham, Protective film formation on AA2024-T3 aluminum alloy by leaching of lithium carbonate from an organic coating, J. Electrochem. Soc. 163 (2015) C45–C53, doi:10.1149/2.0021603jes.
[350] Y. Liu, P. Visser, X. Zhou, S.B. Lyon, T. Hashimoto, A. Gholinia, G.E. Thompson, G. Smyth, S.R. Gibbon, D. Graham, J.M.C. Mol, H. Terryn, An investigation of the corrosion inhibitive layers generated from lithium oxalate-containing organic coating on AA2024-T3 aluminium alloy, Surf. Interface. Anal 48 (2016) 798–803, doi:10.1002/sia.5972.
[351] K. Marcoen, P. Visser, G.F. Trindade, M.L. Abel, J.F. Watts, J.M.C. Mol, H. Terryn, T. Hauffman, Compositional study of a corrosion protective layer formed by leachable lithium salts in a coating defect on AA2024-T3 aluminium alloys, Prog. Org. Coat. 119 (2018) 65–75, doi:10.1016/j.porgcoat.2018.02.011.
[352] M. Meeusen, P. Visser, L.F. Macía, A. Hubin, H. Terryn, J.M.C. Mol, The use of odd random phase electrochemical impedance spectroscopy to study lithium-based corrosion inhibition by active protective coatings, Electrochim. Acta 278 (2018) 363–373, doi:10.1016/j.electacta.2018.05.036.
[353] P. Visser, Y. Gonzalez-Garcia, J.M.C. Mol, H. Terryn, Mechanism of passive layer formation on AA2024-T3 from alkaline lithium carbonate solutions in the presence of sodium chloride, J. Electrochem. Soc. 165 (2018) C60–C70, doi:10.1149/2.1011802jes.
[354] P. Visser, Y. Liu, H. Terryn, J.M.C. Mol, Lithium salts as leachable corrosion inhibitors and potential replacement for hexavalent chromium in organic coatings for the protection of aluminum alloys, J. Coat. Technol. Res. 13 (2016) 557–566, doi:10.1007/s11998-016-9784-6.
[355] P. Visser, Y. Liu, X. Zhou, T. Hashimoto, G.E. Thompson, S.B. Lyon, L.G.J. van der Ven, J.M.C. Mol, H. Terryn, The corrosion protection of AA2024-T3 aluminium alloy by leaching of lithium-containing salts from organic coatings, Faraday. Discuss 180 (2015) 511–526, doi:10.1039/C4FD00237G.
[356] P. Visser, K. Marcoen, G.F. Trindade, M.L. Abel, J.F. Watts, T. Hauffman, J.M.C. Mol, H. Terryn, The chemical throwing power of lithium-based inhibitors from organic coatings on AA2024-T3, Corros. Sci 150 (2019) 194–206, doi:10.1016/j.corsci.2019.02.009.
[357] P. Visser, M. Meeusen, Y. Gonzalez-Garcia, H. Terryn, J.M.C. Mol, Electrochemical evaluation of corrosion inhibiting layers formed in a defect from lithium-leaching organic coatings, J. Electrochem. Soc. 164 (2017) C396, doi:10.1149/2.1411707jes.
[358] Y. Wang, Y. Zhang, B. Zhou, C. Li, F. Gao, X. Wang, D. Liang, Y. Wei, In-situ observation of the growth behavior of ZnAl layered double hydroxide film using EQCM, Mater. Des. 180 (2019) 107952, doi:10.1016/j.matdes.2019.107952.
[359] M.A. Iqbal, M. Fedel, Effect of operating parameters on the structural growth of ZnAl layered double hydroxide on AA6082 and corresponding corrosion resistance properties, J. Coat. Technol. Res. 16 (2019) 1423–1433, doi:10.1007/s11998-019-00227-0.
[360] V. Rizkia, B. Munir, J.W. Soedarsono, B. Suharno, Corrosion resistance enhancement of an anodic layer on an aluminum matrix composite by cerium sealing, Int. J. Technol 7 (2015) 1191–1197, doi:10.14716/ijtech.v6i7.1260.
[361] T.L. Galvão, A.C. Bouali, M. Serdechnova, K.A. Yasakau, M.L. Zheludkevich, J. Tedim, Anticorrosion thin film smart coatings for aluminum alloys. In Advances in Smart Coatings and Thin Films for Future Industrial and Biomedical Engineering Applications (pp. 429-454). Elsevier. https://doi.org/10.1016/B978-0-12-849870-5.00007-0
[362] G.P. Shulman, A.J. Bauman, Organic acid sealants for anodized aluminum—A new method for corrosion protection, Met. Finish 93 (1995) 16–19, doi:10.1016/0026-0576(95)91305-7.
[363] N. Hu, X. Dong, X. He, J.F. Browning, D.W. Schaefer, Effect of sealing on the morphology of anodized aluminum oxide, Corros. Sci 97 (2015) 17–24, doi:10.1016/j.corsci.2015.03.021.
[364] Y. Li, S. Li, Y. Zhang, M. Yu, J. Liu, Enhanced protective Zn–Al layered double hydroxide film fabricated on anodized 2198 aluminum alloy, J. Alloy. Compd. 630 (2015) 29–36, doi:10.1016/j.jallcom.2014.12.176.
[365] Y. Li, S. Li, Y. Zhang, M. Yu, J. Liu, Fabrication of superhydrophobic layered double hydroxides films with different metal cations on anodized aluminum 2198 alloy, Mater. Lett 142 (2015) 137–140, doi:10.1016/j.matlet.2014.11.148.
[366] J. Liu, H. Shi, M. Yu, R. Du, G. Rong, S. Li, Effect of divalent metal ions on durability and anticorrosion performance of layered double hydroxides on anodized 2A12 aluminum alloy, Surf. Coat. Technol 373 (2019) 56–64, doi:10.1016/j.surfcoat.2019.05.066.
[367] M.A. Iqbal, M. Fedel, Protective Cerium-Based Layered Double Hydroxides Thin Films Developed on Anodized AA6082, Adv. Mater. Sci. Eng. 2020 (2020) 1–12, doi:10.1155/2020/5785393.
[368] M.A. Iqbal, H. Asghar, M. Fedel, Double doped cerium-based superhydrophobic layered double hydroxide protective films grown on anodic aluminium surface, J. Alloys Compd 844 (2020) 156112, doi:10.1016/j.jallcom.2020.156112.
[369] R. Arrabal, M. Mohedano, E. Matykina, A. Pardo, B. Mingo, M.C. Merino, Characterization and wear behaviour of PEO coatings on 6082-T6 aluminium alloy with incorporated α-Al2O3 particles, Surf. Coat. Technol 269 (2015) 64–73, doi:10.1016/j.surfcoat.2014.10.048.
[370] A.L. Yerokhin, X. Nie, A. Leyland, A. Matthews, S.L. Dowey, Plasma electrolysis for surface engineering, Surf. Coat. Technol 122 (1999) 73–93, doi:10.1016/S0257-8972(99)00441-7.
[371] X. Lu, M. Mohedano, C. Blawert, E. Matykina, R. Arrabal, K.U. Kainer, M.L. Zheludkevich, Plasma electrolytic oxidation coatings with particle additions–A review, Surf. Coat. Technol 307 (2016) 1165–1182, doi:10.1016/j.surfcoat.2016.08.055.
[372] M. Mohedano, X. Lu, E. Matykina, C. Blawert, R. Arrabal, M.L. Zheludkevich,

Plasma electrolytic oxidation (PEO) of metals and alloys, (2018) 423-438. https://doi.org/ 10.1016/B978-0-12-409547-2.13398-0.
[373] E. Matykina, R. Arrabal, P. Skeldon, G.E. Thompson, Investigation of the growth processes of coatings formed by AC plasma electrolytic oxidation of aluminium, Electrochem. Acta 54 (2009) 6767–6778, doi:10.1016/j.electacta.2009.06.088.
[374] I.P. Mertsalo, V.T. Yavors' kyi, M.D. Klapkiv, R.S. Mardarevych, Wear resistance of anodic-spark coatings on aluminum alloys, Mater. Sci 39 (2003) 136–139, doi:10.1023/A:1026147017445.
[375] V.S. Egorkin, S.V. Gnedenkov, S.L. Sinebryukhov, I.E. Vyaliy, A.S. Gnedenkov, R.G. Increasing thickness and protective properties of PEO-coatings on aluminum alloy, Surf. Coat. Technol 334 (2018) 29–42, doi:10.1016/j.surfcoat.2017.11.025.
[376] B. Dou, Y. Wang, T. Zhang, B. Liu, Y. Shao, G. Meng, F. Wang, Growth behaviors of layered double hydroxide on microarc oxidation film and anti-corrosion performances of the composite film, J. Electrochem. Soc. 163 (2016) C917–C927, doi:10.1149/2.1141614jes.
[377] M. Mohedano, M. Serdechnova, M. Starykevich, S. Karpushenkov, A.C. Bouali, M.G.S. Ferreira, M.L. Zheludkevich, Active protective PEO coatings on AA2024: Role of voltage on in-situ LDH growth, Mater. Des 120 (2017) 36–46, doi:10.1016/j.matdes.2017.01.097.
[378] M. Mohedano, E. Matykina, R. Arrabal, B. Mingo, A. Pardo, PEO of pre-anodized Al–Si alloys: Corrosion properties and influence of sealings, Appl. Surf. Sci 346 (2015) 57–67, doi:10.1016/j.apsusc.2015.03.206.
[379] Y. Zhang, P. Yu, Y. Zuo, H. Tian, X. Chen, F. Chen, Investigating the growth behavior of LDH layers on MAO-coated aluminum alloy: Influence of microstructure and surface element, Int. J. Electrochem. Sci 13 (2018) 610–620, doi:10.20964/2018.01.53.
[380] R. del Olmo, M. Mohedano, B. Mingo, R. Arrabal, E. Matykina, LDH Post-Treatment of Flash PEO Coatings, Coatings 9 (2019) 354, doi:10.3390/coatings9060354.
[381] K. Noweck, K. Diblitz, J. Sohiefler, A. Brasch, Process for producing hydrotalcites and the metal oxides thereof. U.S. Patent No US6517795B1, 11 févr. 2003.
[382] SASOL GmbH, HYDROTALCITES AND SPINELS PURAL MG / PURALOX MG. https://www.sasolgermany.de/index.php?id=hydrotalcites0. (Accessed 26th July 2020).
[383] SINWON CHEMICAL CO., LTD, Synthetic Hydrotalcites (HI-TALTM), http://www.swchem.co.kr/layered-double-hydroxides.html. (Accessed 26th July 2020)
[384] KISUMA CHEMICALS BV, Innovations, https://www.kisuma.com/innovation. (Accessed 26th 2020)
[385] SMALLMATEK., Lda, Home page, https://www.smallmatek.pt/. (Accessed 26th July 2020)
[386] H. Hintze-Bruening and F. Leroux, Nanocomposite based multifunctional coatings, New advances in vehicular technology and automotive engineering. 55 (2012).https://doi.org/ 10.5772/48567.
[387] VISSER, Peter et HAYES, Scott Alan. Anti-corrosive coating composition. U.S. Patent No US8628689B2, 14 janv. 2014.
[388] AkzoNobel Coating GmbH, Chromate-free Systems, https://aerospace.akzonobel.com/featured-product/chromate-free. (Accessed 26th July 2020).
[389] E. Alibakhshi, E. Ghasemi, M. Mahdavian, B. Ramezanzadeh, S. Farashi, Active corrosion protection of Mg-Al-PO43− LDH nanoparticle in silane primer coated with epoxy on mild steel, J. Taiwan. Inst. Chem. Eng 75 (2017) 248–262, doi:10.1016/j.jtice.2017.03.010.
[390] K. Hoshino, S. Furuya, R.G. Buchheit, Effect of Solution pH on layered double hydroxide formation on electrogalvanized steel sheets, J. Mater. Eng. Perform. 28 (2019) 2237–2244, doi:10.1007/s11665-019-03963-x.
[391] T. Ishizaki, S. Chiba, K. Watanabe, H. Suzuki, Corrosion resistance of Mg–Al layered double hydroxide container-containing magnesium hydroxide films formed directly on magnesium alloy by chemical-free steam coating, J. Mater. Chem A. 1 (2013) 8968–8977, doi:10.1039/C3TA11015J.
[392] N. Kamiyama, G. Panomsuwan, E. Yamamoto, T. Sudare, N. Saito, T. Ishizaki, Effect of treatment time in the Mg (OH) 2/Mg–Al LDH composite film formed on Mg alloy AZ31 by steam coating on the corrosion resistance, Surf. Coat. Technol 286 (2016) 172–177, doi:10.1016/j.surfcoat.2015.11.051.
[393] G. Zhang, L. Wu, A. Tang, S. Zhang, B. Yuan, Z. Zheng, F. Pan, A novel approach to fabricate protective layered double hydroxide films on the surface of anodized Mg-Al alloy, Adv. Mater. Interfaces 4 (2017) 1700163, doi:10.1002/admi.201700163.
[394] L. Wu, D. Yang, G. Zhang, Z. Zhang, S. Zhang, A. Tang, F. Pan, Fabrication and characterization of Mg-M layered double hydroxide films on anodized magnesium alloy AZ31, Appl. Surf. Sci 431 (2018) 177–186, doi:10.1016/j.apsusc.2017.06.244.
[395] L. Guo, W. Wu, Y. Zhou, F. Zhang, R. Zeng, J. Zeng, Layered double hydroxide coatings on magnesium alloys: A review, J. Mater. Sci. Technol. 34 (2018) 1455–1466, doi:10.1016/j.jmst.2018.03.003.
[396] M. Bukhtiyarova, M., A review on effect of synthesis conditions on the formation of layered double hydroxides, J. Solid State Chem 269 (2019) 494–506, doi:10.1016/j.jssc.2018.10.018.
[397] W. Zhang, H. Cheng, S. Peng, D. Li, H. Gao, D. Wang, Performance and mechanisms of wastewater sludge conditioning with slag-based hydrotalcite-like minerals (Ca/Mg/Al-LDH), Water Res 169 (2020) 115265, doi:10.1016/j.watres.2019.115265.
[398] Z.X. Xu, H. Song, P.J. Li, X. Zhu, S. Zhang, Q. Wang, P. Duan, X. Hu, A new method for removal of nitrogen in sewage sludge-derived hydrochar with hydrotalcite as the catalyst, J. Hazard. Mater. 398 (2020) 122833, doi:10.1016/j.jhazmat.2020.122833.
[399] M. Eisgruber, J. Ladebeck, J. Koy, H. Schiessling, W. Buckl, H. Ebert, Method for the production of hydrotalcites. U.S. Patent No. 7,897,136. 1 Mar. 2011.
[400] M.L. Parello, R. Rojas, C.E. Giacomelli, Dissolution kinetics and mechanism of Mg–Al layered double hydroxides: a simple approach to describe drug release in acid media, J. Colloid. Interf. Sci. 351 (2010) 134–139, doi:10.1016/j.jcis.2010.07.053.
[401] L.P.F. Benício, R.A. Silva, J.A. Lopes, D. Eulálio, R.M.M. Santos, L.A. Aquino, L. Vergütz, R.F. Novais, L.M. Costa, F.G. Pinto, J. Tronto, Layered double hydroxides: nanomaterials for applications in agriculture, Revista Brasileira de Ciência do Solo 39 (2015) 1–13, doi:10.1590/01000683rbcs2015081.
[402] Z.H. Xie, L. Wu, Corrosion inhibition of layered double hydroxide coating for Mg alloy in acidic corrosive environments, Mater. Corros 71 (2020) 118–124, doi:10.1002/maco.201910995.
[403] A.U. Kura, N.M. Ain, M.Z. Hussein, S. Fakurazi, S.H. Hussein-Al-Ali, Toxicity and metabolism of layered double hydroxide intercalated with levodopa in a Parkinson's disease model, Int. J. Mol. Sci 15 (2014) 5916–5927, doi:10.3390/ijms15045916.
[404] T.A. Silva, T.A. Silva, T.G. Nascimento, R.E. Yatsuzuka, L.A.M. Grillo, C.B. Dornelas, Recent advances in layered double hydroxides applied to photoprotection, Einstein (São Paulo) 17 (2019) 2317–6385, doi:10.31744/einstein_journal/2019rw4456.
[405] M.L. Zheludkevich, M.G.S. Ferreira, S. Poznyak, Self-healing corrosion protection coatings with nanocontainers of corrosion inhibitors, in: Physics, Chemistry And Application Of Nanostructures: Reviews and Short Notes, World Scientific, 2007, pp. 380–383, doi:10.1142/9789812770950_0085.
[406] J. Rodriguez, E. Bollen, T.D. Nguyen, A. Portier, M.G. Olivier, Incorporation of layered double hydroxides modified with benzotriazole into an epoxy resin for the corrosion protection of Zn-Mg coated steel, Prg. Org. Coat 149 (2020) 105894, doi:10.1016/j.porgcoat.2020.105894.
[407] A. Seniski, R.F. Monteiro, G.T. Carrera, M.O.G.P. Bragança, K.F. Portella, The inhibitory and comparative effects of Zn-Al layered double hydroxide microcontainers intercalated with benzotriazole and nitrite for corrosion protection coatings on AISI 1010 carbon steel, Matéria (Rio de Janeiro) 25 (2020) 1–10, doi:10.1590/s1517-707620200002.1064.
[408] Y. Cao, S. Dong, D. Zheng, J. Wang, X. Zhang, R. Du, G. Song, C. Lin, Multifunctional inhibition based on layered double hydroxides to comprehensively control corrosion of carbon steel in concrete, Corros. Sci 126 (2017) 166–179, doi:10.1016/j.corsci.2017.06.026.
[409] F. Zhong, Y. He, P. Wang, C. Chen, P. Xie, H. Li, J. Chen, One-step hydrothermal synthesis of reduced graphene oxide/aspartic acid intercalated layered double hydroxide for enhancing barrier and self-healing properties of epoxy coating, React. Funct. Polym. 145 (2019) 104380, doi:10.1016/j.reactfunctpolym.2019.104380.
[410] Y. Dong, L. Ma, Q. Zhou, Effect of the incorporation of montmorillonite-layered double hydroxide nanoclays on the corrosion protection of epoxy coatings, J. Coat. Technol. Res. 10 (2013) 909–921, doi:10.1007/s11998-013-9519-x.
[411] H. Hayatdavoudi, M. Rahsepar, Smart inhibition action of layered double hydroxide nanocontainers in zinc-rich epoxy coating for active corrosion protection of carbon steel substrate, J. Alloys Compd 711 (2017) 560–567, doi:10.1016/j.jallcom.2017.04.044.
[412] Q.S. Yao, F. Zhang, L. Song, R.C. Zeng, L.Y. Cui, S.Q. Li, Z.L. Wang, E.H. Han, Corrosion resistance of a ceria/polymethyltrimethoxysilane modified Mg-Al-layered double hydroxide on AZ31 magnesium alloy, J. Alloys Compd 764 (2018) 913–928, doi:10.1016/j.jallcom.2018.06.152.
[413] X. Wang, L. Li, Z.H. Xie, G. Yu, Duplex coating combining layered double hydroxide and 8-quinolinol layers on Mg alloy for corrosion protection, Electrochim. Acta 283 (2018) 1845–1857, doi:10.1016/j.electacta.2018.07.113.
[414] J. Wang, D. Li, X. Yu, X. Jing, M. Zhang, Z. Jiang, Hydrotalcite conversion coating on Mg alloy and its corrosion resistance, J. Alloys Conpd 494 (2010) 271–274, doi:10.1016/j.jallcom.2010.01.007.
[415] F. Zhang, Z.G. Liu, R.C. Zeng, S.Q. Li, H.Z. Cui, L. Song, E.H. Han, Corrosion resistance of Mg–Al-LDH coating on magnesium alloy AZ31, Surf. Coat. Technol 258 (2014) 1152–1158, doi:10.1016/j.surfcoat.2014.07.017.
[416] M.J. Anjum, J. Zhao, V.Z. Asl, G. Yasin, W. Wang, S. Wei, Z. Zhao, W.Q. Khan, In-situ intercalation of 8-hydroxyquinoline in Mg-Al LDH coating to improve the corrosion resistance of AZ31, Corros. Sci 157 (2019) 1–10, doi:10.1016/j.corsci.2019.05.022.